(12)

Mechanical Properties for the Grasp of a Robotic Hand

Mark R. Cutkosky

CMU-RI-TR-84-24

Carnegie-Mellon University
The Robotics Institute

Technical Report

Unclassified

SECURITY CLASSIFICATION OF THIS PAGE (When Data Entered)

REPORT DOCUMENTATION PAGE	READ INSTRUCTIONS BEFORE COMPLETING FORM
1. REPORT NUMBER CMU-RI-TR-84-24	2. GOVT ACCESSION NO. AD-A150062	3. RECIPIENT'S CATALOG NUMBER
4. TITLE (and Subtitle) Mechanical Properties for the Grasp of a Robotic Hand	5. TYPE OF REPORT & PERIOD COVERED Interim 6. PERFORMING ORG. REPORT NUMBER
7. AUTHOR(s) Mark R. Cutkosky	8. CONTRACT OR GRANT NUMBER(s)
9. PERFORMING ORGANIZATION NAME AND ADDRESS Carnegie-Mellon University The Robotics Institute Pittsburgh, PA. 15213	10. PROGRAM ELEMENT, PROJECT, TASK AREA & WORK UNIT NUMBERS
11. CONTROLLING OFFICE NAME AND ADDRESS Office of Naval Research Arlington, VA 22217	12. REPORT DATE September 1984 13. NUMBER OF PAGES 78
14. MONITORING AGENCY NAME & ADDRESS (if different from Controlling Office)	15. SECURITY CLASS. (of this report) UNCLASSIFIED 15a. DECLASSIFICATION/DOWNGRADING SCHEDULE

16. DISTRIBUTION STATEMENT (of this Report)

Approved for public release; distribution unlimited

17. DISTRIBUTION STATEMENT (of the abstract entered in Block 20, if different from Report)

Approved for public release; distribution unlimited

18. SUPPLEMENTARY NOTES

19. KEY WORDS (Continue on reverse side if necessary and identify by block number)

20. ABSTRACT (Continue on reverse side if necessary and identify by block number)

The subject of this paper forms part of a broader effort to model the mechanics of grasping and fine-manipulation for robots. Grasping is the act of acquiring and holding (gripping) an object. Fine-manipulation is an extension of grasping to include control of the object using an end-effector such as a gripper or a hand. A mechanical model of grasping and manipulation forms the basis for contr as grippers and paves the way for robots that can make independent judgments about how to pick up and handle the objects they encounter. In this paper a procedure is developed for computing physical properties with which a grasp may be described.

DD FORM 1 JAN 73 1473 EDITION OF 1 NOV 65 IS OBSOLETE
S/N 0102-014-6601

UNCLASSIFIED
SECURITY CLASSIFICATION OF THIS PAGE (When Data Entered)

(20. cont'd.)

Among these properties are grip strength, stability, compliance and mobility. The results depend strongly on the interaction between the gripping surfaces and the object. For example, a grasp may be unstable when the fingertips are pointed, but stable for rounded fingertips. The analysis suggests that particular kinds of sensory information are especially useful in controlling a grasp and supports the notion that general grasping "rules of thumb" can be identified for use by robots.

12

Mechanical Properties for the Grasp of a Robotic Hand

Mark R. Cutkosky

CMU-RI-TR-84-24

The Robotics Institute
Carnegie-Mellon University
Pittsburgh, Pennsylvania 15213

September 1984

This report is adapted from sections of a doctoral thesis to be submitted to The Department of Mechanical Engineering.

Table of Contents

List of Figures

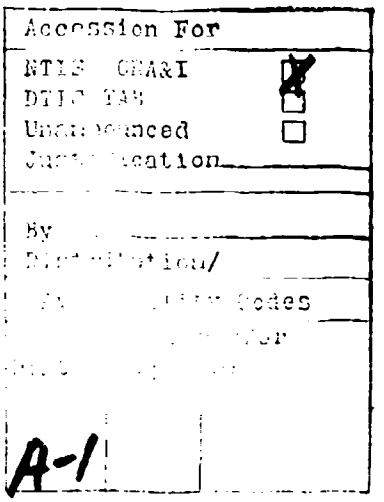

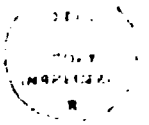

List of Tables

Abstract

The subject of this paper forms part of a broader effort to model the mechanics of grasping and fine-manipulation for robots. Grasping is the act of acquiring and holding (gripping) an object. Fine-manipulation is an extension of grasping to include control of the object using an end-effector such as a gripper or a hand. A mechanical model of grasping and manipulation forms the basis for controlling grippers and paves the way for robots that can make independent judgments about how to pick up and handle the objects they encounter. In this paper a procedure is developed for computing physical properties with which a grasp may be described. Among these properties are grip strength, stability, compliance and mobility. The results depend strongly on the interaction between the gripping surfaces and the object. For example, a grasp may be unstable when the fingertips are pointed, but stable for rounded fingertips. The analysis suggests that particular kinds of sensory information are especially useful in controlling a grasp and supports the notion that general grasping "rules of thumb" can be identified for use by robots.

Additional keywords: mechanical properties, three dimensional, fingers, kinematics.

1. Introduction

What is the best way to hold an object given a particular gripper and a particular task to perform? If we look to natural examples of gripping we find that the answer to this question is a function of many things including friction, the softness of the object, the fragility of the object, and how well the object "fits" the geometry of the gripper. For example, all other things being equal, human beings will favor gripping positions that comfortably fit the size and shape of the hand. We avoid gripping positions that require us to stretch or to cramp our fingers, unless other considerations predominate. Over years of experience, we seem to acquire a database of suitable gripping configurations which we apply to the world at large. We choose gripping positions without much conscious thought until we are faced with a completely unfamiliar object shape (especially if the object is also slippery or heavy).

For the current generation of industrial robots there is little need to calculate suitable gripping positions. Today's robots are play-back machines repeating sequences of instructions; they may be programmed to assemble various shapes or to load them into machine tools but they never have to decide how to grasp an object. The grasp is chosen for them when they are programmed and is part of the information associated with the task. This approach is adequate as long as robots continue to perform a narrow range of tasks with a limited selection of parts, but it becomes impractical if robots are to work under less structured circumstances. For example, a robot working on the ocean floor, or in a nuclear power plant, would be more effective if it did not have to ask for instructions about how to pick up every new object it encountered. This goal prompts us to ask whether a suitable grasp is something that can be determined analytically and expressed to the robot in terms of an algorithm. But first, we need a model that describes different grasps and predicts how a grasp will respond to forces and motions applied to the object as the robot proceeds with a task.

The present paper draws upon previous work on the kinematics of an object being manipulated by a gripper and develops a procedure for determining mechanical properties which may be used to characterize grips and to discriminate between them. The result is a linearized model of how a grasp will behave in response to task-induced forces and motions. Using the grasp model, the paper considers the importance of gripper contact surfaces, frictional properties and gripping forces in determining the overall behavior of the grasp.

1.1 Previous Investigations on Prehension

Recently, a few works have appeared that cover grasping kinematics, gripper control and related topics.

Asada [1] begins by describing the force balance for an object held by a gripper with several fingers. He assumes that the gripper has k_a actuators each driving l fingers of which m are actually touching the held object at a particular time. Thus there are a total of $k_a \times m$ fingers in contact with the object, of which k_a are independent. He next assumes that each finger has a small contact area so that the contact between each

finger and the object can be treated as a point contact. With this assumption the force exerted by each finger can be resolved into forces perpendicular and tangential to the object surface. The assumption is a limiting one because it removes the possibility that a single finger can apply a torque about its own axis and ignores rolling or rocking motion between the fingertip and the object. However, it is often a reasonable approximation for grippers with small gripping surfaces made of hard materials (a pair of tongs, for example). Generally, the point-contact approximation results in an overestimate of the gripping force required to maintain equilibrium. Salisbury [2] and Okada [3, 4] make similar assumptions in describing the forces exerted by their three-fingered hands, although Salisbury discusses the effects of having a "soft" finger that can apply moments, twisting about its central axis.

Having described the equilibrium requirements for an object held by several fingers, Asada addresses the problem of choosing a suitable finger configuration. He treats the held object as a rigid body and models the fingers as elastic members with one degree of freedom, along a specified trajectory or locus. He simplifies the grasping model by ignoring friction at the contact points between the fingers and the object. With this model he is able to construct a potential function, based on the shape of the object, which indicates the relative stability of different finger configurations. In the absence of friction, an object held in a stable grasp will return to its original position if displaced slightly. The theory works well for slippery objects and whenever the chief concern is that the object should not be dropped (when we wash dishes we hold them in a stable grasp.) Unfortunately, the utility of the model for industrial robots is very limited. Friction is an important consideration and is often used to advantage. According to Asada's theory there is no satisfactory way for a two-fingered gripper to grip many shapes. For example, there is no "stable" configuration for a two-fingered gripper grasping a sphere. In practice, people depend on friction when they design grippers and when they program robots to grasp and manipulate objects. A stable grip guarantees that the gripper will not drop an object, but often a great deal more is required. It may be required that none of the fingers of a gripper should slip with respect to an object while it is manipulated because if they do, the object will not return to the same equilibrium position.[1] Industrial robots are ofte . programmed based on a precise knowledge of the position and orientation of a grasped object with respect to the robot coordinate system. As soon as any of the fingers slip, this information is lost.

Salisbury [2, 5] and Okada [4, 3] are concerned with developing control laws for multi-jointed three-finger grippers. The hand designed by Okada can perform a variety of manipulation tasks such as screwing a nut onto a bolt and manipulating a match box in three dimensions. When the motions of the manipulated object are not very small it becomes necessary to treat the fingertips not as points but as surfaces of finite radius. The fingertips roll with respect to the manipulated object and the kinematic description of the fingertip locus becomes extremely complicated.

Salisbury [2, 5] draws upon his earlier work in manipulator control [6] in which he discusses how to determine the correct servo stiffnesses for the joints of a robot to achieve some desired set of suffnesses

[1] In the absence of friction the object would return to its orginal, stable position.

expressed with respect to the robot hand (or any other convenient coordinate system). Salisbury considers several contact types, including point, line and planar contact (with and without friction), and discusses the constraints imposed on the object by each. He also introduces a "soft" finger with friction which can apply torques about its own axis in addition to forces at the contact point. The effects of rolling and deformation of the fingertip are not considered. He also considers the interaction of groups of contacts about an object and discusses the conditions under which arbitrary motions and forces can be applied to the object. Like Asada, he shows that for pointed fingers a jacobian matrix can be found which relates forces exerted at the fingertips to an equivalent force and torque at the centroid of an object held by the fingers. He augments this jacobian matrix to include internal forces which essentially measure the magnitude of the "pinch" exerted by pairs of opposed fingers.

Hanafusa *et al* [7] also consider the kinematics of an object held by point-contact fingers. They discuss the conditions under which the the object is free to move in any direction if the finger joints are loose, but becomes completely constrained if the finger joints are locked. They consider a gripper with an arbitrary number of fingers, each with an arbitrary number of joints, and discuss methods for specifying the redundant degrees of freedom.

Orin and Oh [8] have considered the related problem of determining the optimum distribution of forces in closed kinematic chains. They are primarily interested in extending earlier work in the control and analysis of walking machines, but they point out that a walking machine and a multi-fingered gripper handling an object both contain closed kinematic chains.[2] Usually, the number of independent joint actuators in the chains is greater than the number required to impart a desired set of velocities and forces to the body of the walking machine or the grasped object. They compute the dynamic terms for all the legs and then use a linear programming approach to minimize the energy expenditure in the motors, subject to a number of constraints. The constraints include friction limitations at the feet (or fingertips) and maximum joint torques at the actuators. Normally, friction limitations result in non-linear constraints, but by approximating the conventional "friction cones" with friction pyramids a conservative set of linear inequality equations is obtained. The contacts between the feet and the ground are treated as point contacts in the kinematic model. To measure the energy expenditure, a power term is established, where the power at each joint is a function of the joint torque and velocity. The simplex method is used to find the minimum of the cost function.

The linear programming method described by Orin and Oh [8] allows a sequence of joint torques to be determined off-line for a walking machine, but is too slow for real-time use. However, for a hand making small motions with the fingers, inertial terms can be ignored, considerably reducing the computation time. Power expenditure might actually be of little consequence in a robot gripper, but other terms might be added to the overall cost function to determine an optimum set of joint torques and stiffnesses for a given grasp geometry.

---

[2] In fact, a hand supporting a basketball is like a very large animal walking upon a very small planet.

Mason [9] investigates the effects of friction on basic operations in which a robot grasps an object or pushes it into place. He points out that the role of friction in simple tasks performed by manipulators has not been adequately studied. The few investigators who have considered friction have been content to use the model developed by Coulomb in 1781. For tasks involving grippers and objects with hard, flat surfaces, the Coulomb model gives accurate results. Using it, Mason derives analytic solutions predicting, for example, the direction and the rate of rotation of an object pushed along a flat surface.

For grippers with soft fingers (and particularly the human hand) the Coulomb model of friction may not accurately describe what we observe from experience:

> "When there is a possibility of the object slipping over the skin, a resistance, namely friction, intervenes which is proportional to the area of the surfaces in contact. ...Sweat glands, by moistening the skin, tend to increase friction and make the skin more adhesive." [10]

At light pressures, adhesion contributes greatly to the tangential force that a contact can sustain without slipping. The adhesion is not directly related to the normal force, but depends on surface chemistry, surface roughness, and the past history of normal forces. As an illustration, a compliant elastomer, once it has been pressed against the surface of an object, can often resist tangential loads even after the normal pressure is reduced to zero. The Coulomb coefficient of friction in this case would be infinite.

1.2 Current Investigation

In the following sections a procedure is given for determining mechanical properties with which a grip may be described. In the analysis, the arrangement of the fingers upon the object, and the stiffness and kinematic design of each finger are assumed to be known. The object is given arbitrary small displacements and the resulting motions and changes in forces are computed. From these, the overall stiffness of the grip, the ability of the grip to resist slipping and the ability of the grip to recover equilibrium in the presence of disturbances may be established. The procedure is initially illustrated with some two-dimensional examples. It is shown that the results may contain not only stiffness terms of the kind discussed by Salisbury [2] but also terms due to differential changes in the grip geometry. Unlike the stiffness terms, the geometric terms may make the grip *unstable*. A concept of grip stability is then developed which includes friction. A robot may choose between competing grips by selecting one which is stable in the presence of disturbances, which is most able to resist slipping and which matches the stiffnesses of the fingers to the compliance requirements of the task.

The analysis is extended to three-dimensional examples and explicit consideration is paid to the importance of the interaction between the fingertips and the object. Different contact conditions involving pointed, curved, soft and hard fingertips are modeled. A summary of the contact types is shown in Table 6-1. The point-contact model used in earlier analyses sometimes gives misleading results, especially when the object is small compared to the hand and when compliant gripping surfaces are employed. Finally, the results of the analysis are discussed in terms of designing and controlling dextrous hands or grippers. The results suggest that certain kinds of sensory information will be especially useful for grasp control and that a number of grasping "rules of thumb" may be argued on mechanical grounds. For example, an argument can be made

for gripping as gently as possible without letting the object slip. A gentle grip not only helps to prevent damage to the object and fingers, but also (for a given combination of finger stiffnesses) results in a grip that is more likely to be stable.

Nomenclature for Section 2

f_i = scalar magnitude of force applied by the i^{th} finger

$\alpha_i\mu_i$ = acting coefficient of friction at the i^{th} finger ($0 \le \alpha_i \le 1$)

μ_i = coefficient of friction at the i^{th} finger (from surface properties)

$\mathbf{n}_i$ = unit normal vector at the i^{th} finger

$\mathbf{l}_i$ = unit vector tangential to the object at the i^{th} finger

$\mathbf{r}_i$ = vector from origin fixed in the object to the i^{th} finger

$\mathbf{f}_e$ = external force taken at the origin

$\mathbf{m}_e$ = external moment taken at the origin

δn_i = normal component of displacement of i^{th} finger

δl_i = tangential displacement of i^{th} finger

β_i = angle between unit normal and $\mathbf{r}_i$ for i^{th} finger

k_{ni} = normal stiffness of i^{th} finger

k_{li} = tangential or lateral stiffness of i^{th} finger

$\mathbf{q}$ = a unit vector in an arbitrary direction

θ_q = angle between $\mathbf{q}$ and the x axis.

δq = small displacement of the object in the $\mathbf{q}$ direction

$\delta\theta$ = small rotation of the object

k_q = translational stiffness of the grip in direction $\mathbf{q}$

k_θ = rotational stiffness of the grip

$f_{\theta r}$ = restoring torque due to finger stiffnesses

$f_{\theta g}$ = grasp torque due to rotation

(*see also* Figure 2-2)

2. Determining Mechanical Properties of a Grasp

In this section the concepts of grip stiffness, strength and stability are discussed and the general procedure is described for determining the force/displacement characteristics of a grip. The concepts are illustrated at the end of the section with some simple, two-dimensional examples.

2.1 Grasping Model and Assumptions

A gripper may be modeled as a device with several fingers in contact with an object. The "fingers" need not resemble human fingers. They may be contact points on the jaws of a standard commercial gripper. If, for the moment, we adopt the Coulomb model of friction the static equilibrium equations become:

$$\mathbf{f}_e = \sum_{i=1}^{m} f_i(-\mathbf{n}_i) + \alpha_i \mu_i f_i(\mathbf{l}_i) \quad = \quad \sum_{i=1}^{m} f_i(-\mathbf{n}_i + \alpha_i \mu_i \mathbf{l}_i)$$

$$\mathbf{m}_c = \sum_{i=1}^{m} \mathbf{r}_i \times f_i(-\mathbf{n}_i) + \mathbf{r}_i \times \alpha_i \mu_i f_i(\mathbf{l}_i) \quad = \quad \sum_{i=1}^{m} f_i[\mathbf{n}_i \times \mathbf{r}_i + \alpha_i \mu_i (\mathbf{r}_i \times \mathbf{l}_i)]$$

(*see* Nomenclature *and Fig 2-1 for explanation of terms*)

The problem described by the above equations is in general statically indeterminate. The values f_i and $\alpha_i \mu_i \mathbf{l}_i$ are the unknowns. In the above equations α_i is taken as a variable parameter between 0 and 1, so that $0 \le \alpha_i \mu_i \le \mu_i$, where μ_i is the standard coefficient of friction determined from surface properties. The unit vector $\mathbf{l}_i$ is tangential to the surface of the body but its direction is otherwise unspecified. Until the object starts to slip with respect to the fingers, $\mathbf{l}_i$ and α_i cannot be further defined. We can require that the above equations have at least one solution such that all $\alpha_i \le 1$ but this is not particularly useful. It eliminates absurd finger arrangements (eg. all fingers on the same side of the object).

The presence of friction means that there are generally many grasps that will satisfy static equilibrium and it is possible to choose between them to find the one best suited for a given task. In fact, when we pick up objects with our own hands the grip we choose often depends more on what we intend to do with the object than on its shape or surface properties. For example, if we are asked to pick up a tall, thin candle that is lying on a table we may grasp it near the middle so that it balances in our hand; but if we want to push the candle into a candlestick holder we usually hold the candle near the base. Similarly, if we pick up a pen to hand it to somebody the grip we choose is entirely different from the one we use for writing.

To proceed further with a mechanical analysis it is necessary to adopt a force/deflection model for the gripper and the object. This is analogous to the use of Hookes' stress/strain relations in solid mechanics in which a model for the material provides the necessary additional equations. The force/deflection model used in the following sections incorporates a number of simplifying assumptions which are listed below.

- The fingers are modeled as elastic structures and the object as a rigid body. This is usually a good approximation for robots assembling parts or holding tools since the servoed joints in the robot arm and fingers make them considerably less stiff than the grasped object. For robots handling such materials as textiles, foamed plastic or rubber, the elasticity of the object would have to be taken into account.

- The analysis is static. There is no consideration of dynamic terms and no explicit treatment of slipping motion. However, the model can predict when a finger will start to slip upon the object and different grips may be compared by finding the one which will resist the largest task-related force or torque before slipping occurs.

- The analysis does not attempt to solve for the optimum grip for a given task but provides a mechanism for evaluating mechanical properties such as the stiffness, stability and resistance to slipping of a grip. Competing grips may be compared on the basis of such properties.

- The analysis is not concerned with geometric constraints, such as whether a gripper is actually able to achieve a given grip, or whether it is possible to place the fingers underneath an object that will be picked up from a flat surface. These are important considerations and a number of them are addressed in [11, 12, 13], but they are beyond the scope of this analysis. Basically, it is assumed that the grips under consideration have already met such criteria.

- The analysis is concerned only with small motions about an initial position. The small-motion assumption permits linear force and displacement transformations. The results of the analysis are invalid if the fingers make large motions with respect to the object, for example if they are used to turn a nut onto a bolt or to flip an object over in the hand. However, there are many tasks in which a grip is chosen and then the fingers make small motions with respect to the object. When tools such as wrenches or screwdrivers are used, the fingers usually make small motions with respect to the tool, while larger motions are accomplished with the wrist. As another example, when assembling parts, an initial grasp is chosen and then the fingers make small adjustments as the mating parts are slid together.

- Only motions with respect to the hand are considered. The interaction of the hand and the robot arm is not considered. This is not a severe restriction, however, since the compliance (inverse of stiffness) of the arm can always be added to the compliance of the hand when determining the overall force/deflection characteristics. For small and relatively low speed movements of the fingers there is little concern that dynamic coupling between hand and the arm will cause difficulties.

2.2 Stiffness, Strength and Stability of a Grasp

Stiffness

The first criterion that might be considered for evaluating a grip is the stiffness of the grip in response to externally imposed loads. The grip stiffness is a function of the stiffnesses of the fingers and of their arrangement about the object. Given a variety of possible grips, it may be useful to find the one that is stiffest with respect to torsional or translational loads. A stiff grip is useful when manipulating objects at high speeds. It helps to ensure that the displacements caused by inertial forces and torques will be small and that the natural frequency or bandwidth of the gripper/object ensemble will be high.

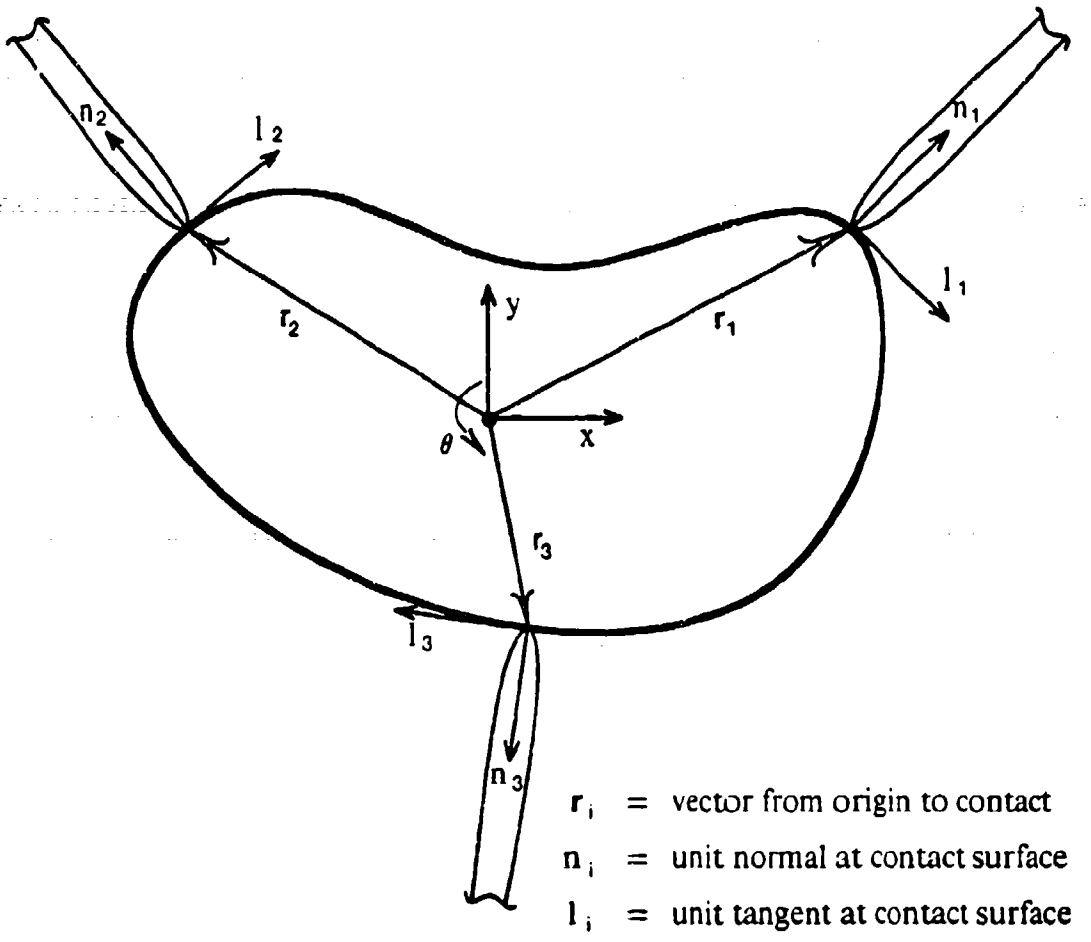

Figure 2-1: A two dimensional object held by three fingers

Robots moving freely in space are generally position-servoed and under these conditions the stiffest grip is often the best, but when a robot interacts with other objects, as during an assembly task, it becomes useful to control the mechanical *impedance* of the arm and the grip [14, 15]. Impedance control is especially well suited to servoing the fingers of the gripper or hand [6]. At low speeds, dynamic effects become negligible and impedance control reduces to stiffness control. For example, the robot hand can be made stiff in directions which are not constrained by contact with fixtures and compliant in the directions which are. In terms of choosing a grip, the best grip is the one which best matches the requirements of the task to the achievable range of finger stiffnesses.

Resistance to slipping

A second way to discriminate between grips is to find the one that, for a given combination of servo stiffnesses, grasping forces and fingertip geometries, can resist the greatest possible applied force or torque before any of the fingers slip. This again is desirable when manipulating objects at high speed. For tasks involving contact forces and torques the same analysis may be used to find the grip for which the fingers are least likely to slip in response to the expected range of forces and torques.

Stability

A third criterion is grip stability. Since the analysis is linearized and only small motions are considered it is only possible to determine whether a grip is *infinitesimally stable*, that is, whether the grip will return to its original position if the object is displaced by an arbitrary small amount. This amounts to determining whether the changes in the forces on the object that result from disturbing it will tend to oppose or to increase the disturbance.

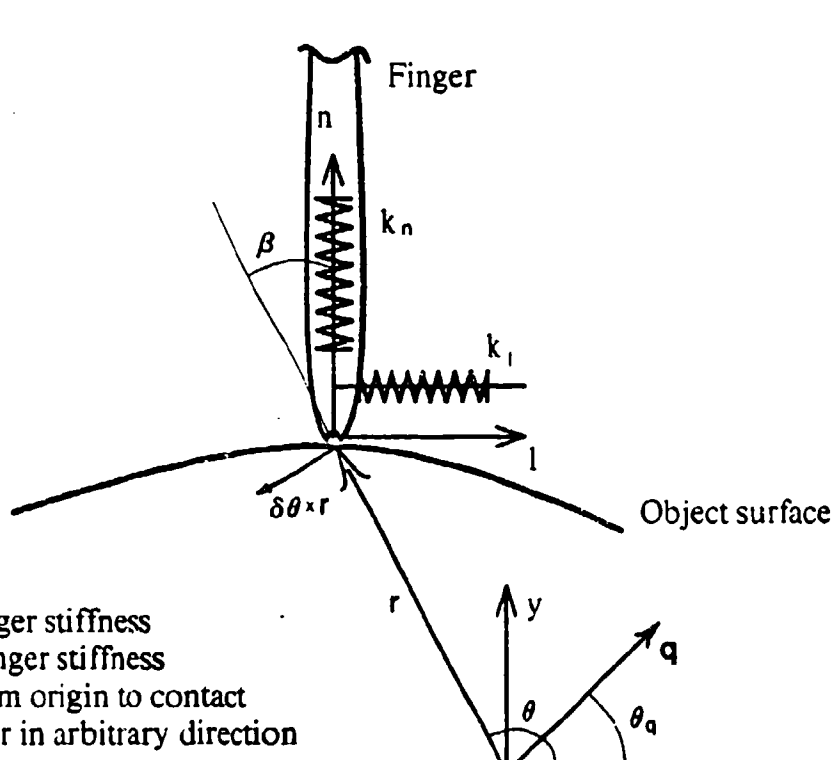

k_l = lateral finger stiffness
k_n = normal finger stiffness
r = vector from origin to contact
q = unit vector in arbitrary direction
l = unit tangent vector at contact
n = unit normal vector at contact
β = angle between unit normal and **r**

Figure 2-2: Detail of a single two-dimensional finger from Figure 2-1

2.3 Procedure for Establishing Grip Properties

The procedure used in determining the above grip properties is outlined below.

1. Displace the object an arbitrary, small amount.

2. Determine the resulting motions of the fingers. These will depend on the finger geometries, contact types and stiffnesses.

3. Determine the changes in the forces at the finger/object contact areas that result from the motions of the object and fingers. There are two contributors to these changes. The first are restoring forces that result from the stiffnesses of the fingers. The second result from changes in the grip. The fingers and the object do not move together as a rigid ensemble and the resulting modification of the grip geometry changes the way in which the finger forces act upon the object.

4. Compare the new forces at the finger/object contact areas with the maximum forces that the contacts can sustain without slipping. Also determine whether the normal forces would become negative at any of the fingers (meaning that they would lose contact with the object).

5. Compare the new resultant forces and torques on the object with the original forces and torques and with the displacement of the object to determine the stiffness and infinitesimal stability of the grip.

In later sections, particular attention is paid to the interactions between different kinds of fingertips and an object. Curved, soft, and pointed fingertips are discussed and their effects on the grip are investigated. It is shown that the point-contact model adopted in earlier analyses is only accurate when the fingertips are small compared to the object being held. Thus, if we hold a large cardboard box or a basketball, a point-contact model of our fingertips is fairly accurate, but when we hold a matchbox or a golf ball it is not.

2.4 Two-Dimensional Examples

The concepts of grip stiffness, stability and resistance to slipping can be illustrated with some short examples. In these two-dimensional examples, the forces and motions are broken into scalar components, but a matrix notation will be used for the three-dimensional analysis in later sections. Figure 2-1 shows a rigid body held by three fingers which are assumed to have some characteristic stiffness. The actual stiffness of each finger need not be prescribed; only the *relative* stiffness with respect to the other fingers is required. In the following two-dimensional examples, the finger stiffnesses may be resolved into components k_{ni} and k_{li}, perpendicular and parallel to the surface of the object. As before, the fingers need not resemble human fingers but may be the contact areas of an industrial gripper. It is required only that their stiffness and friction characteristics be known. Figure 2-2 shows the coordinates and stiffnesses for a single finger.

Looking first at torsional loading, if a force is externally applied to the object, (perhaps by a wrench at the x,y origin in Figure 2-1), the object will be rotated by a small amount, $\delta\theta$. Each fingertip in contact with the object must move $\delta\theta \times \mathrm{r}_i$ along with the object surface. The finger motions can be resolved into components parallel and perpendicular to the surface of the object.

$$\delta n_i = (\delta\theta \times \mathrm{r}_i)\cdot \mathrm{n}_i = -r_i \delta\theta \sin\beta_i$$

$$\delta n_i = (\delta\theta \times \mathrm{r}_i)\cdot \mathrm{l}_i = -r_i \delta\theta \cos\beta_i$$

We can equate the potential energy stored in rotating the body with the energy stored in the fingers to express the rotational stiffness of the grip in terms of the finger stiffnesses.

$$\tfrac{1}{2} k_\theta \delta\theta^2 = \sum_{i=1}^{m} \tfrac{1}{2} k_{ni} \delta n_i^2 + \tfrac{1}{2} k_{li} \delta l_i^2$$

Substituting for δn_i and δl_i,

$$k_\theta = \sum_{i=1}^{m} r_i^2 (k_{ni} \sin^2\beta_i + k_{li} \cos^2\beta_i)$$

The stiffest grip for torsional loading is that for which k_θ is greatest.

To find the grip that will resist the greatest torsional load without slipping we first look at each of the grips under consideration and discover which finger (or fingers in a symmetrical grip) is nearest to slipping for a given applied moment, m_e, at the origin. As the body is rotated $\delta\theta$, the changes in the forces at each finger are

$$\delta f_{ni} = k_{ni}\,\delta n_i \quad \text{and} \quad \delta f_{li} = k_{ll}\,\delta l_i.$$

From the discussion earlier in this section, $f_{li} = \alpha_i \mu_i f_{ni}$ for the Coulomb law of friction, where slipping will occur as $\alpha \rightarrow 1$. Then, for example, if initially $f_{li} = 0$, slipping will occur when

$$k_{li}\,\delta l_i > \mu_i f_{ni}$$

Thus, for a given rotation, $\delta\theta$, the finger nearest to slipping will be the one for which α is closest to 1, or for which

$$\alpha_i = \frac{k_{li}\,\delta l_i}{\mu_i f_{ni}} = \frac{m_c k_{li}(-r_i \cos\beta_i)}{k_\theta \mu_i f_{ni}}$$

is greatest.

Having found the "worst case" finger for each grip we chose between grips by finding the one for which m_e is greatest before $\alpha = 1$ at the finger.

$$m_{emax} = -\frac{k_\theta \mu_j f_{nj}}{k_{lj} r_j \cos\beta_j}$$

(where j is the subscript of the "worst case" finger)

We do not have to worry that $\cos\beta_j$ will approach zero since it will never be zero for the finger closest to slipping unless all fingers are equally likely to slip.

For motion in an arbitrary direction, q, the angle at each finger between q and n_i is $\varphi_i = \theta_i - \beta_i - \theta_q$, (where q, n, θ, β and θ_q are shown in Figure 2-2 for a typical finger). Equating potential energies allows the translational stiffness to be expressed in terms of the finger stiffnesses.

$$k_q = \sum_{i=1}^{m} k_{ni} \cos^2\varphi_i + k_{ll} \sin^2\varphi_i$$

Following the procedure used for the rotational case, we can choose between grips to find the one that will withstand the largest force, f_e, in a given direction, q, before any of the fingers slip. The "worst case" finger is the one for which

$$\alpha_i = \frac{k_{li}\,\delta l_i}{\mu_i f_{ni}} = \frac{f_e k_{li} \sin\varphi_i}{k_q \mu_i f_{ni}}$$

is greatest. The best grip is then the one for which f_e can be greatest before the "worst case" finger will slip.

$$f_{emax} = \frac{k_q \mu_j f_{nj}}{k_{lj} \sin\varphi_j}$$

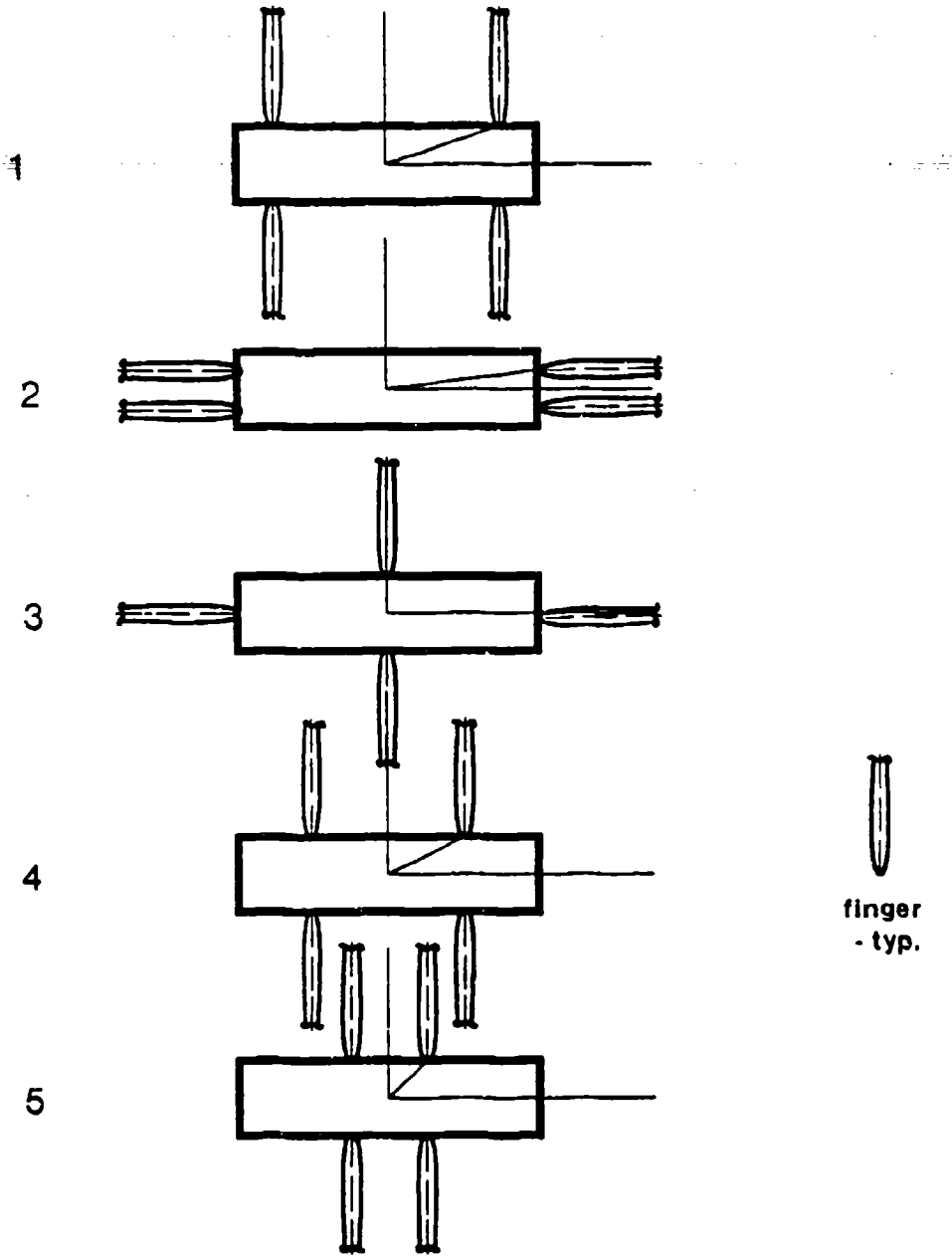

Figure 2-3: Five ways to grip a rectangle with four fingers

2.4.1 Choosing between five grips: an example

Figure 2-3 shows five grips on a rectangular block. Grips 1, 4 and 5 share the same configuration, but with different finger spacings. We can use the above results to discriminate between the grips. To simplify the computation we assume that the fingers are all identical and that their stiffness components, k_{ni} and k_{ti}, are independent of the orientation of the finger. This is a reasonable approximation for long fingers with several joints.

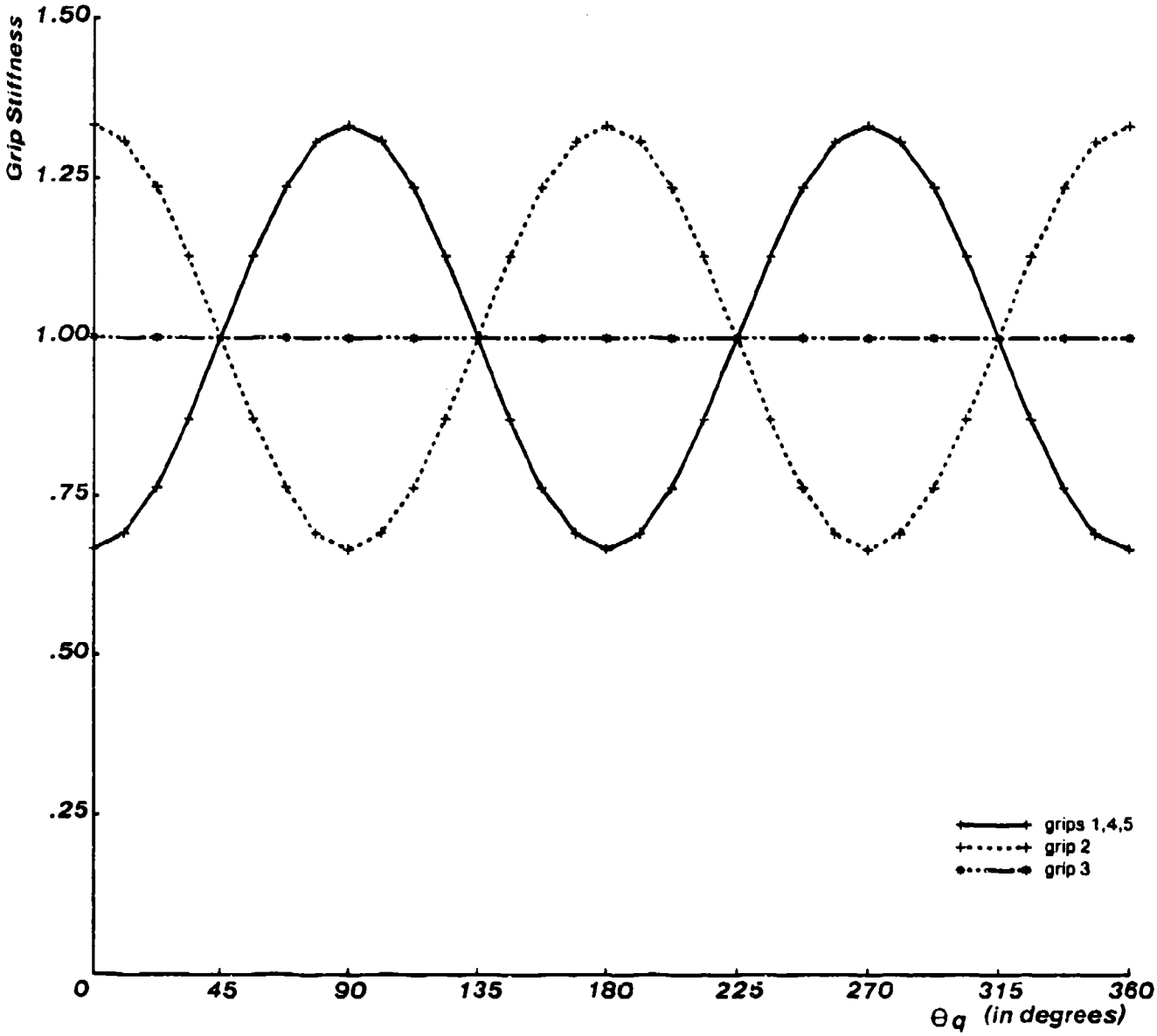

Figure 2-4: Grip stiffness for force at angle θ_q

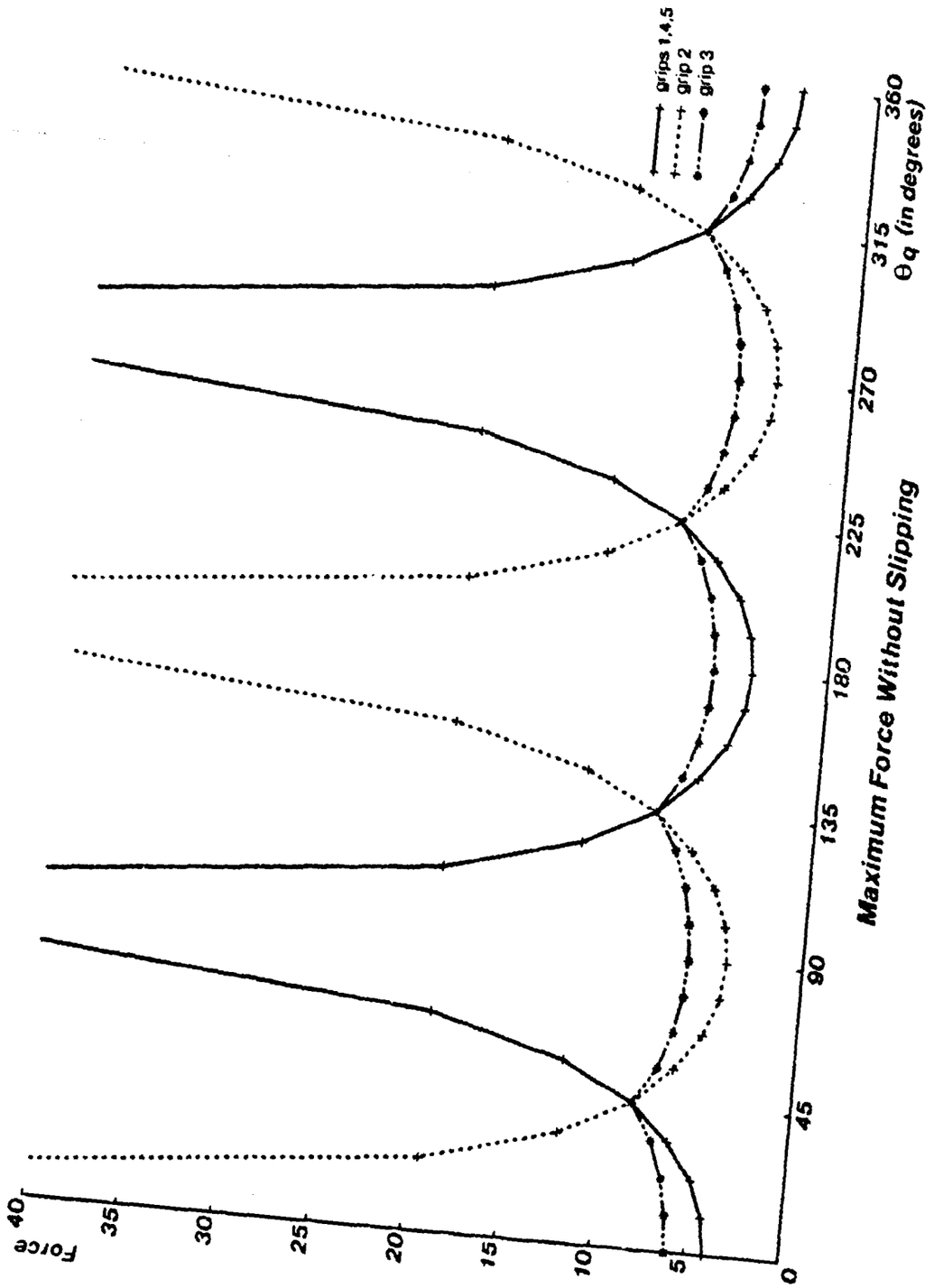

Figure 2-5: Maximum force without slipping at angle θ_q

The highest rotational stiffness is achieved either with grip 1 or grip 2, depending on whether k_{ni} or k_{li} is greater. If it is most important that none of the fingers slip when a moment is applied to the rectangle, then grips 1, 4 or 5 should be chosen. Grip 1 offers the best combination of rotational stiffness and resistance to slipping.

For translations the picture is a bit more complicated since the stiffness and the resistance to slipping vary as the direction of q varies. Intuitively, one might suggest that Grip 3 is the safest choice. Figures 2-4 and 2-5 show plots of the stiffness and the maximum force without slipping as a function of angle, θ_q. For these plots, k_{ni} was arbitrarily taken twice as large as k_{li}. Actual values of k_{ni} and k_{li} might be quite different, but the plots provide an example of how grip stiffness varies as a function grip geometry. In this case, the stiffness of grip 3 is constant, regardless of the direction of f_e. Grip 3 also offers the most nearly constant resistance to slipping and is therefore the safest choice for arbitrary loads, although other grips offer more stiffness or resistance to slipping when the object is pulled in a single direction.

2.4.2 An unstable example

The foregoing discussion has focused on determining whether the stiffness of a grip is suitable and on determining when the fingers slip. The next question is whether the grasp will be stable if perturbed slightly. A potentially unstable grip is shown in Figure 2-6. If the grasp forces are large, and if the fingers are not stiff enough in the lateral direction, the rectangle will continue to rotate when disturbed by a small angle, $\delta\theta$, instead of returning to the initial position. The same effect can be seen by gripping a coin on edge between two opposed fingers. If one squeezes too hard, the coin "collapses" to a more stable position in which one's fingers are pressing against the faces. In general the coin will also slip with respect to the fingers when this occurs, but before slipping occurs it is possible to determine whether the grip is stable.

As the rectangle in Figure 2-6 is rotated by a small angle, $\delta\theta$, the lateral stiffnesses of the two fingers produce a restoring torque, $f_{\theta r}$

$$f_{\theta r} = 2k_l r^2 \delta\theta$$

At the same time, due to the rotation of the body, a torque is generated by the grasp forces,

$$f_{\theta g} = 2f_n r \delta\theta$$

The net change in the torque upon the object is

$$\delta m_e = (f_n - k_l r)2r\delta\theta$$

The grip is unstable if the change in the torque is positive for a positive rotation, $\delta\theta$. Thus, for the grip to be infinitesimally stable it is required that $f_n < k_l r$. Evidently, for a given rectangle size and finger stiffness, pressing harder makes the grip less stable. This result appears again in later examples and provides an incentive for not gripping harder than necessary because for a given grip geometry, the stability of the grip *decreases* with increased gripping force. Another result is that for a given finger stiffness and gripping force, the grip is more stable for a longer rectangle (one for which r is large).

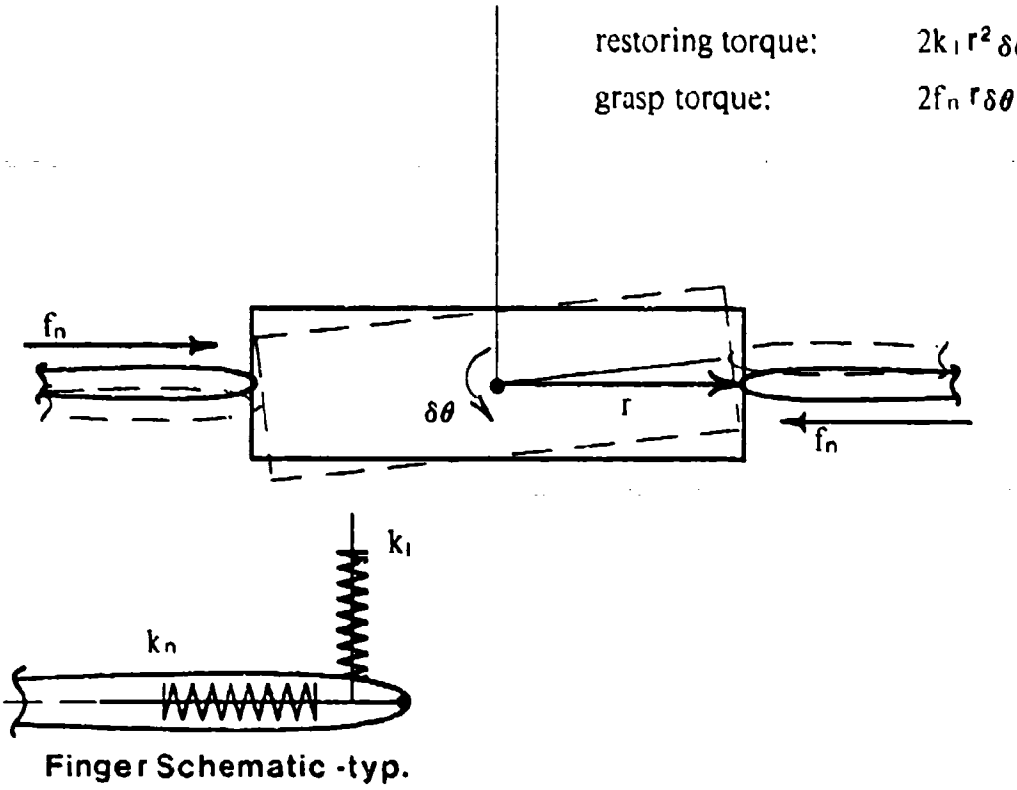

Figure 2-6: Instability of a rectangle held by two fingers

These effects can be demonstrated by pressing a pencil lengthwise between the index fingers of each hand. As one presses harder the grip is likely to collapse unless one also tenses (stiffens) one's arm and finger muscles. If the experiment is repeated for an old, short pencil and for a new, long one it will be seen that the grip collapses more easily for the short one.

Unfortunately, if we return to the example of gripping a coin between two fingers of one hand, a problem appears. If the fingers are now pressing against the faces of the coin instead of the edges, the grip should, according to the above equation, become *less* stable. This is clearly incorrect and demonstrates that the point-contact fingertip model gives inaccurate results for human fingers pressing against the faces of a coin. If we repeat the example, using ball-point pens instead of our fingers to press against the faces of the coin, we find that the grip is indeed very unstable. The problem is resolved if we model the finite curvature and deformation of our fingertips. Thus, in the following sections, a framework is established in which examples like those above can be extended to three dimensions and in which fingers with pointed, curved and soft contacts are considered.

Nomenclature for Three-Dimensional Analysis

o	= origin of (x,y,z) system
bp	= origin of (l,m,n) system and contact point on object
fp	= contact point on fingertip
f	= origin of (a,b,c) system
r_b	= 3x1 vector from (x,y,z) origin to (l,m,n) origin
r_f	= 3x1 vector from (a,b,c) origin to (l,m,n) origin
d_b	= vector of small translations and rotations of the object in (x,y,z) coordinates
d_{bp}	= vector of small translations and rotations of the object in (l,m,n) coordinates
d_c	= vector of displacements transmitted through the contact
d_{fp}	= vector of small finger translations and rotations in (l,m,n) coordinates
d_f	= vector of small finger translations and rotations in (a,b,c) coordinates
d_q	= vector of small finger translations and rotations in joint coordinates
g_b	= vector of forces and torques on the object in (x,y,z) coordinates
g_{bp}	= vector of forces and torques on the object in (l,m,n) coordinates
g_c	= vector of forces transmitted through the contact
g_{fp}	= vector of finger forces and torques in (l,m,n) coordinates
g_f	= vector of finger forces and torques in (a,b,c) coordinates
g_q	= vector of finger forces and torques in joint coordinates
[Jb]	= 6x6 jacobian relating d_b to d_{bp}
[Jf]	= 6x6 jacobian relating d_f to d_{fp}
[Jq]	= nfx6 jacobian relating d_q to d_f
[Jfq]	= nfx6 product of [Jf] and [Jq]
[P]	= partition of [Jfq]
[P*]	= non-singular partition of [Jfq]
[G]	= 9x9 grasp jacobian for three fingers
[Kq]	= stiffness matrix of a finger in joint coordinates
[Kf]	= stiffness matrix of a fingertip for three-fingered hand
[Kx]	= [Kf] rotated to world coordinates
[Kb]	= stiffness matrix of the grasp
[Cf]	= compliance matrix for finger and fingertip
[A]	= 3x3 orthonormal rotation matrix
[R]	= 3x3 skew-symmetric matrix for r
[I]	= the identity matrix
[M]	= matrix of contact degrees of freedom
[L]	= square matrix assembled from [P] and [Kq]
l	= vector of Langrange multipliers for [L]
λ_i	= i^{th} Langrange multiplier

$\mathbf{q}_f$ = set of nf independent elements in $\mathbf{d}_{fp}$

$\mathbf{u}_f$ = 3x1 unit tangent vector on fingertip

$\mathbf{u}_b$ = 3x1 unit tangent vector on object

nf = number of degrees of freedom of finger

nc = number of force or displacement components transmitted through contact

s = arclength along fingertip or object surface

r_c = magnitude of radius of curvature of fingertip

r_o = outer radius of contact area

E = modulus of elasticity

G = shear modulus

A = contact area

I_{ij} = ij moment or product of inertia

I_p = polar moment of inertia

σ_{ii} = stress in ii direction

τ_{ij} = ij shear stress

k = scalar stiffness component

f = scalar force component

w = width

t = thickness

3. Extension to Three-Dimensional Problems

3.1 Forward Force and Displacement Relations

In the general case, the gripper fingers and the object may have up to three translational and three rotational degrees of freedom. It becomes convenient to use matrix equations to express the grip stiffness, strength and stability. In the following discussion, force vectors, g or f, include force and moment components and displacement vectors, d, include small translation and rotation components:

$$f^t = [f_x,\ f_y,\ f_z,\ f_{\theta x},\ f_{\theta y},\ f_{\theta z}]$$

$$d^t = [d_x,\ d_y,\ d_z,\ d_{\theta x},\ d_{\theta y},\ d_{\theta z}]$$

The goal of this analysis is to express the interaction between grasping forces and small motions of the object. If g_b is the resultant grasp force on the object and d_b is a vector of small motions of the object then the desire is to determine

$$\frac{\partial g_b}{\partial d_b} = ?$$

Since d_b is a small quantity this may be approximated by the linear relationship

$$\Delta g_b = [?]\, d_b$$

where [?] is a matrix that must be determined. To do this it is necessary to first establish how the forces applied by the fingers, g_f, determine the grasp force, g_b, and to establish the relationship between a small motion of the object, d_b, and the resulting motions of the fingers, d_f. If g_b and d_b were scalars, δf and δx, the relationship between them could be written

$$\frac{\partial f}{\partial x} = k \quad \text{or} \quad \delta f \approx k\,\delta x$$

Under certain circumstances, for example if the fingers do not move relative to the object when the object moves slightly, an equivalent stiffness expression can be written for forces and displacements of the object

$$g_b = [Kb]\, d_b$$

where [Kb] is a symmetric stiffness matrix. More commonly, the fingertips and the contact areas will shift with respect to the grasped object as it moves and new terms are added to the above stiffness relationship. Such terms are discussed later in this section.

In Figure 3-1, the coordinate systems are shown for a fingertip touching an object. The fingertip may be the last segment of a multijointed finger or it may be a contact surface on the jaw of an industrial gripper. The global coordinate system, (x,y,z), is embedded in the object at o. The (a,b,c) coordinate system is embedded in the fingertip at f and, like the (x,y,z) system, may be chosen with any convenient position and orientation. The (l,m,n) coordinate system is shared by the fingertip contact area, fp, and the object contact area, bp. The n axis is perpendicular to both the object and fingertip surfaces and the l,m axes lie in the

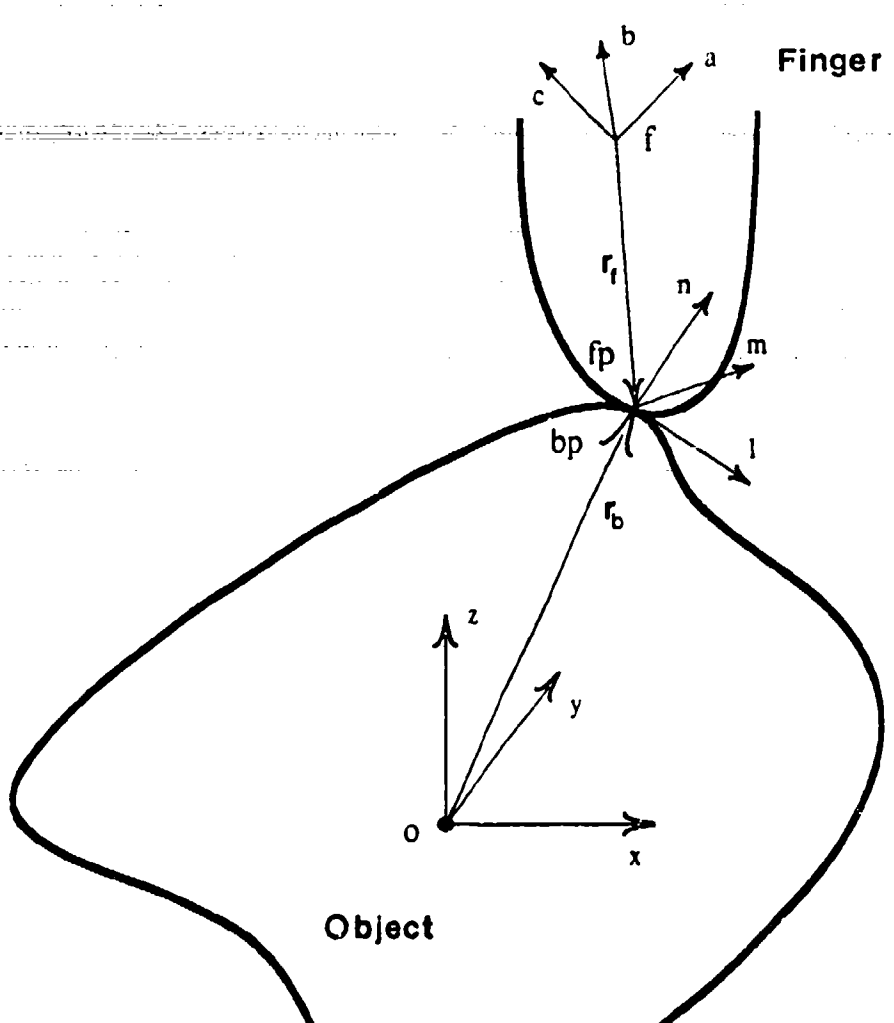

Figure 3-1: Coordinate systems for a finger touching an object

common tangent plane. The finger joint coordinates are not shown in Figure 3-1 since they will be different for each finger design.

It is assumed that the position and orientation of the (a,b,c) coordinate system can be determined with respect to (x,y,z) from the geometry of the gripper and knowledge about the initial position and orientation of the object. Salisbury [2] has shown that the position and orientation of the tip of a multijointed finger may be established in the same way that the position and orientation of the end link of a manipulator are determined from the joint angles. The result is often expressed as a 4x4 transformation matrix, [T], [16]. The elements of [T] are given in Appendix A.

Usually, the fingertip will have less than 6 degrees of freedom and the compliance of the fingertip will be

negligible in one or more directions. For example, a finger with $nf < 6$ joints is often considered to have nf degrees of freedom since the structural compliance of the finger links is negligible in comparison to the compliance of the servoed joints. In this case, the displacement vector of the finger in joint coordinates, $\mathbf{d_q}$, will be an nfx1 vector.

The fingertip is also assumed to have known stiffness properties, represented by the nfxnf stiffness matrix $[\mathbf{Kq}]$ in joint coordinates. Salisbury [2] has shown that the stiffness matrix for the tip of a multi-jointed finger, valid for small motions, may be derived from the finger kinematics and joint servo gains.

Frequently, the fingertip may be treated as a rigid body so that small displacements of the finger in joint coordinates may be related to displacements in the (a,b,c), which in turn, may be related to displacements in the (l,m,n) system with the linear transformations:

$$\mathbf{d_f} = [\mathbf{Jq}]\,\mathbf{d_q} \quad \text{(where } [\mathbf{Jq}] = \frac{\partial \mathbf{d_f}}{\partial \mathbf{d_q}} \text{ defines a Jacobian)} \tag{3.1}$$

$$\mathbf{d_{fp}} = [\mathbf{Jf}]\,\mathbf{d_f} \tag{3.2}$$

$$\mathbf{d_{fp}} = [\mathbf{Jfq}]\,\mathbf{d_q} \quad \text{where} \quad \underset{(nf\text{x}6)}{[\mathbf{Jfq}]} = \underset{(6\text{x}6)}{[\mathbf{Jf}]}\,\underset{(nf\text{x}6)}{[\mathbf{Jq}]} \tag{3.3}$$

The fingertip displacement vector, $\mathbf{d_{fp}}$, will contain 6 elements of which nf will be linearly independent. A set of nf linearly independent elements within $\mathbf{d_{fp}}$ is called $\mathbf{q_f}$.

The object is treated as a rigid body and consequently, a small motion, $\mathbf{d_b}$, of the object in the (x,y,z) system produces a displacement of the contact area, $\mathbf{d_{bp}}$, in the (l,m,n) system.

$$\mathbf{d_{bp}} = [\mathbf{Jb}]\,\mathbf{d_b} \tag{3.4}$$

For generality, $\mathbf{d_b}$ and $\mathbf{d_{bp}}$ are taken as 6 element vectors (possibly with some zero elements). A number of identities for 6x6 Jacobians are given in Appendix A.

It can be shown [16], by equating virtual work, that small displacements and forces transform in a complementary way. If the grasping force, $\mathbf{g_{fp}}$, at the fingertip contact area is known then the equivalent force in the (a,b,c) system is found by equating the work done in displacing the fingertip by $\mathbf{d_{fp}}$ and the finger by $\mathbf{d_f}$.

$$\mathbf{d_{fp}}^t \cdot \mathbf{g_{fp}} = \mathbf{d_f}^t \cdot \mathbf{g_f}$$

Then, substituting from equation (3.2),

$$\mathbf{d_f}^t \cdot \mathbf{g_f} = \mathbf{d_f}^t\,[\mathbf{Jf}]^t\,\mathbf{g_{fp}} \quad \text{or} \quad \mathbf{g_f} = [\mathbf{Jf}]^t\,\mathbf{g_{fp}} \tag{3.5}$$

Similarly,

$$g_q = [Jq]^t g_f \tag{3.6}$$

and

$$g_b = [Jb]^t g_{bp}. \tag{3.7}$$

3.2 Summary of Forward Transformations

The forward displacement and force transformations are summarized in Figure 3-2.

Starting at the lower left corner with a displacement, d_b, of the object in (x,y,z) coordinates, and following the arrows, the displacements transmitted through the contact are determined as d_c. Then, starting with the contact forces, g_c, on the object in (l,m,n) coordinates, and following the arrows, one computes the forces upon the object

Starting at the lower right corner with displacements of the finger joints, d_q, the displacement of the fingertip, d_{fp} ca be determined. Finally, if the contact forces, g_{fp}, are known for the finger, following the arrows gives the forces in the finger joints, g_q.

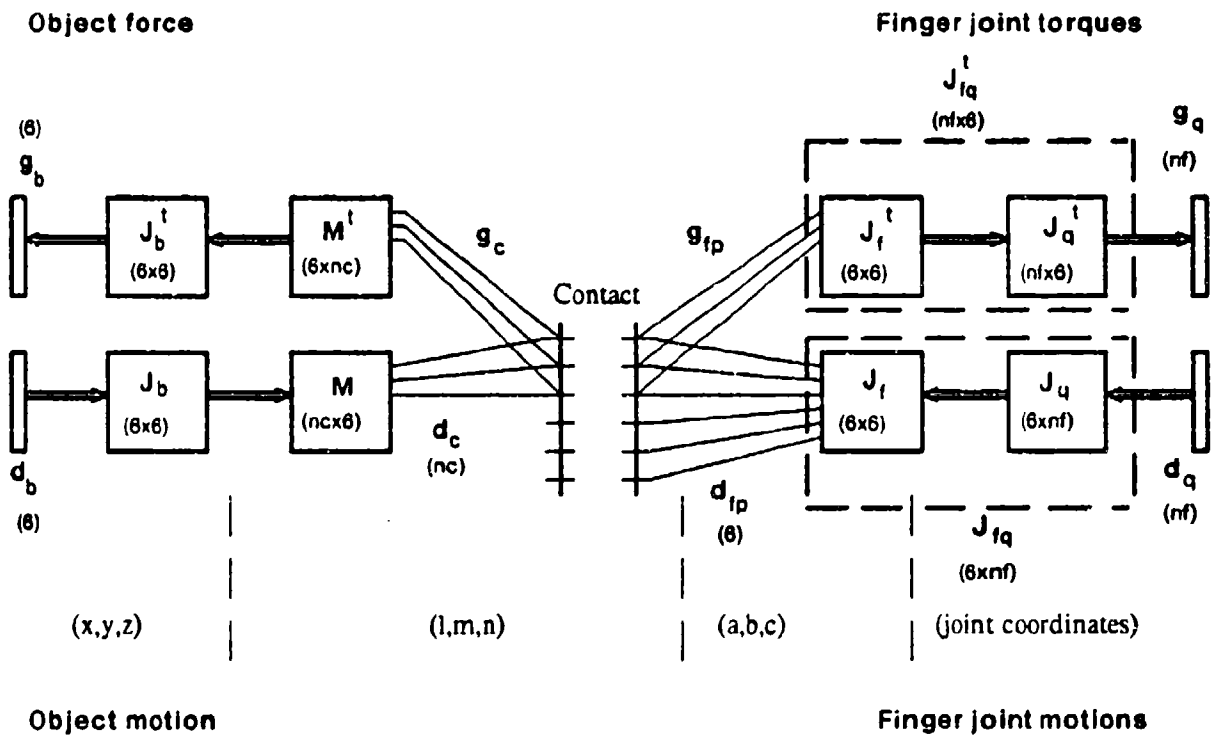

Figure 3-2: Flow chart for forward force and displacement transformations

The forward *displacement* relations provide transformations starting with the object or the finger and working towards the common contact. The forward *force* relations start with the contact and work outward toward the object or the finger. Unfortunately, these relations are not sufficient to complete steps 2 and 3 of the procedure outlined in Section 2.3. Once d_c has been determined, an *inverse* relationship giving d_q in terms of d_c must be used. The solution depends on the type of contact and the number of degrees of freedom of the finger, and is discussed in Section 3.3. Once d_q has been determined, another inverse relation is required to determine the change in g_{fp}. This solution also depends on the contact and the finger, and is discussed in Section 3.4. A forward force transformation can then be used to determine the change in g_b from the change in g_{fp}.

3.3 Finger Motions and Constraints

The mobility of an object represents the number of degrees of freedom with which the object can make arbitrary motions. The mobility is subject to constraints imposed at each contact point which may prevent motions in certain directions and couple the motions of the object in others. Generally, the mobility of the object decreases as the number of contact points increases.

The determination of mobility involves first finding the constraints imposed at each contact point and then determining how the different contacts interact to limit the mobility of the object. In this section, the emphasis is on characterizing the constraints and contact conditions for a single contact so that various fingertips may be compared.

Once the constraints at each finger have been identified, the way in which they combine to constrain an object is discussed in previous analyses [2, 7]. For such an analysis it is convenient to adopt the terminology of *wrenches* and *twists* in which the magnitudes of the components of the force and displacement vectors, g_{bp} and d_{bp}, are considered separately from their directions. The number of degrees of freedom of the object depends on the *intersection* over all contacts of the degrees of freedom from each [7]. The number of independent forces that may be applied to the object by the hand increases as the *union* over all contacts of the forces that each can apply. When more than one contact can apply forces in the same directions, it becomes possible to specify internal forces on the object [2, 7]. These may be set to ensure that all fingers remain in contact with the object.

3.3.1 Constraints at a Contact

At each contact point, the constraints depend on how many degrees of freedom are transmitted through the contact and on how many degrees of freedom the finger has. Basically, there are three categories. In the first case a motion of the object *exactly determines* the motion of the finger (this is the simplest case, in which a part of $[J_{fq}]$ is simply inverted for the inverse displacement and force relations). In the second case the motion of the finger is *under determined* and in the third case the motion of the finger is *over determined.*

Forces and motions at the fingertip-object contact area are transmitted through a coupling matrix, $[M]$.

The elements of [M] depend on the contact geometry (*see* Figure 4-1) and friction conditions. These are discussed further in Section 4. If there is complete coupling in six degrees of freedom between the object and the fingertip (as in the case of a soft, sticky finger adhering to the object) [M] becomes a 6x6 identity matrix. The elements of d_{fp} that are transmitted to the finger form the vector d_c and the elements of the grasp force, g_{fp}, that are transmitted to the object form the vector g_c which has *nc* components.

$$d_c = [M]d_{bp} \qquad g_c = [M]^t g_{fp} \tag{3.8}$$

The contact constraints are found by comparing the elements of d_c with the independent members of d_{fp}. As mentioned in the last section, *nf* elements of d_{fp} will usually be linearly independent for a finger with *nf* joints. A set of *nf* independent elements within d_{fp} is called q_f and, for the purposes of describing the contact constraint, there are three conditions:

1. A set of independent elements in d_{fp} can be found such that $d_c = q_f$ and $nc = nf$. In this case arbitrary motions of the object at *bp* are possible and the motion of the fingertip is completely determined. Similarly, the joint torques of the finger completely determine the set of forces, g_c, that can be transmitted through the contact to the object.

2. A set of independent elements in d_{fp} can be found such that $d_c \subset q_f$. If d_c is a subset of q_f, arbitrary motions of the object at *bp* are possible but the finger motion is not completely determined. The remaining undetermined elements of d_{fp} or d_q may be solved for by requiring that the finger move so as to minimize its potential energy.

3. $d_c \not\subset q_f$. If d_c contains elements that are not included in q_f, the finger and contact limit the possible motions of the object. At the same time, it is possible that $q_f \not\subset d_c$, in which case a (constrained) motion of the object does not completely determine d_{fp}. If this happens, the undetermined elements of d_{fp} must be determined as above.

Methods for solving for the motions of the finger are discussed below for each of the above situations. In each case, a submatrix, [P], is extracted from [Jfq] that relates the *nc* elements of d_c to the *nf* elements of d_q: $d_c = [P]d_q$. The three cases are identified by evaluating the rank of [P].

3.3.1.1 Case 1: exactly determined

An example for which $d_c = q_f$ and $nc = nf$ is a finger with three joints, constructed so that the fingertip can move in three directions, always touching the object at a single point fixed on the object surface. This is mathematically the most convenient situation and forms the basis of previous investigations on grip stiffness [2]. The matrix, [P], that is extracted from [Jfq] will be square and non-singular. The relations are:

$$\text{rank}([P]) = nf = nc$$

$$d_q = [P]^{-1}d_c \tag{3.9}$$

3.3.1.2 Case 2: under determined

When $\mathbf{d}_c \subset q_f$, the submatrix, [P], that relates the *nc* members of $\mathbf{d}_c$ to the *nf* joint variables, $\mathbf{d}_q$, will have rank *nc*. The motion of the fingertip will minimize the potential energy of the finger, subject to the *nc* constraint conditions that make up the rows of [P]. The change in the potential energy of the finger may be expressed as

$$\Delta P.E. = \mathbf{g}_q{}^t\mathbf{d}_q + \tfrac{1}{2}(\mathbf{d}_q{}^t[\mathbf{Kq}]\mathbf{d}_q) \tag{3.10}$$

in which first term is due to work done against the grasping joint torques and the second is due to the stiffnesses of the finger joints. The second term is what provides the grasp stiffness discussed in previous investigations [2, 5], but the first term may be of comparable magnitude.

To minimize the potential energy, the magnitude of the above expression must be at a maximum. If the elements of $\mathbf{d}_q$ were all independent (*i.e.* if there were no coupling between $\mathbf{d}_c$ and $\mathbf{d}_q$) then the maximum would be found by taking the partial derivative of the above equation with respect to each member of $\mathbf{d}_q$ and setting the resulting expressions equal to zero. In the present case, a flexible and systematic approach is to use Lagrange multipliers. The resulting equation is conveniently expressed as

$$\begin{bmatrix} \mathbf{d}_q \\ \hline \boldsymbol{l} \end{bmatrix} = [\mathbf{L}]^{-1} \begin{bmatrix} \mathbf{g}_q \\ \hline \mathbf{d}_c \end{bmatrix}$$

where [L] can be assembled from [P] and [kq] and $\boldsymbol{l}$ is a vector of Langrange multipliers. Details are given in Appendix A.1.

Once all the members of $\mathbf{d}_q$ have been found, the motion of the finger in (l,m,n) coordinates is found using $\mathbf{d}_{fp} = [\mathbf{Jfq}]\mathbf{d}_q$. The restoring forces in the joints are given by $\Delta\mathbf{g}_q = [\mathbf{Kq}]\mathbf{d}_q$. Since [P] is not square, $[\mathbf{P}]^{-t}$ cannot be used as in Case 1 to determine the changes in the forces at the fingertip, $\delta\mathbf{g}_{fp}$. However, since $\mathbf{d}_c \subset q_f$ and since $\mathbf{d}_q$ have been determined subject to the constraints of [P], some columns may be removed from [P] so as to leave a square matrix, $[\mathbf{P}^*]$ relating $\mathbf{d}_c$ to *nc* of the *nf* elements in $\mathbf{d}_q$.

3.3.1.3 Case 3: over determined

When $\mathbf{d}_c \not\subset q_f$ the elements of $\mathbf{d}_c$ become coupled and the object is constrained by the finger and contact. The submatrix, [P], will have a rank of less than *nc*. In this case, rows of [P] corresponding to particular elements of $\mathbf{d}_c$ may be eliminated to produce a smaller matrix, $[\mathbf{P}^*]$ that has the same rank as [P]. The elements of $\mathbf{d}_c$ corresponding to $[\mathbf{P}^*]$ form the vector, $\mathbf{d}_c^*$. If the new submatrix, $[\mathbf{P}^*]$ has rank *nf* then it may be inverted as in Case 1 to determine $\mathbf{d}_q$ from $\mathbf{d}_c^*$. All the elements of $\mathbf{d}_{fp}$ can then be recovered as $[\mathbf{Jfq}]\mathbf{d}_q$. Thus, the kinematic coupling between the elements of $\mathbf{d}_{fp}$ is defined.

If the rank of [P] is less than *nf* then the motion of the finger is not completely determined and potential energy methods must be used as in Case 2 to determine $\mathbf{d}_q$ from $\mathbf{d}_c^*$. Again, the complete motion of the fingertip is recovered from $[\mathbf{Jfq}]\mathbf{d}_q$.

The general method for determining the motions of a finger from the motions of the contact is illustrated in the left hand portion of Figure 3-4. For the particular case in which [P] is invertible, the method is summarized in Figure 3-3.

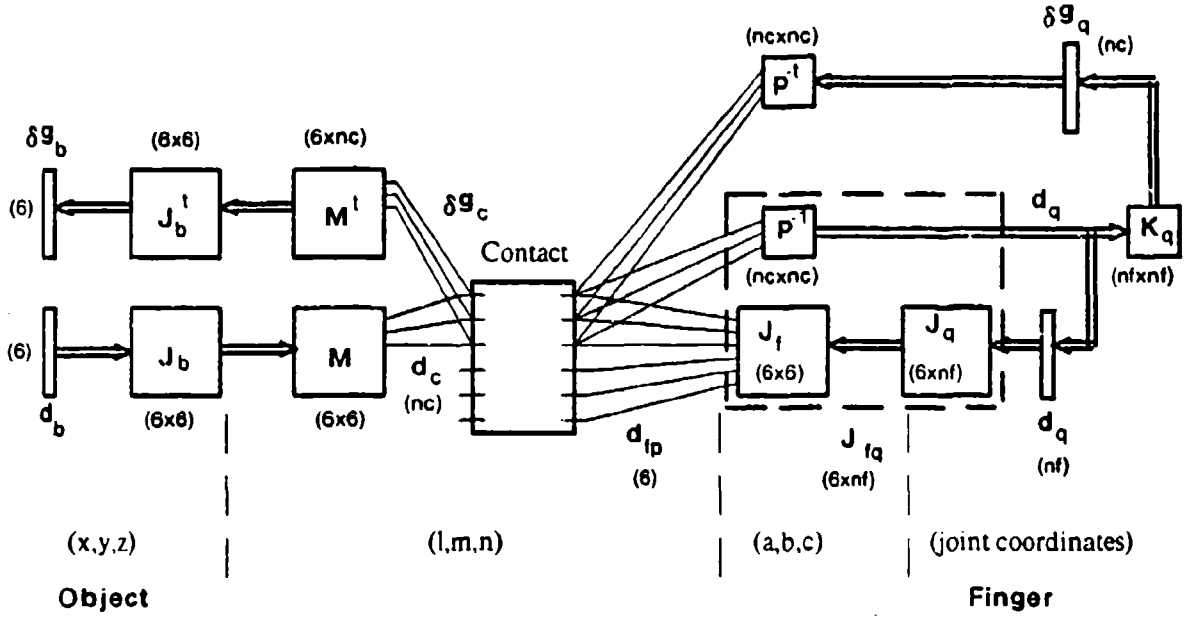

Figure 3-3: Flow chart for cases in which [P] is invertible (Case 1)

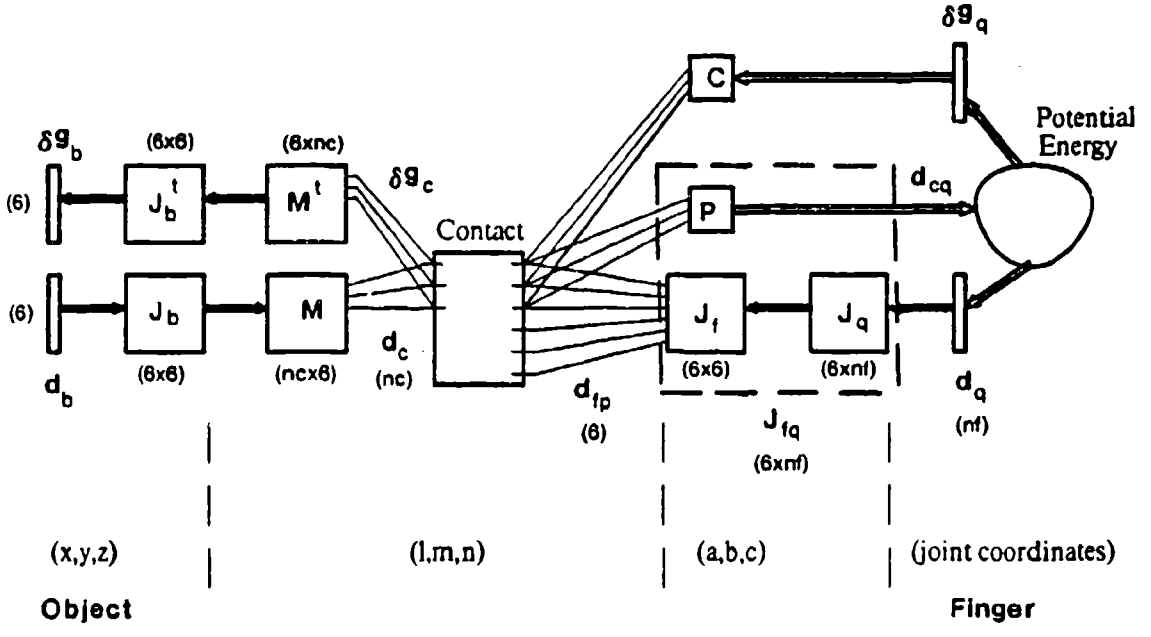

Figure 3-4: Flow chart for relationships between displacements and forces (Case 2 or 3)

3.4 Computing Changes in Grip Force

As mentioned in Section 2, the changes in the grip forces will be due to two effects. The first consists of the restoring forces in the finger joints produced by displacing the fingers. The second stems from relative motion between the object and the fingers which modifies the grasp geometry so that the grasp forces produce different forces and torques on the object.

The change in grip geometry can be broken into two parts. The first is due to the contact area shifting upon the object and the second is due to relative motion between the finger and the object. For the first part, recalling that the forces upon the object, g_b, are given in terms of g_{fp} by equations (3.7) and (3.8), the total change in the forces upon the object becomes

$$\Delta g_b = \Delta([Jb]^t[M]^t g_{fp}) = \Delta([Jb]^t[M]^t) g_{fp} + [Jb]^t[M]^t \Delta g_{fp}.$$

The change in the product of the jacobians above may be expanded to give terms involving $\Delta[Jb]^t$ and $\Delta[M]^t$.

$\Delta[Jb]^t$ will be zero if the contact area does not move with respect to the object when the object is displaced by d_b. This is true for point contacts and for contacts in which a very soft finger adheres to the surface. For curved finger/object contact surfaces, the contact area usually moves on the surface of the object due to rolling of the finger and $\Delta[Jb]^t$ cannot be ignored.

$\Delta[M]^t$ will be zero provided that the coupling between the finger and the object does not change. This is true for many contact geometries, although there are a few exceptions, such as a flat-ended finger touching a flat surface on the object. If the flat finger rocks slightly with respect to the object, the contact changes from a line contact to a point contact or from a planar contact to a line contact. When this happens the number of components of force and motion transmitted between the fingertip and the object is reduced and some additional elements of $[M]^t$ become zero. Such transitions, however, are not smooth and continuous and cannot be represented by a matrix $\Delta[M]^t$. In the following analysis it will be assumed that that $\Delta[M]^t$ is zero. The case of a flat-tipped finger on a flat object can be regarded as a limiting case in which the radii of curvature of the fingertip and object approach infinity.

The expression for Δg_b is now given by

$$\Delta g_b = \Delta[Jb]^t [M]^t g_{fp} + [Jb]^t[M]^t \Delta g_{fp}.$$

In Appendix A.2, a method is given for determining the elements of $\Delta[Jb]$ for a given translation and rotation of the contact area with respect to the object.

Next, it is necessary to determine the change in g_{fp}. This will be due partly to the relative motion of the finger with respect to the (l,m,n) coordinate system and partly to the restoring forces in the finger joints.

The motion of the fingertip is d_{fp}, where d_{fp} is determined by the methods of Section 3.3. The motion of

the (l,m,n) coordinate system is given by d_{bp} and therefore the relative motion is $(d_{fp} - d_{bp})$. The resulting 6-element vector is used to determine the elements of $\Delta[Jf]^{-t}$ in the same way that the motion of the contact point on the object determines the elements of $[Jb]^t$. There may also be a contribution to Δg_{fp} due to relative motion between the (a,b,c) coordinate system and the joint space in which d_q is defined. However, this will depend on the particular finger design and is not considered in the current analysis.

The restoring forces in the finger joints are given by

$$\Delta g_q = [Kq]d_q$$

where d_q is found using the methods in Sections 3.1 and 3.3. The contribution of these restoring forces to Δg_{fp} may be computed for each of the constraint cases discussed in Section 3.3.

For the first case in Section 3.3, in which the motion of the object exactly determines the motion of the finger, the contribution of Δg_q to Δg_{fp} follows from equation (3.9).

$$\Delta g_{fp} = [P]^{-t}\Delta g_q \tag{3.11}$$

For the second case, the contribution of the restoring forces in the joints to the change in the forces at the fingertip is $[P^*]^{-t}\Delta g_q^*$. It does not matter which columns are removed from $[P]$ provided that the remaining square matrix, $[P^*]$, is non-singular and that the elements of g_q corresponding to the eliminated rows of $[P]$ are removed from g_q^*.

For the third case the problem is statically indeterminate and there are not enough equations for the number of unknowns. If no motion is possible in one of the directions of the (l,m,n) coordinate system, the change in force for that direction may reasonably be set to zero. This is equivalent to removing null rows and columns from the compliance matrix in (l,m,n) coordinates. If the remaining compliance matrix is still singular or in other words, if there are remaining non-zero (but coupled) motions in d_{fp} then a useful technique is to add "virtual joints" to the finger to provide enough equations. The virtual joints can be chosen in directions orthogonal to the existing joints. The motion about their axes is zero and consequently, the change in the torques about their axes will also be zero.

For the particular case in which fingers with three degrees of freedom are used to hold an object, with point contact between the fingertips and the object, the relations above reduce to

$$d_q = [P]^{-1}[M][Jb]d_b$$

$$\Delta[Jb]^t = [0]$$

$$\Delta g_b = [Jb]^t[M]^t(\Delta[Jf]^{-t}g_f + [P]^{-t}g_q)$$

If, in addition, it can be assumed that $\Delta[Jf]^{-t}$ is negligible, the change in the force upon the body becomes

$$\Delta g_b = [Jb]^t[M]^t[P]^{-t}[Kq][P]^{-1}[M][Jb]d_b$$

or, letting $[P]^{-1}[M][Jb] = [J]$

$$\Delta g_b = [J]^t[Kq][J]d_b.$$

For a grip with m fingers, the net change in the grasping force becomes

$$\Delta g_b = \sum_{i=1}^{m} [J_i]^t[Kf_i][J_i]\, d_b$$

$$\text{or} \quad \Delta g_b = [Kb]d_b \tag{3.12}$$

Three Fingered Hand

For a hand with three fingers, each having three degrees of freedom and point contacts at the fingertips, Salisbury [2] derives an equivalent expression to (3.12). If the finger axes, (a,b,c) are chosen to parallel to (x,y,z) and their origin, f, is moved to the contact point, fp, then

$$\underset{(3x3)}{[P]^{-1}}\ \underset{(3x6)}{[M]}\ [Jb] \quad = \quad \underset{(3x6)}{[\ I\ |\ R^t\ ]} \quad = \quad [J] \tag{3.13}$$

where $[I]$ is a 3x3 identity matrix and $[R]$ is given in Appendix A. The jacobians, $[J]$, for each finger are assembled into a single grasp jacobian (*see* Figure 3-5). The 6x9 grasp jacobian is augmented by a 3x9 matrix that gives the dot products between the forces exerted by opposing fingers. These "pinch" terms are related to the magnitude of the internal forces on the object. The resulting 9x9 grasp matrix is $[G]^{-t}$. The fingertip displacements are concatenated into a single 9x1 vector d_f and the vector of resultant forces, with respect to equilibrium, on the object becomes $f_b = \Delta g_b$. The 3x3 finger stiffness matrices are also assembled into a single, block-diagonal 9x9 matrix, $[K]$.

$$[K] \quad = \quad \begin{bmatrix} Kf & | & \\ \hline & Kf & | \\ \hline & | & Kf \end{bmatrix}$$

The relationship between displacements of the fingers and the net restoring force upon the body, f_b, may then be expressed as

$$f_b = [G]^{-t}[K]d_f$$

and the stiffness of the object computed as

$$[Kb] = [G]^{-t}[Kf][G]^{-1}.$$

The relationship between the above expressions and equation (3.12) can be seen by dropping the "pinch" terms from $[G]$ and f_b, and by allowing an arbitrary number of fingers which have arbitrary orientations, $[A_i]$ with respect to the (x,y,z) system:

$$\begin{bmatrix} A & A & A & \cdots \\ \hline RA & RA & RA & \cdots \end{bmatrix} \begin{bmatrix} Kf & & & \\ \hline & Kf & & \\ \hline & & Kf & \\ \hline & & & \cdots \\ \hline & & & Kf \end{bmatrix} \begin{bmatrix} A^t & [RA]^t \\ \hline A^t & [RA]^t \\ \hline A^t & [RA]^t \\ \hline \cdots & \cdots \end{bmatrix}$$

Multiplying the partitioned matrices above gives

$$[Kb] = \begin{bmatrix} \sum_{i=1}^{m} [Kx_i] & \sum_{i=1}^{m} [Kx_i][R_i]^t \\ \sum_{i=1}^{m} [R_i][Kx_i] & \sum_{i=1}^{m} [R_i][Kx_i][R_i]^t \end{bmatrix}$$

(where $[Kx_i] = [A_i][Kf_i][A_i]^t$)

which is identical to (3.12), when $[J_i]$ are given by (3.13).

Grasp Jacobian for Three Fingers:

$$f_b = [G]^{-t} f_f = \left[\begin{array}{c|c|c} I & I & I \\ \hline R & R & R \\ \hline P & P & P \end{array}\right] \left[\begin{array}{c} f1 \\ \hline f2 \\ \hline f3 \end{array}\right]$$

or:

$$\left[\begin{array}{c} fx \\ fy \\ fz \\ \hline mx \\ my \\ mz \\ \hline p12 \\ p13 \\ p23 \end{array}\right] = \left[\begin{array}{ccc|ccc|ccc} 1 & 0 & 0 & 1 & 0 & 0 & 1 & 0 & 0 \\ 0 & 1 & 0 & 0 & 1 & 0 & 0 & 1 & 0 \\ 0 & 0 & 1 & 0 & 0 & 1 & 0 & 0 & 1 \\ \hline 0 & -rz & ry & 0 & -rz & ry & 0 & -rz & ry \\ rz & 0 & -rx & rz & 0 & -rx & rz & 0 & -rx \\ -ry & rx & 0 & -ry & rx & 0 & -ry & rx & 0 \\ \hline r12 & & & -r12 & & & 0 & 0 & 0 \\ r13 & & & 0 & 0 & 0 & & -r13 & \\ 0 & 0 & 0 & & r23 & & & -r23 & \end{array}\right] \left[\begin{array}{c} f1x \\ f1y \\ f1z \\ \hline f2x \\ f2y \\ f2z \\ \hline f3x \\ f3y \\ f3z \end{array}\right]$$

In the above:

$[R]$ are cross-product matrices such that if $r = (rx, ry, rz)$ are vectors from the origin of the global coordinate system to each of the finger contact points, and f are three-component force vectors then $[R]f = r \times f$.

$[P]$ are matrices formed of 3 element vectors rij which point from finger i to finger j. The products $[P]f$ produce three scalar internal forces, pij, which measure the "pinch" between fingers i and j.

Figure 3-5:
(from Salisbury [6])

4. A Closer Look at Contact Conditions

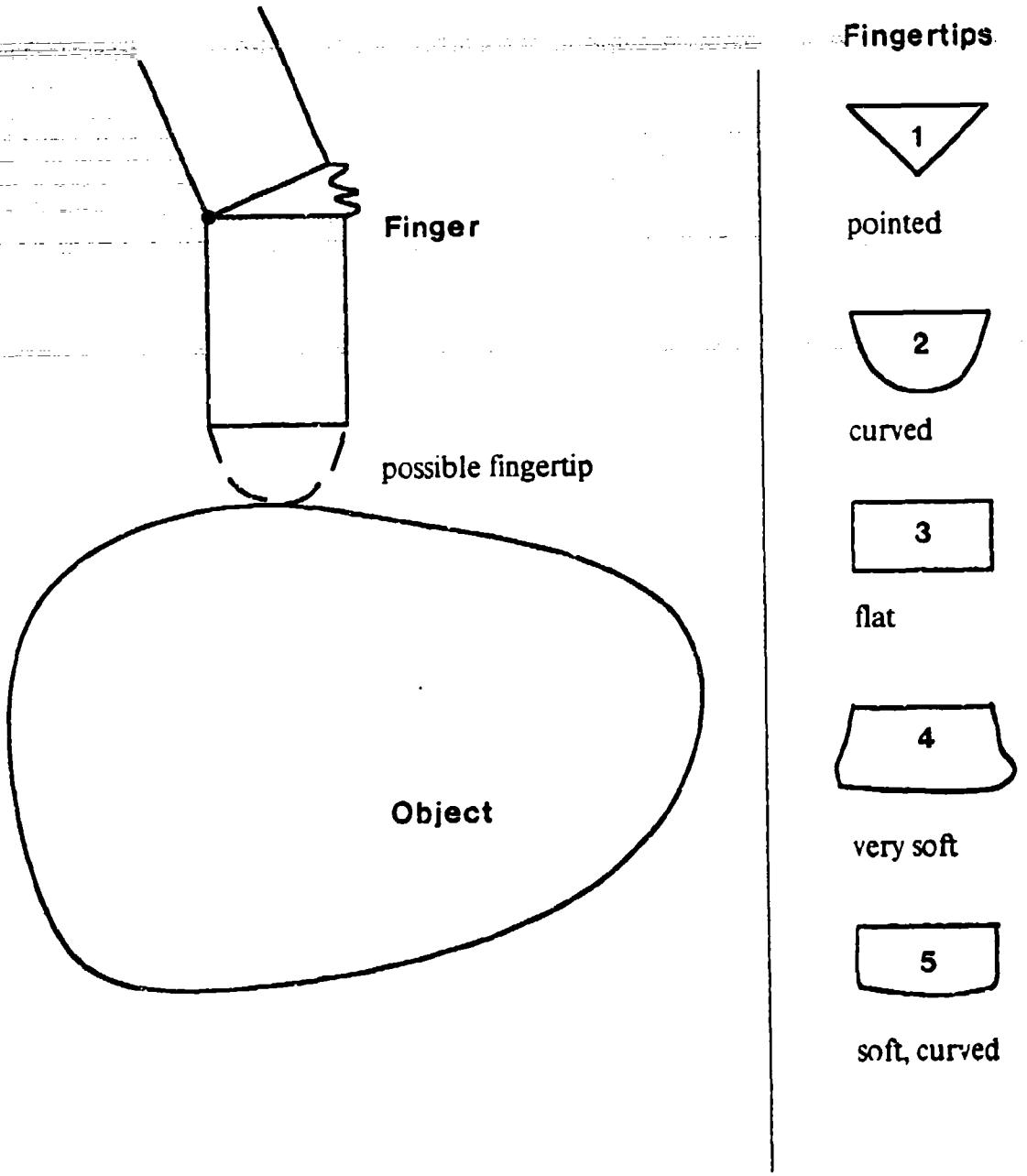

Figure 4-1: Examples of fingertip geometry

Contact conditions between the gripper and the object depend on friction, adhesion, surface geometry and surface deformation under load. The contact conditions have a profound effect on the strength and stability of a grip and determine the extent of kinematic coupling between the gripper fingertips and the object.

Previous analyses [1, 2, 3, 4, 6] have used the assumption of hard surfaces and small contact areas to treat

the contact areas as point contacts. This turns out to be the simplest case to handle analytically, but it becomes inaccurate when the radius of curvature of the fingertips is not small compared to the size of the object or when the fingertips deform. The effects of different assumptions concerning the fingertip geometry are shown in several examples below. In a later section, the effects of different friction models are discussed.

Models that may be used for the fingertip geometry include: point contacts, hard curved contacts, flat contacts, elastic curved contacts and very soft contacts. These models are shown schematically in Figure 4-1.

4.1 Point Contact

In a point contact with friction, forces are transmitted between the fingertip and the object but torques are not. Similarly, translation of the fingertip is coupled with that of the object, but rotation is not. The result is that the coupling matrix, $[M]$, is a 3x6 matrix in which the left partition is a 3x3 identity matrix and the right partition is zero.

In point contact, there is no rolling motion and consequently no movement of the contact area upon the object or the fingertip. As the object is displaced, the fingers can only rotate about the contact points. Consequently, there is no change in the jacobian $[Jb]^t$ and only a rotational change in $[Jf]^{-t}$ as the object is displaced.

4.2 Curved finger contact

A hard, curved finger is similar to a point contact in that the contact area is small so that forces may be transmitted, but torques may not. The main difference arises from the possibility of the fingertip rolling upon the surface of the object. As the finger rolls, the location of the contact point will shift. This shift produces non-zero terms in the differential jacobians, $\Delta[Jb]^t$ and $\Delta[Jf]^{-t}$ introduced in Section 3.4.

A general analysis of rolling becomes quite complex. As a first step, if we assume that the finger does not twist about its own axis, (perpendicular to the surface of the object) then for small displacements the problem can be approximated by a two-dimensional one involving an instantaneous plane of rolling. The plane is defined by the common perpendicular (n in Figure 3-1) and the vector of translational motion of the initial contact points, bp and fp. In the following discussion, second-order approximations are derived to express the translation and rotation of the contact points on the fingertip and the object as functions of the fingertip and object curvature.

Figure 4-2 shows the cross sections of a finger and an object in the instantaneous plane of rolling motion. The fingertip and the object profiles may be described parametrically as $r_{f(s)}$ and $r_{b(s)}$, where s is equal to the arclength along either curve. The conditions for pure rolling, without slipping or losing contact, are

1. There will be a common tangent plane at the points of contact.

2. The contact points on the fingertip and the object (fp and bp in Figure 3-1) must have the same

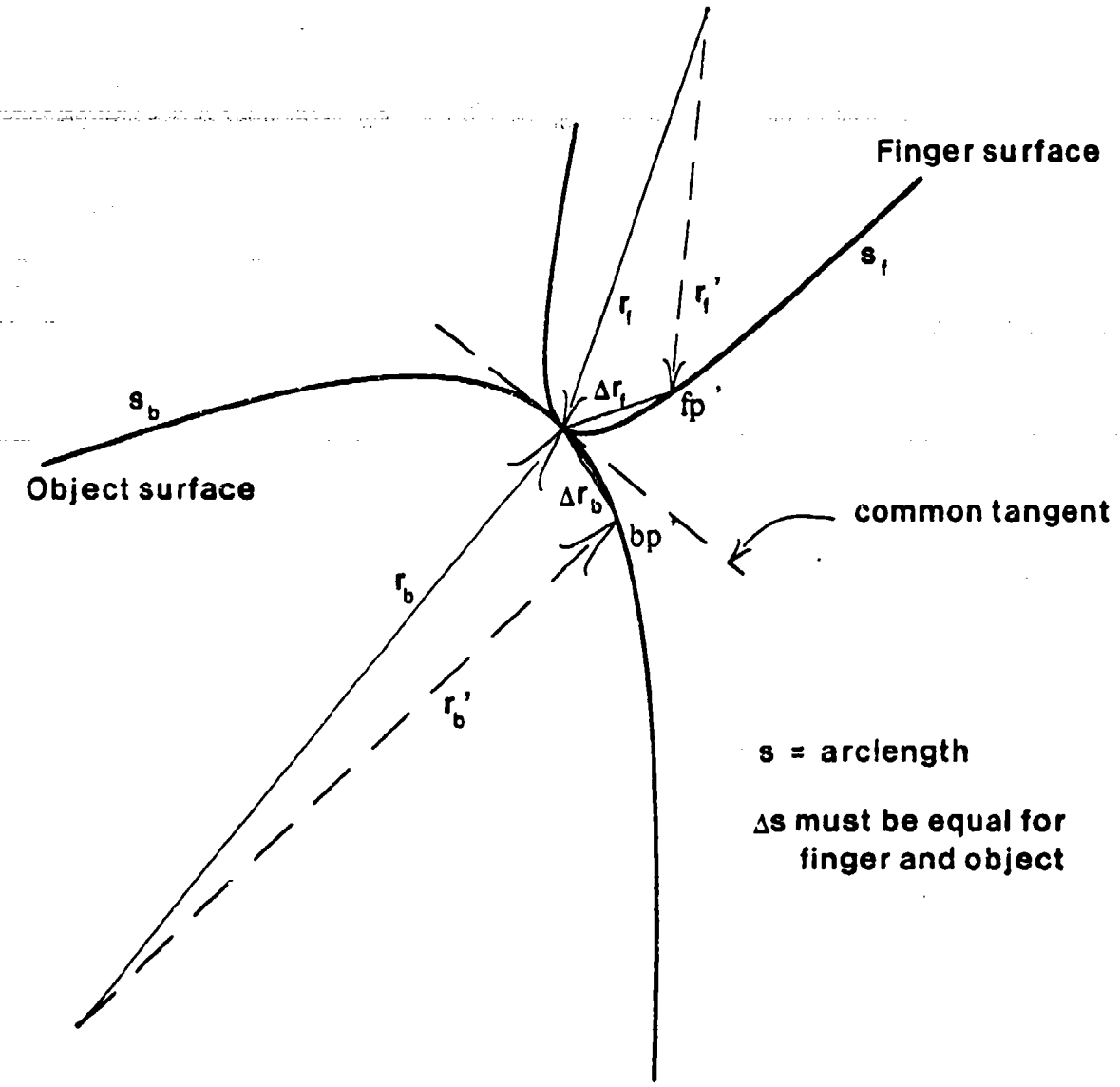

Figure 4-2: Rolling contact

translational velocity. For a differential motion this means that the translational components of d_{bp} and d_{fp} must be equal.

3. The arc length, δs, traversed along $r_{b(s)}$ and $r_{f(s)}$ must be equal as the fingertip rolls on the object.

The tangent at any point, s, along each curve in Figure 4-2 is given by the unit vector

$$u = \frac{dr}{ds}.$$

At the contact point, the tangent is the same for both curves so that

$$\frac{dr_f}{ds} = \frac{dr_b}{ds}.$$

After the fingertip rolls a small amount, the new contact point will be at the location r_b' on the body and the new tangent will have the direction

$$u' = \frac{dr_b'}{ds}.$$

The contact point on the fingertip will be at the location r_f' with respect to the finger coordinate system and the direction of the tangent will be

$$u_f' = \frac{dr_f'}{ds}.$$

For pure rolling it is required that $\delta s_f = \delta s_b$, where for small motions, $\delta s = \sqrt{\Delta r \cdot \Delta r}$. Thus for a small rolling motion, the contact point translates Δr_b upon the body and rotates through the angle between u_b and u_b'. At the same time, the fingertip must translate by $\Delta r_b - \Delta r_f$ (the distance between bp' and fp') and rotate through the angle between u_f' and u_b'. The translations and rotations are functions of $r_{f(s)}$, $r_{b(s)}$ and δs.

Δr and u' may be expressed as Taylor's series expansions in $r_{(s)}$ and δs (Appendix B). To look at the effects of curvature, terms involving the first and second derivatives of r_b and r_f are kept in the expansions.

translation of bp with respect to object:

$$\Delta r_b \approx \delta s \frac{dr_b}{ds} + \frac{(\delta s)^2}{2}\frac{d^2 r_b}{ds^2} = u\,\delta s + \frac{du_b}{ds}\frac{(\delta s)^2}{2} \tag{4.1}$$

translation of fp' with respect to object:

$$\Delta r_b - \Delta r_f \approx \frac{(\delta s)^2}{2}\left(\frac{d^2 r_b}{ds^2} - \frac{d^2 r_f}{ds^2}\right) \tag{4.2}$$

rotation of bp with respect to object:

$$u_b \times u_b' \approx \delta s\left(\frac{dr_b}{ds} \times \frac{d^2 r_b}{ds^2}\right) \tag{4.3}$$

rotation of fp' with respect to object:

$$u_f' \times u_b' \approx \delta s\left(\left(\frac{d^2 r_f}{ds^2} - \frac{d^2 r_b}{ds^2}\right) \times u\right) + (\delta s)^2\left(\frac{d^2 r_f}{ds^2} \times \frac{d^2 r_b}{ds^2}\right) \tag{4.4}$$

In (4.4) and (4.1), $u = u_{b(s)} = u_{f(s)}$.

For a given object shape, the fingertip curvature determines the magnitudes of the translation and rotation of bp and the translations of fp and fp', as the fingertip rolls through the small angle given by equation (4.4).

The above equations can be simplified by dropping second order terms. Since $|u| = 1$, equation (4.4) will be dominated by a term on the order of

$$\delta s\left(\frac{d^2 r_f}{ds^2} - \frac{d^2 r_b}{ds^2}\right).$$

The second term in (4.4) is at least a factor of δs smaller and, for infinitesimal motions, may be dropped. In (4.2), the translation of fp' is also smaller than the rotation vof the fingertip by a factor of δs, which leads to the conclusion that for infinitesimal rolling, the fingertip may be considered to rotate about the contact point, fp. The translation of the contact point on the object, bp, contains one term on the order of δs, and a second term which may be dropped. The simplified equations are

translation of contact point with respect to object: $\Delta r_f \approx \Delta r_b \approx u\delta s$ (4.5)

rotation of contact point with respect to object: $u_b \times u_b' \approx \delta s(\frac{dr_b}{ds} \times \frac{d^2 r_b}{ds^2})$ (4.6)

rotation of fingertip with respect to object: $u_f' \times u_b' \approx \delta s\left((\frac{d^2 r_f}{ds^2} - \frac{d^2 r_b}{ds^2}) \times u\right)$. (4.7)

4.2.1 Effects of rolling motion

The meaning of the above equations becomes apparent in Figures 4-3 and 4-4, which show a finger with a curved tip of constant radius rolling on a flat surface on an object. For convenience, the coordinate systems are chosen so that (a,b), (l,m), and (x,y) all lie in the same plane. In Figure 4-3 the radius of curvature, r_c, of the fingertip is large while in Figure 4-4 it is small. In both cases $u_f = u_b = (1)\mathbf{i} + (0)\mathbf{j}$. Since the object is flat, the second derivative of r_b is zero and equation (4.7) reduces to $\delta\theta_f = \delta s(1/r_c)$ (Appendix B).

The fingertip undergoes virtually same motion in Figures 4-3 and 4-4, but there is a significant difference in Δr_b and Δr_f between the two cases, which stems from the difference in δs. In Figure 4-4, there is no appreciable change between r_b and r_b'. Consequently $\Delta[\mathbf{Jb}]^t = [\mathbf{0}]$. There is also virtually no difference between r_f and r_f', when expressed with respect to the (a,b) coordinate frame. Consequently $\Delta[\mathbf{Jf}]^{-t}$ contains only a rotation term resulting from the rotation of the (a,b) coordinate system with respect to the contact point and the (x,y) system. In other words, as the radius of curvature becomes small, the model reduces to the case of a pointed finger rotating about its tip.

In Figure 4-3, Δr_b and Δr_f are significant. Consequently, $\Delta[\mathbf{Jb}]^t$ contains a translation term and $\Delta[\mathbf{Jf}]^{-t}$ reflects both the rotation of the (a,b) system and the addition of Δr_f to r_f. The way in which such terms are incorporated into the elements of the differential jacobians is discussed in Appendix A.2, and an example is given in Section 5.

A flat-tipped finger can be seen as a limiting case in which the radius of curvature becomes infinite so that Δr_b and Δr_b become infinite and produce an infinite displacement of the contact area for any rotation of the finger with respect to the object. In practice, of course, the contact point will jump to the edge of the flat fingertip, at which point the radius of curvature becomes zero rather than infinite.

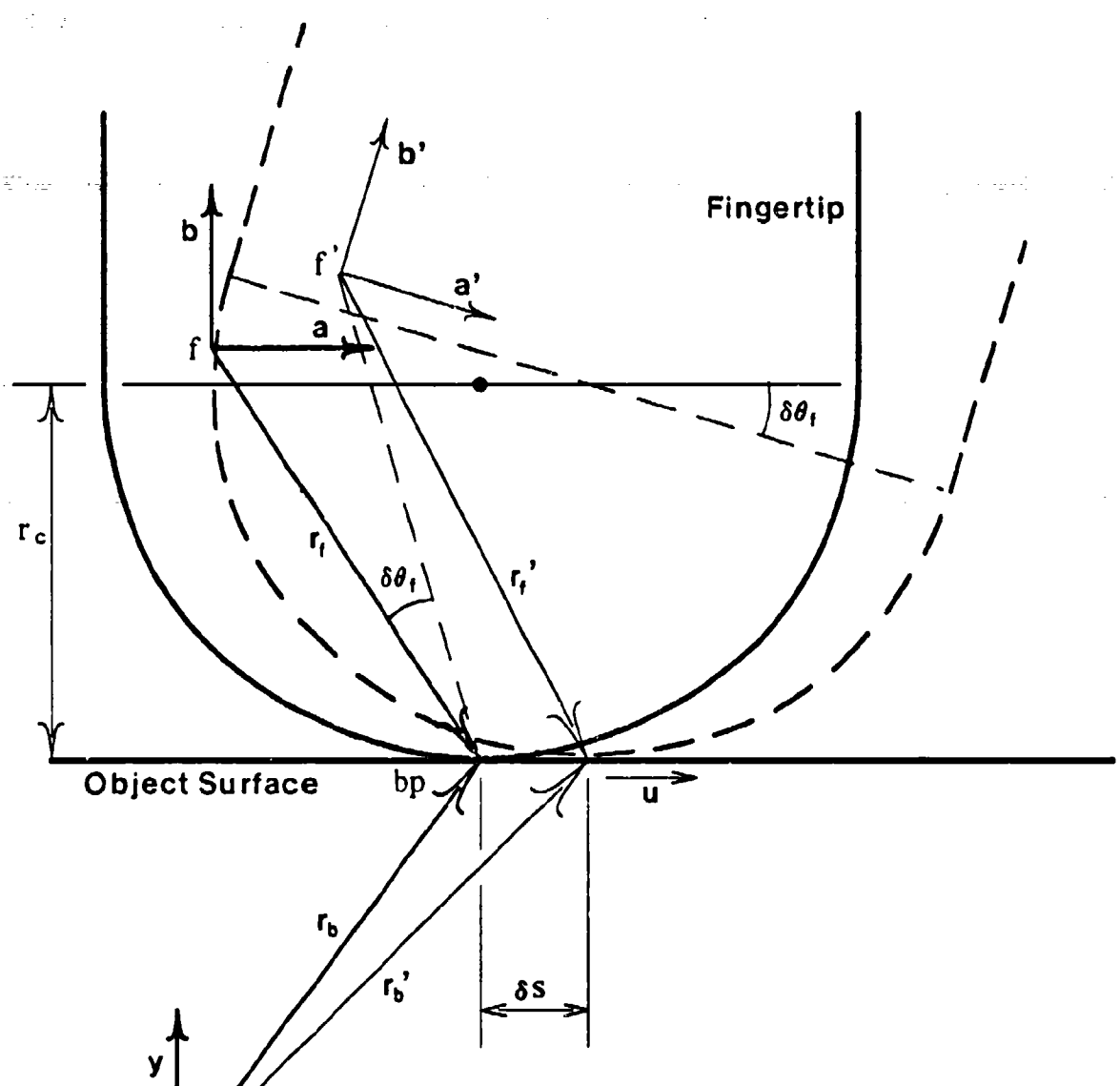

Figure 4-3: Cross section of a large-radius hemispherical fingertip on a flat object surface

4.3 Very soft finger

The bottom fingertip example shown in Figure 4-1 represents the extreme case of a compliant fingertip pressing against the object surface. In this model it is assumed that the fingertip conforms to the object surface, and adheres slightly. Such characteristics are found in many natural gripping surfaces, including the fingertips of the human hand. The coefficient of friction for such a fingertip will be high (greater than one). However, since deformation and adhesion are the primary mechanisms, it is not advisable to assume the Coulomb friction law.

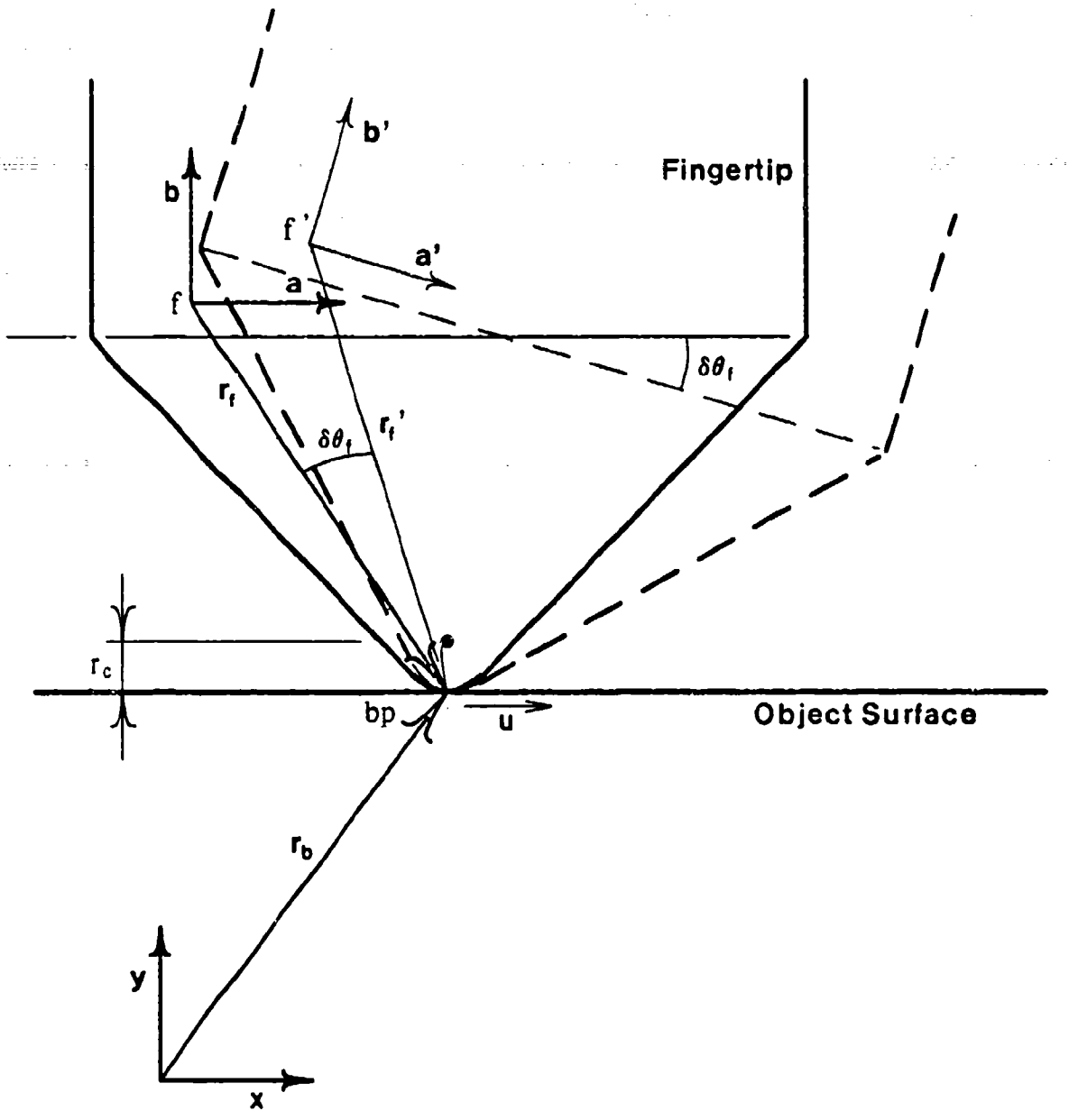

Figure 4-4: Cross section of a small-radius hemispherical fingertip on a flat object surface

The soft finger model is further specialized with the assumption that no rolling occurs and that the compliant medium at the fingertip is elastic. With these assumptions the fingertip becomes a less accurate model of human fingertips. Human skin is visco-elastic and after being deformed will not generally return to its original position. Depending on the curvature of the object being held and the degree of adhesion present, the human fingertip will also roll slightly upon the object, exhibiting a rolling resistance of the kind discussed in Section 4.4. Nonetheless, the elastic soft-finger model is useful to demonstrate a limiting case in which there is complete kinematic coupling between the fingertip and the object.

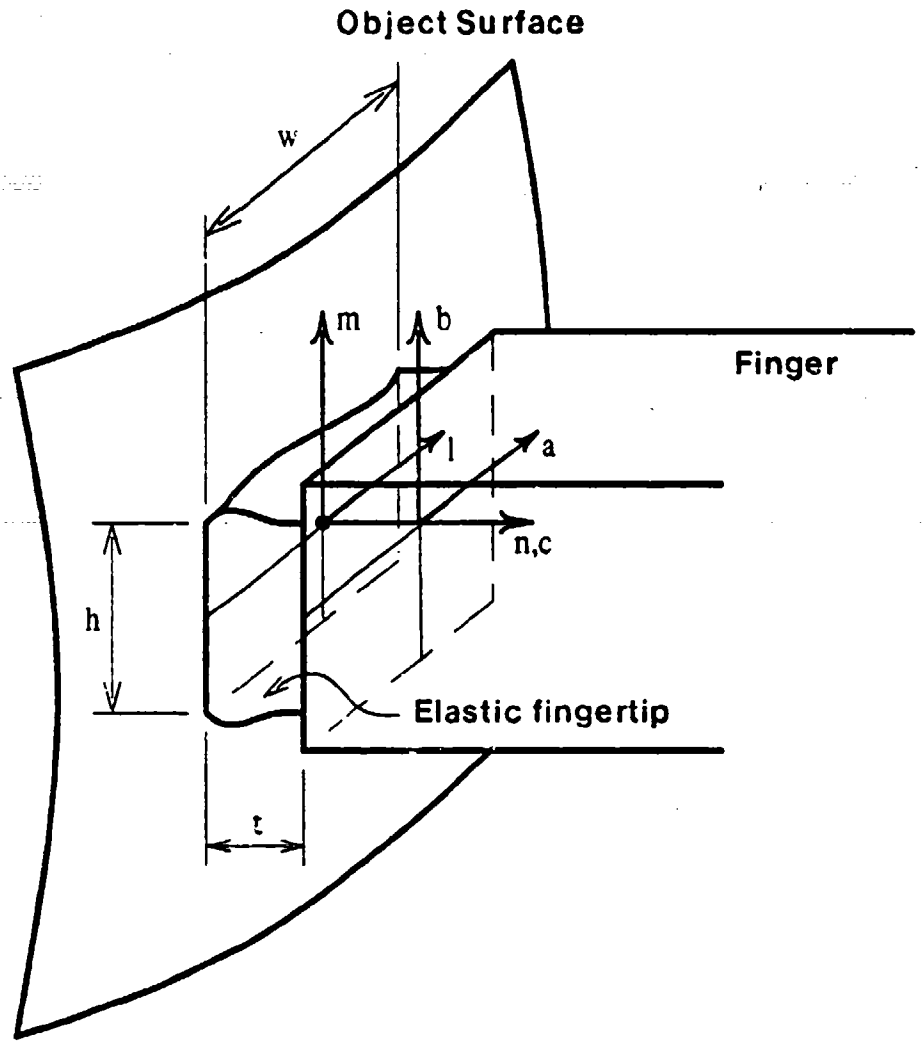

Figure 4-5: Elastic fingertip in contact with object surface

Figure 4-5 shows the fingertip in contact with the surface of an object. The fingertip material is assumed to be much softer than that of either the object or the finger substrate, which are treated as rigid bodies. For convenience, the finger (a,b,c) coordinate system has been moved to the interface between the fingertip material and the finger substrate. As explained in Section 3.1, the forces, displacements and stiffness characteristics of the finger can easily be transformed from another coordinate system to the one chosen in Figure 4-5. The (l,m,n) coordinate system remains, as usual, at the contact area between the fingertip and the object, with the n axis normal to the object surface.

The grasping forces at the object surface, g_{bp}, can be expressed as integrals of the stresses over the contact area:

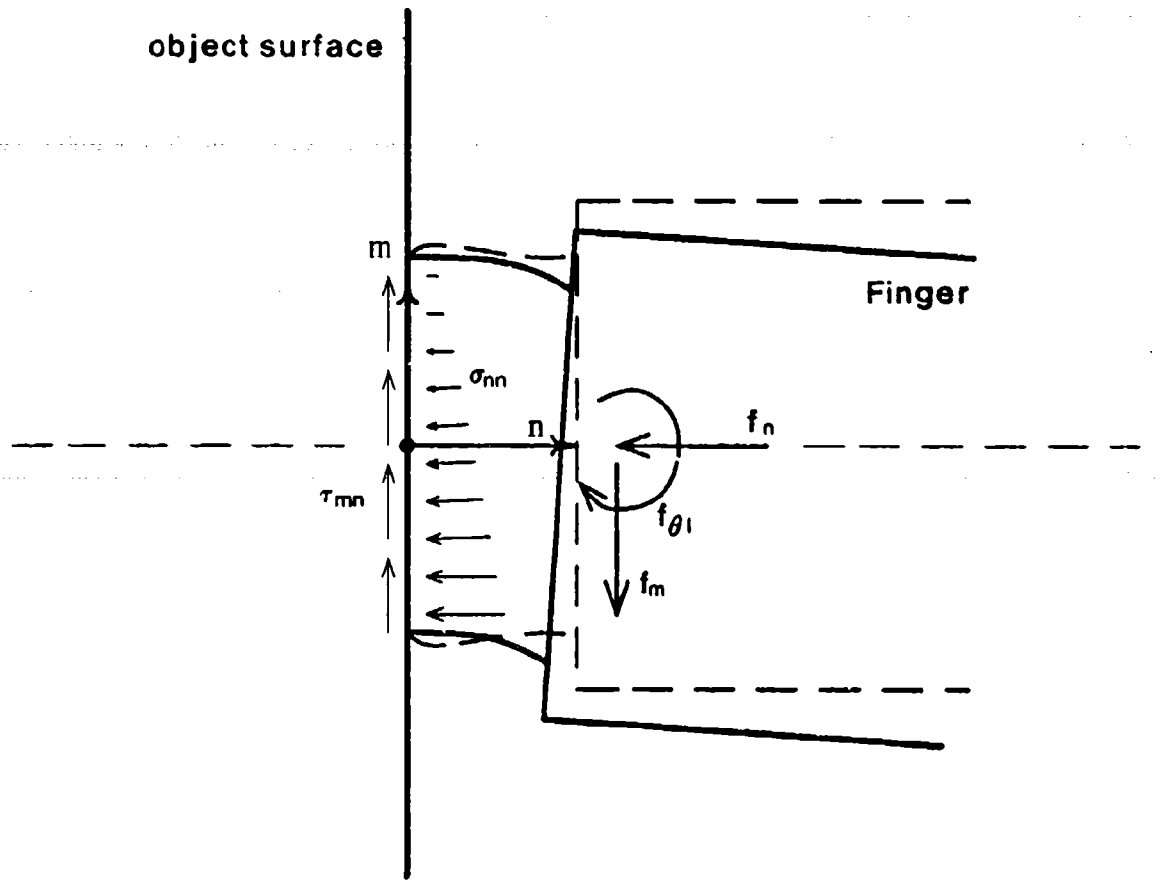

Figure 4-6: Elastic fingertip in contact with object surface

$$g_l = \int_A \tau_{ln}\, dA \qquad g_m = \int_A \tau_{mn}\, dA \qquad g_n = \int_A \sigma_{nn}\, dA$$

$$g_{\theta l} = \int_A m\sigma_{nn}\, dA \qquad g_{\theta m} = \int_A l\sigma_{nn}\, dA \qquad g_{\theta n} = \int_A (\sqrt{l^2 + m^2})\tau_{lm}\, dA$$

The elastic contact represents a compliant coupling in which small motions of the finger with respect to the object are possible in any direction. Such relative motions produce changes in the above forces and a model of the system permits the deflection/force relationships to be expressed as the stiffness of the contact.

The fingertip can be treated as a short elastic member clamped between two rigid boundaries. To obtain the exact stress field for such a problem is a formidable task — even if the assumption is made that the material is perfectly elastic and isotropic. Numerical results could be obtained using a finite element analysis, but the analysis would be time consuming and would have to be re-computed for different cross sections and materials. The problem can be simplified by observing that the stresses at any given location within the material are of little interest, provided that

- estimates of the integral quantities can be computed at the object surface

- the combined stress field nowhere exceeds the strength of the material
- the normal stress, σ_{nn}, never becomes sufficiently tensile to cause the fingertip material to separate from the object surface.

The last requirement can be satisfied by assuming a large grasping force normal to the object surface and/or some adhesion between the fingertip and the object. If one edge of the fingertip *does* start to separate from the object when the finger rotates slightly, then the finger is starting to roll.

Since an exact elastic solution is impractical (and would in any event be an approximation to the visco-elastic behavior of compliant polymers and skin-like materials) an approximate elastic solution is used to estimate the force/deflection relationship for the fingertip. The behavior of the fingertip in shear, torsion, compression and bending is discussed below, and the separate solutions are superposed to produce a 6x6 stiffness matrix for the contact.

Bending stiffness and resistance to rolling

The bending model for the elastic fingertip is similar to that used in classical beam theory. A rotation about the a axis by the finger produces a rotation in the material of $\delta\theta/t$ per unit thickness. The bending strain and stress at a distance m above the centerline are

$$\varepsilon_{nn} = \frac{m\delta\theta}{t} \quad \text{and} \quad \sigma_{nn} = E\varepsilon_{nn}$$

where E is the modulus of elasticity. As in beam theory, it is assumed that plane sections remain plane and $\gamma_{ln} = \gamma_{mn} = 0$. It is also assumed that since the stresses τ_{lm}, σ_{mm} and σ_{ll} are zero at the surfaces of the material that they are approximately zero throughout. This assumption is somewhat less supportable than in beam theory since the elastic element cannot be considered slender. However, it is not actually necessary that τ_{lm}, σ_{mm} and σ_{ll} be zero everywhere but only that their resultant does not significantly affect the estimated bending rigidity of the element. The bending rigidity may then be found by equating the energy stored in rotating the finger with the energy stored in deforming the material

$$1/2k_{\theta l}(\delta\theta_l)^2 = 1/2\int_V \sigma_{nn}\varepsilon_{nn}dV = \frac{EI_{mm}(\delta\theta_l)^2}{2t}$$

$$\text{or} \quad k_{\theta l} = \frac{EI_{mm}}{t}$$

where I_{mm} is the moment of inertia of the cross section about the m axis and V is the volume of the material.

The bending stiffness for rotations about the m axis is similarly found as

$$k_{\theta m} = \frac{EI_{ll}}{t}.$$

As mentioned earlier, the maximum bending moment that the contact can sustain is limited by the adhesion between the fingertip and the object surface. The limitation is easily demonstrated for the example

of a square contact area of length w on each side. Referring to Figure 4-6, a normal force of magnitude f_n produces a uniform contribution to the normal stress of

$$\sigma_{nn} = -\frac{f_n}{w^2} \quad \text{(compression)}.$$

A bending moment of magnitude $f_{\theta l}$ produces a contribution to the normal stress that is maximum at the edges of the contact.

$$\sigma_{nn} = \pm\frac{f_{\theta l}}{I} = \pm\frac{6 f_{\theta l}}{w^3} \quad \text{(bending)}$$

The combined normal stress will become tensile at one edge when

$$f_{\theta l} > \frac{w f_n}{6}.$$

Thus, unless the adhesion between the fingertip and the object is able to resist tensile loads, the finger will start to roll whenever the bending moment is more than one sixth the normal load times the length of the side. For small contact areas the fingertip is likely to start rolling unless considerable adhesion is present.

Shear stiffness and resistance to slipping

For a beam with an end load, the variation in the moment over the length of the beam is balanced by a distribution in shearing stress over the cross section of the beam [17]. For the elastic fingertip, however, it is assumed that the variation in the moment produced by a shear force in the (a,b,c) system is negligible compared to the effect of rotating the finger. Consequently the bending moment is approximately constant over t and the shear stress is assumed to be uniform over the cross section. The shear stiffness is found by equating the energy required to displace the finger in shear with the energy stored internally in the material.

$$1/2 k_{\theta m} (\delta_m)^2 = 1/2 \int_V \tau_{mn} e_{mn} dV = GA \frac{(\delta\theta_l)^2}{2t}$$

$$\text{or} \quad k_m = \frac{GA}{t}$$

In the above, G is the shear modulus of the material and A is the cross section area, wh.

The maximum shearing force that the contact can sustain is limited by the shear strength of the fingertip/object interface, which depends on the bonding strength between the fingertip and object materials and on the area of intimate contact between them. The area of intimate contact is generally much smaller than the overall contact area, A, and depends not only on the current normal force, f_n, but on such factors as how clean the surfaces are, how rough they are, and how long they have been held together. In general, the shear strength of the contact will be some fraction, β, of the shear strength of the fingertip material. The fraction will be a function of (but not directly proportional to) the normal force, and slipping will occur when τ_{mn} or τ_{ln} exceeds that fraction.

$$\tau_{slip} = \beta_{(f_n, \ldots)} \tau_{yield}$$

Compressive stiffness

Displacement of the fingertip toward the object results in a uniform compressive strain, $-\varepsilon_{nn}$, across the cross section. The compressive stiffness is found in the same way as the shear stiffness, with G replaced by E.

$$k_n = \frac{EA}{t}$$

Torsional stiffness and resistance to slipping

The torsional rigidity of a cylindrical member can easily be found as

$$k_{\theta n} = \frac{\pi G r_o^4}{2} = G I_p$$

where r_o is the radius of the cylinder and I_p is the polar moment of inertia [17]. For non-circular cross sections the expression becomes more complicated due to warping of the cross sections, although for the present case the warping may be negligible since t is small and since the material is constrained by a rigid boundary at each end. For a bar of elliptical cross-section the torsional rigidity per unit length has been determined as

$$k_{\theta n} = \frac{G A^4}{4\pi^2 I_p}$$

and it has been found that this formula holds approximately true for other compact cross sections [18].

For a round bar, the shear stress in torsion is

$$\tau_{lm} = \frac{r f_{\theta n}}{I_p}. \tag{4.8}$$

Thus, if the fingertip were a cylinder ending in a circular contact area, slipping would begin at the periphery when

$$f_{\theta n} = \frac{\tau_{slip} I_p}{r_o} \tag{4.9}$$

(where τ_{slip} is given above for shear loading.) Once slipping has occurred at the periphery, the fingertip will not return to exactly the same orientation when the torque is removed. As the torque is increased, the region of slipping will spread from the periphery toward the center. The phenomenon resembles the yielding of an elastic/perfectly plastic bar in torsion. At any stage, the moment balance is given by

$$f_{\theta n} = \int_0^{r_{slip}} 2\pi \tau_{lm} r^2 \, dr + \int_{r_{slip}}^{r_o} 2\pi \tau_{slip} r^2 \, dr. \tag{4.10}$$

The above equation can be integrated and condensed by expressing τ_{lm} and r_{slip} in terms of r and the angle of rotation of the finger, $d_{\theta n}$.

$$\tau_{lm} = \frac{2\pi G d_{\theta n} r}{t}$$

$$r_{slip} = \frac{t \tau_{slip}}{G d_{\theta n}}$$

The result for the torque is

$$f_{\theta n} = \tfrac{2}{3}\pi \tau_{slip}(r_0^3 - \tfrac{1}{4} r_{slip}^3)$$

Thus, the torque required for complete slipping is $\frac{4}{3}$ the torque required to initiate slipping at the periphery, although this would theoretically only be reached for an infinite rotation, $d_{\theta n}$ or $d_{\theta c}$, of the fingertip. For a square or rectangular contact area the qualitative behavior is the same, with slipping initiating at the periphery and spreading inwards. However, the expression for $f_{\theta n}$ becomes more complex due to the more involved expression for τ_{lm}.

Fingertip Stiffness Matrix

The above stiffness terms form the elements of a 6x6 diagonal matrix [Kc] where

$$Kc_{11} = Kc_{22} = \frac{GA}{t} \tag{4.11}$$

$$Kc_{33} = \frac{EA}{t} \tag{4.12}$$

$$Kc_{44} = \frac{EI_{mm}}{t} \tag{4.13}$$

$$Kc_{55} = \frac{EI_{ll}}{t} \tag{4.14}$$

$$\frac{GA^4}{4\pi^2 I_p} < Kc_{66} < GI_p \tag{4.15}$$

If t were larger than w and h, then shear loads would produce bending moments that varied along t, and bending loads would produce shear deflections, as in classical beam theory. The result would be off-diagonal terms in [Kc].

4.3.1 Effects of deforming fingertips

The comparative importance of the above quantities can be determined for a fingertip of given proportions. The table below shows the results for two fingertips. For the first, $w = h = 1.0$ cm and $t = 0.5$ cm. In the second $w = h = 2.0$ cm and $t = 0.5$ cm. The modulus of elasticity, E, is assumed to be 250 N/cm^2 and Poisson's ratio is taken as 1/2, so that $G = E/3$. These are typical values for rubber. A force of 4.0N (a little less than one lbf.) is used to produce deflections for comparison.

Table 4-1: Soft fingertip deflections for 4.0 N load and $1cm^2$ and $4cm^2$ contact area

Fingertip material properties: $E = 250\ N/cm^2$, $\nu = 0.5$, $G = 83.3\ N/cm^2$

	$w = h = 1.0$ cm, $t = 0.5$ cm	$w = h = 2.0$ cm, $t = 0.5$ cm
Kc_{11}, Kc_{22}	167 N/cm	667 N/cm
deflection for 4.0 N shear force	0.024 cm	0.006 cm
Kc_{33}	500 N/cm	2000 N/cm
deflection for 4.0 N compressive force	0.008 cm	0.002 cm
Kc_{44}, Kc_{55}	42 Ncm	672 Ncm
rotational deflection for 4.0 N at 1.0 cm lever arm	0.096 radian	0.006 radian
Kc_{66}	27 Ncm	432 Ncm
torsional deflection for 4.0 Ncm torque	0.15 radian	0.009 radian

For the smaller area, the rotational stiffness terms are much lower that the translational terms and the fingertip is clearly less constrained with respect to rotations than translations. However, the bending and torsion stiffnesses increase as the square of the contact area, while the shear and compressive stiffness increase linearly with the contact area. Thus, for the larger contact patch, the rotational and translational stiffnesses become comparable. If w and h were doubled again, bending and torsional deflections would become negligible in comparison to shear deflections. This result matches what one would expect intuitively.

If the grasping force is varied proportionately with the contact area, then, as the contact area becomes small, the fingertip begins to behave like a point contact in which significant rotations are possible but translations are not. As the contact area becomes large, rotations are negligible compared to shear deflections. If the grasping force is held constant for different contact areas then the contact becomes much less compliant as the area increases, and rotational deflections become negligible faster than translational deflections.

For the forces given in the table above, unless some adhesion exists between the fingertip and the object, the bending moment will cause the fingertip to roll for both the $1cm^2$ or the $4cm^2$ area. The largest bending

moment that the contact could sustain without tension is 0.67Ncm for the $1cm^2$ case and 1.33Ncm for the $4cm^2$ case. In torsion, depending on the shear strength of the interface, the contact will probably slip for the $1cm^2$ area but might not for the $4cm^2$ area. If the shear strength is roughly equal to $4.0N/cm^2$ in the first case (corresponding to a coefficient of friction of 1.0) and $1.5N/cm^2$ in the second, (corresponding to a coefficient of friction of 1.5)[3] the maximum torques that can be exerted are 1.7Ncm and 5.3Ncm respectively. This supports the idea that a soft finger with a small contact area can exert torques about an axis normal to the contact surface more readily than it can exert torques in the plane of the surface. For a soft, curved fingertip, as discussed below, the difference is more pronounced.

Once the fingertip stiffness matrix has been computed, the net compliance matrix may be formed by adding the compliances for the finger and the fingertip.

$$[Cf] = [Jfq][Kq]^{-1}[Jfq]^t + [Kc]^{-1}.$$

This matrix is invertible and therefore, the restoring forces at the contact become

$$\Delta g_{fp} = [Cf]^{-1} d_{bp}$$

Using equations (3.5) and (3.6), the changes in the forces at the finger joints are $\Delta g_q = [Jfq]^t \Delta g_{fp}$, and the finger motions are $d_q = [Kq]^{-1} \Delta g_q$.

4.4 Soft, Curved Fingertip

The hard curved fingertip and the very soft fingertip represent extremes between which real, deformable fingertips may be expected to lie. Human fingers and rounded robot fingers with rubber surfaces exhibit both rolling and substantial deformation. The analysis of such fingertips becomes quite involved, combining the rolling calculations of Section 4.2 with the deformation calculations of Section 4.3. A complete model is not attempted in the discussion below, but the properties of soft, rolling fingers are discussed and it is seen that they are bracketed by the models developed in the last two sections.

A number of insights can be gained by considering the analyses applied to the rolling of rubber tires and metal cylinders or spheres. For a hard, elastic sphere rolling on an elastic surface, the pressure distribution is described by the Hertzian contact model of solid mechanics, which predicts a hemispherical pressure distribution [18]. For the much larger deformations that occur when a soft, curved finger presses against an object the distribution is expected to be qualitatively similar. The pressure will be maximum at the center of the contact, diminishing smoothly to zero at the periphery. For progressively softer fingertips, the pressure distribution becomes more uniform, especially toward the center of the contact area. In the limiting case, the pressure is essentially uniform throughout, as assumed in the very soft finger model described in Section 4.3. The pressure distributions are compared for elastic, soft, and very soft fingertips in Figure 4-7.

---

[3] According to the Coulomb theory, the coefficient of friction would be independent of the contact area, but for compliant materials it is generally not independent.

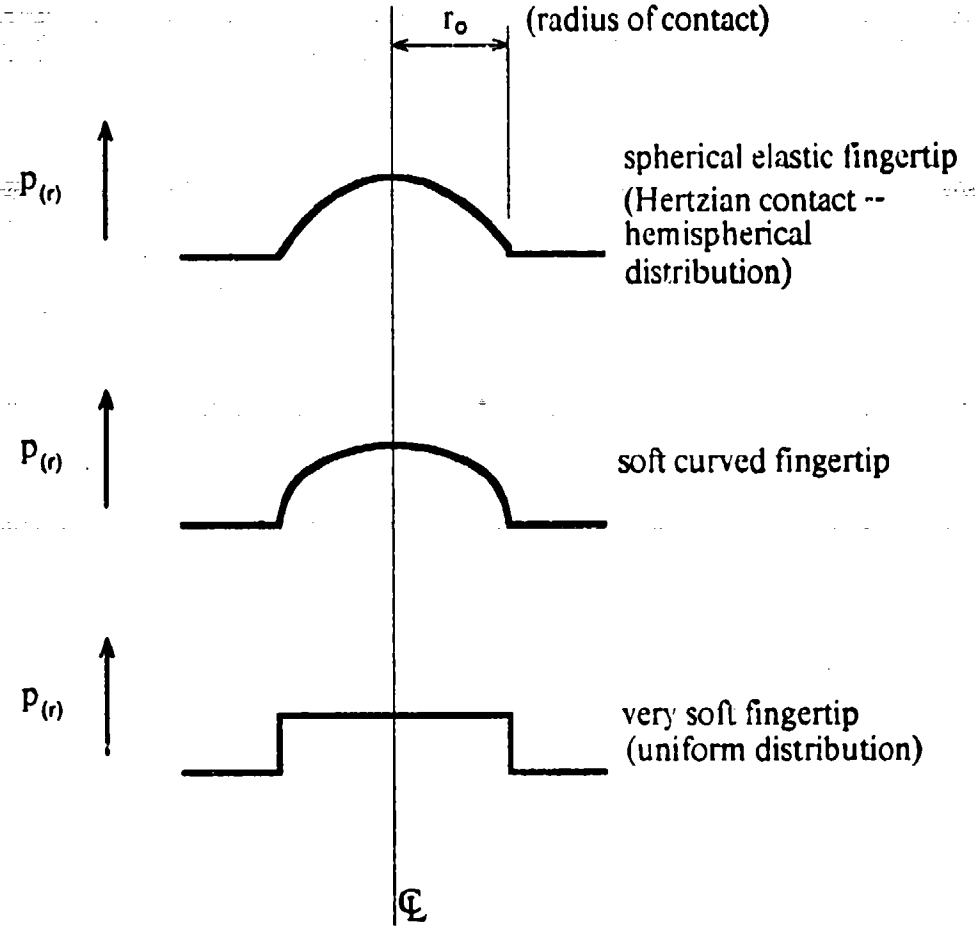

Figure 4-7: Pressure distributions for elastic, soft, and very soft fingertips

For a perfectly elastic curved finger, it is impossible to transmit moments in the plane of the contact since the finger rolls easily upon the object. Thus, in the absence of rolling resistance, the soft curved finger would behave in the same manner as the hard curved finger discussed earlier, the only difference being that r_f would vary due to flattening of the fingertip under load. If the degree of flattening could be predicted as a function of fingertip loading, then the methods discussed in section 4.2 could be used to predict the motion of the finger and the contact point. Elastic flattening formulas have been developed for cylinders and spheres, but these are unlikely to give accurate results for a soft fingertip.

In practice, there is generally a resistance to rolling. At low speeds, the rolling resistance is due largely to hysteresis losses and microslip at the contact area. Rolling resistance is an important subject in the literature on wheels and tires and is discussed at length in [19, 20, 21]. For an elastic sphere or cylinder rolling upon a plane surface, the deformation of the material results in a hysteresis loss which can be used to derive a "coefficient of rolling resistance" [19]. Microslip results from the elastic strain of the fingertip material as it is pressed against the surface. If the fingertip is loaded with a normal load, f_n, against the object surface, the material ahead of the centerline of the contact will spread forwards slightly and the material behind the centerline will spread backwards slightly. The spreading produces regions of microslip toward the front and

rear of the contact area. In the absence of tangential forces, the strains, and the shear tractions that result from them, must cancel each other. When a tangential force is present, there will be a region of sticking toward one side of the contact area, and microslip elsewhere. The microslip results in rolling losses and "creep." The end result is that soft curved fingertips do not rotate quite as freely with respect to the object as pointed or hard curved fingertips do.

The static resistance to slipping of the soft, curved fingertip will be similar to that of the very soft finger of Section 4.3, except that since the pressure distribution is not uniform over the contact area, the value of the stress at which slipping occurs also varies over the contact. As in Section 4.3, the interface shear strength τ_{slip}, may be expressed as a fraction of the material shear strength, where the fraction, β, is a function of factors including the normal pressure and the surface roughness. Since the pressure is least at the edges of the contact, slipping may be expected to initiate there.

For loads in the plane of the contact, the shear stress may be uniform inside the region where there is no sliding, but will have an upper limit of τ_{slip} outside the region.

For a moment about the axis normal to the contact, the shear stress inside the sticking region will have the same distribution as for the very soft finger, the magnitude at any point being proportional to the distance from the center of the contact as in equation (4.8). In the slipping region, the shear stress will again be equal to the upper limit of τ_{slip}. A cross section of shear stress distribution is shown in the lower part of Figure 4-8. The distribution for the very soft fingertip of Section 4.3 is shown in the upper part for comparison. The maximum torque about the axis of the finger is equal to the polar moment of the shear stress shown in Figure 4-8.

$$f_{\theta n} = \int_0^{r_{slip}} 2\pi \tau_{lm} r^2 dr + \int_{r_{slip}}^{r_o} 2\pi \tau_{slip} r^2 dr \qquad (4.16)$$

where $\tau_{lm(r)}$ is proportional to r and $\tau_{slip(r)}$ is a function of $\sigma_{nn(r)}$

Thus, unlike the hard curved finger or the pointed finger, the soft curved finger is able to exert small torques about its own axis.

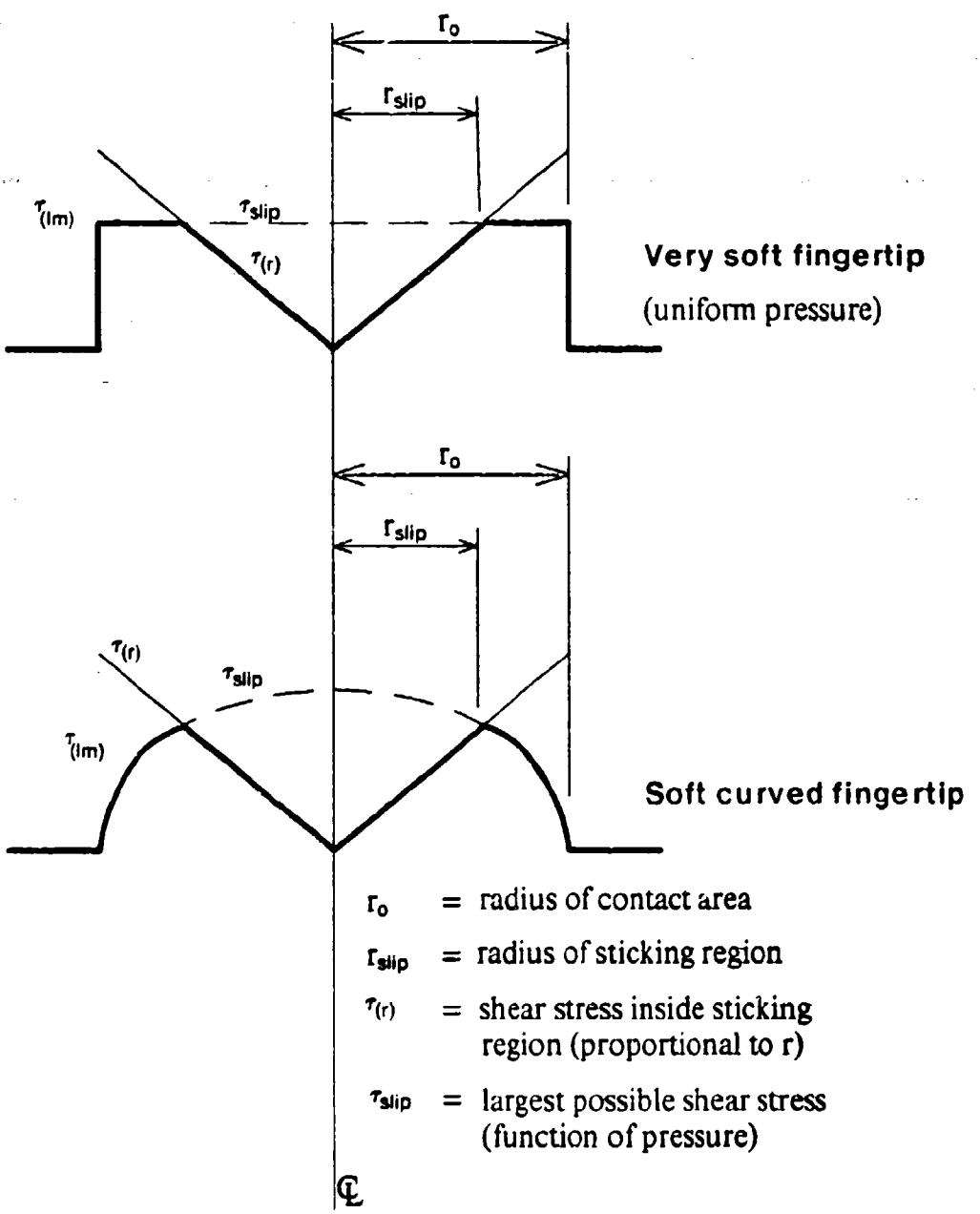

Figure 4-8: Maximum shear stress for moment about finger axis

5. Examples

In this section, results from the last three sections are used in three examples that also illustrate some of the differences between pointed, curved and soft fingers. Figure 5-1 shows three rectangles, each held by two fingers. In the first case the fingers are pointed, in the second case they have finite radii of curvature and in the third case they have very soft tips that adhere to the surface of the rectangle. In all three cases, the fingers are assumed to have three degrees of freedom, being restricted to motions within the plane of the paper. For simplicity, it is assumed that the finger joints correspond to translations, a and b, and a rotation, θc, in the (a,b,c) frames.

The sizes and orientations of the rectangular object and fingers, and the finger stiffnesses, $[Kf]$, are identical in each case. However, the different contact conditions produce substantially different results for the mobility, stiffness, strength and stability of the grasp.

In each case the change in the resultant grasp force on the object, Δg, is calculated for small displacements of the object. The grip stiffness is computed and the maximum force and torque that the grip can resist without slipping is calculated.

5.1 Pointed Fingers

The transformation matrices, $[Jb]$, $[M]$, $[Jf]$, and $[Jq]$, are given in Appendix C for the left or first finger. As the object is moved an arbitrary amount, d_b, the motions at the contact points on the object are given by $d_{bp} = [Jb]d_b$. Premultiplying by $[M]$ gives the vectors d_c, which contain just the first three elements of d_{bp} since, for point contact conditions, only the translations are transmitted.

The fingers have three degrees of freedom and consequently $d_q = [dq_a, dq_b, dq_c]$. A motion, d_q, produces a motion d_{fp} at the fingertip, given by equation (3.3). The elements of d_{fp} and d_c are compared below for the left and right fingers. The (l,m,n) coordinate systems are shown in Figure 5-1.

Matching d_{c1} with d_{fp1} and d_{c2} with d_{fp2} reveals that $dz + \frac{w}{2} d\theta y = 0$ and $dz - \frac{w}{2} d\theta y = 0$ or, $dz = d\theta y = 0$. In other words, the object is constrained by the fingers to move within the plane, except for rotations about the x axis. In the following discussion it will be assumed that the object is given displacements in the x and y directions and a rotation about the z axis. Thus, dl_1 and dm_2 will be zero and the only motions transmitted to the fingers will be dm_1, dn_1, dl_2 and dn_2.

The procedure for calculating the finger motions, the changes in the finger forces and the change in force on the body is given below for the first finger. The contribution from the second finger follows from symmetry.

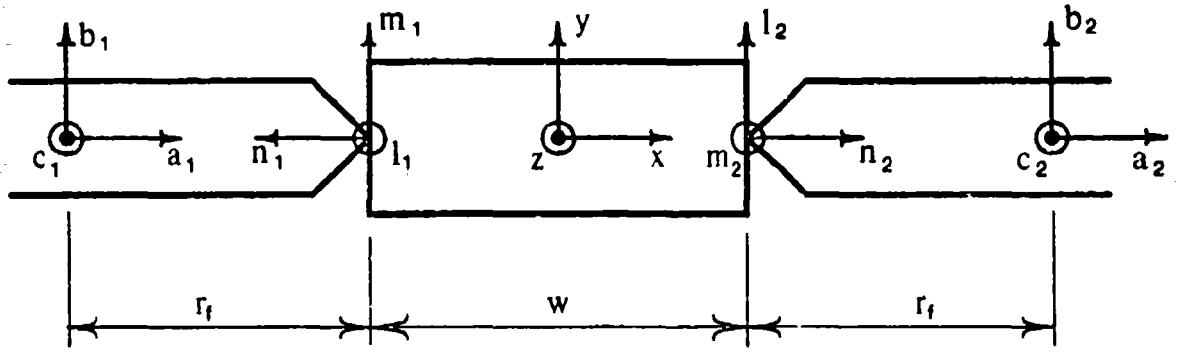

Pointed fingertips

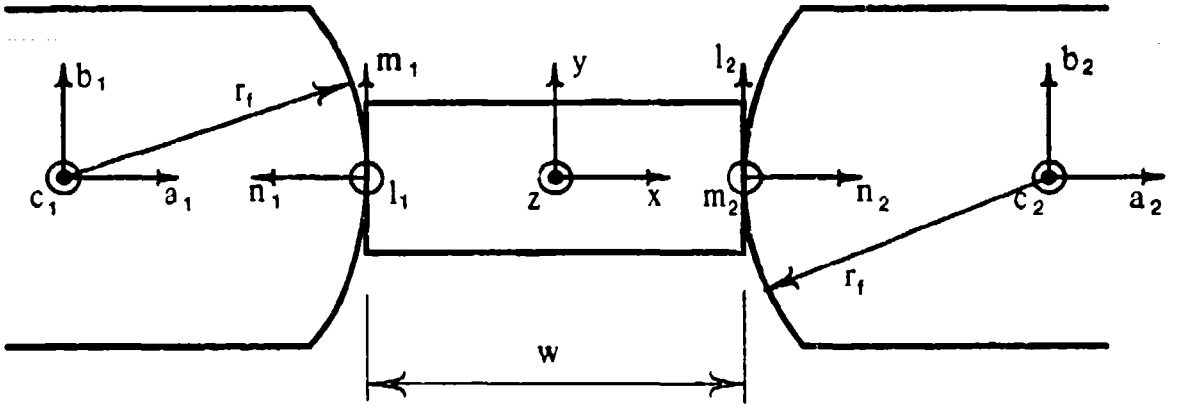

Rounded fingertips

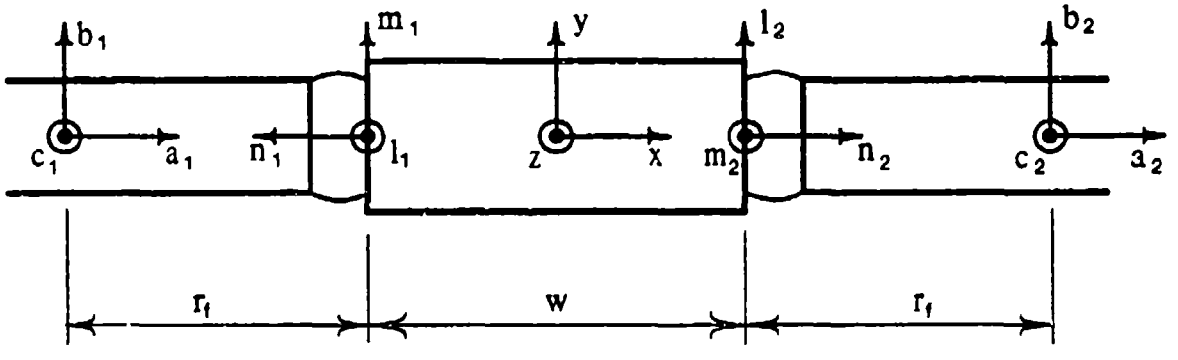

Soft fingertips

Figure 5-1: Holding a rectangle between two fingers — 3 examples

	d_{c1}	d_{fp1}	d_{fp2}	d_{c2}
dl	$dz + \frac{w}{2} d\theta y$	0	$dq_b - rf\, dq_c$	$dy + \frac{w}{2} d\theta z$
dm	$dy - \frac{w}{2} d\theta z$	$dq_b + rf\, dq_c$	0	$dz - \frac{w}{2} d\theta y$
dn	$-dx$	$-dq_a$	dq_a	dx
$d\theta l$		dq_c	0	
$d\theta m$		0	dq_c	
$d\theta n$		0	0	

Table 5-1: Motions of left and right finger and object contact areas (pointed fingertips)

5.1.1 Procedure for Left Finger

The first step is to determine the motions of the first finger given dm_1 and dn_1. A motion in the dm direction can be accommodated either by a movement of the finger in the b direction or by a rotation about c. In practice, both will occur and the contribution from each will be balanced to minimize the potential energy of the finger. The two rows of $[Jfq]$ that relate finger motions dq_b and dq_c to dm and dn are extracted to form the 3x2 matrix $[P]$. Following the method in Section 3.3.1.2, a Lagrange multiplier matrix, $[L]$ is assembled from $[Kq]$ and $[P]$. The matrices and the matrix equations are shown in Appendix C. Inverting $[L]$ produces the finger motions, d_q. Multiplying the finger joint motions by $[Kq]$ determines the changes in the joint forces.

The changes in the forces at the fingertip, δg_{fp}, depend both on the restoring forces δg_q and the change in geometry, $\Delta[Jf]^{-t}$, due to the motion of the finger with respect to the object. The motion of the (l,m,n) coordinate system is given by d_{bp} and the motion of the fingertip is given by $[Jfq]d_q$. The translations of each are the same, but the finger rotates relative to the object by the angle

$$\delta\theta = \delta\theta l - \delta\theta c.$$

which appears as a rotation term in $\Delta[Jf]^{-t}$ in Appendix C.

For a grasping force of f in the a direction and for a motion $(dx, dy, d\theta z)$ applied to the body, the change in the force applied by the first finger to the object is shown in Table 5-2.

When the second finger is added, the expressions for the change in the force on the object become simpler due to combinations and cancellations of symmetrical terms. The contributions to δg_y from each finger cancel for rotations, $d\theta z$, and add for translations, dy. Similarly, the contributions to $\delta\theta z$ from each finger cancel for motions, dy, and add for rotations $d\theta z$. The final result is given in Table 5-3.

δg_x	$= -k_a\, dx$
δg_y	$= (\alpha f - \beta)\, dy - (f + \frac{w}{2}(\alpha f - \beta))\, d\theta z$
δg_z	$= 0$
$\delta g_{\theta x}$	$= 0$
$\delta g_{\theta y}$	$= 0$
$\delta g_{\theta z}$	$= -\frac{w}{2}(\alpha f - \beta)\, dy + \frac{w}{2}(f + \frac{w}{2}(\alpha f - \beta))\, d\theta z$

where $\alpha = \dfrac{k_b r_f}{k_b r_f^2 + k_c}$ and $\beta = \dfrac{k_b k_c}{k_b r_f^2 + k_c}$

Table 5-2: Contribution from left finger to δg_b (pointed fingertip)

δg_x	$= -2 k_a\, dx$
δg_y	$= 2(\alpha f - \beta)\, dy$
$\delta g_{\theta z}$	$= w(f + \frac{w}{2}(\alpha f - \beta))\, d\theta z$

Table 5-3: Change in g_b due to motions dx, dy, and $d\theta z$ (pointed fingertips)

5.1.2 Discussion

Whenever any of the above quantities becomes positive, the grasp will be unstable for infinitesimal displacements in the corresponding direction. Thus, if k_c is small, ($k_c < f r_f$), the change in the grasp force for a motion in the y direction will be positive, tending to continue the motion. This result matches one's intuition that a rectangle squeezed between two fingers will be unstable if the finger pivots freely, without springs, about axes c_1 and c_2.

Similarly if $\frac{w}{2}\beta < (f + \frac{w}{2}\alpha f)$, the rectangle will be unstable with respect to rotations about the z axis. This result is less intuitively clear but it becomes apparent if k_c is very large, in which case the fingers do not rotate about their c axes. For this case, $\alpha \rightarrow 0$ and $\beta \rightarrow k_b$. If the object is rotated by $d\theta_z$ the change in the torque upon the body is

$(wf - \frac{w}{2} k_b)\, d\theta z$.

This is exactly the result obtained earlier in Section 1 for the rotation of a rectangle squeezed between two fingers, where $k_b = k_f$ and $\frac{w}{2} = r$.

5.2 Curved Fingertips

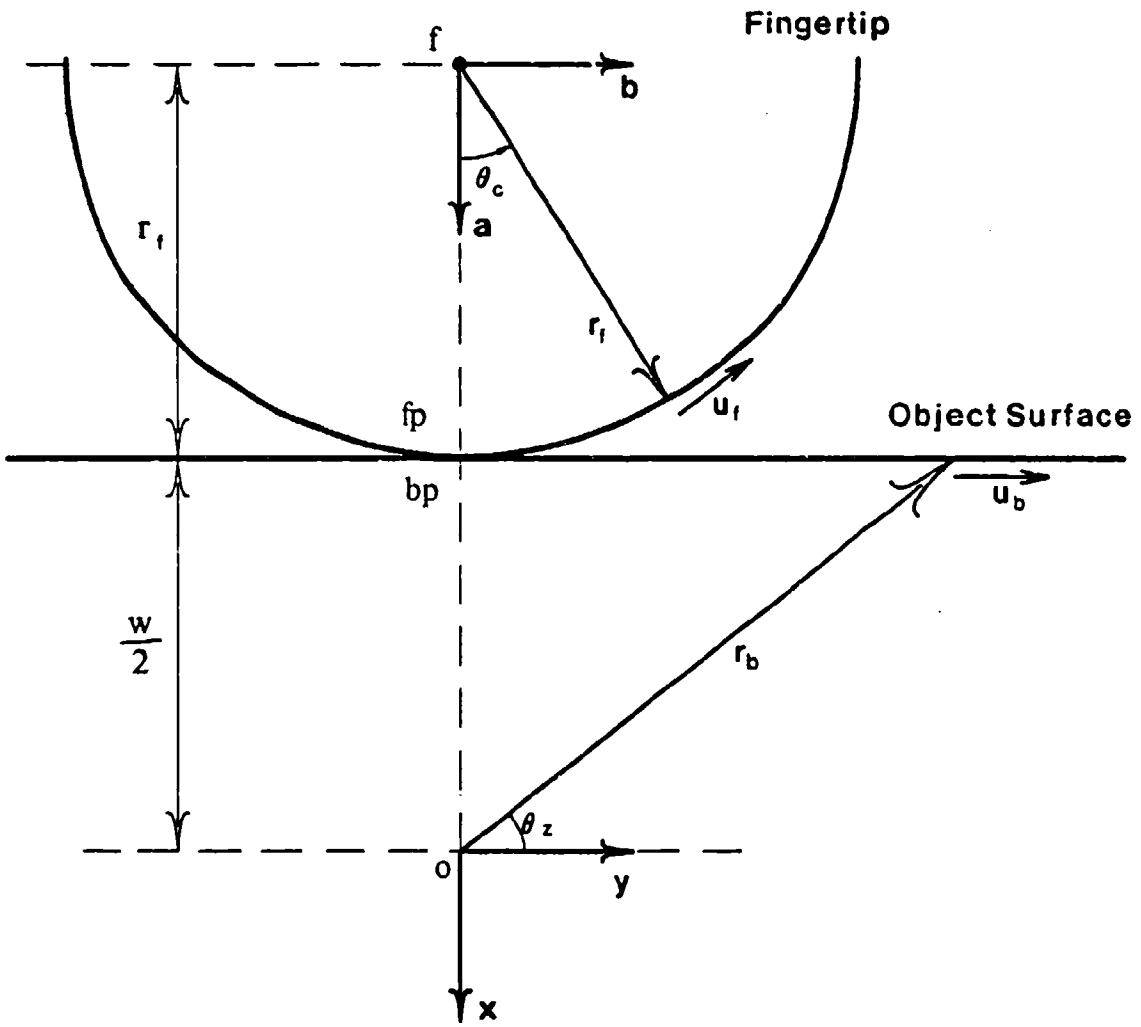

Figure 5-2: Curved finger before rolling

Most of the results from the last example also apply for fingers with curved surfaces. The difference is that the contact point is no longer fixed with respect to the object and consequently $\Delta[Jf]^{-t}$ is slightly different from above and $\Delta[Jb]^{t}$ is no longer zero. The new matrices are given in Appendix C.

As with the pointed finger example, results are derived for the first or left finger. In the current example, the algebra has been simplified by assuming that the (a,b,c) finger coordinate systems are also the centers of curvature of the finger tips. The rolling condition is therefore as shown in figures 5-2 and 5-3, before and

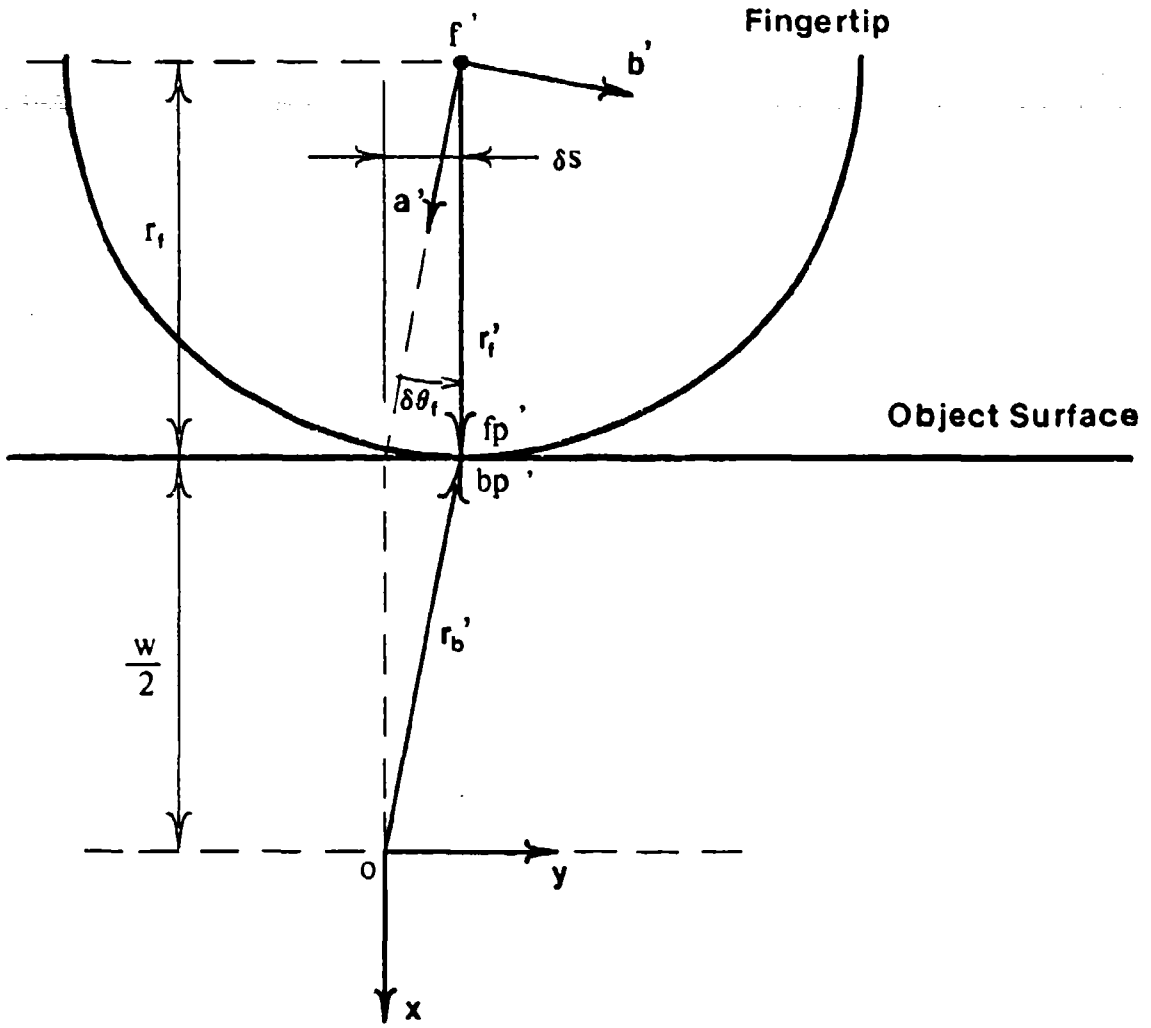

Figure 5-3: Curved finger after rolling $\delta\theta$ with respect to object

after the finger has rotated a small amount, $\delta\theta$, with respect to (l,m,n) coordinate system on the object. As the figures show, $\delta s = r_f \delta\theta$.

Since the center of curvature of the finger is also the origin of the (a,b,c) system, the translation of the contact point *exactly cancels* the product $\delta\theta \times r_f$. The contribution from the left finger to Δg_b is shown in Table 5-4.

When the results from the second finger are added, the changes in the force upon the object are as shown in Table 5-5.

δg_x	$= -k_a\, dx$
δg_y	$= (\alpha f - \beta)\, dy - (f + \frac{w}{2}(\alpha f - \beta))\, d\theta_z$
δg_z	$= 0$
$\delta g_{\theta x}$	$= 0$
$\delta g_{\theta y}$	$= 0$
$\delta g_{\theta z}$	$= \frac{1}{4}\left((\alpha f - \beta)w^2 + 2f(1 - \alpha r_f)w - 4f r_f\right) d\theta_z - \frac{1}{2}\left((\alpha f - \beta)w + 4\alpha f r_f\right) dy$

where $\alpha = \dfrac{k_b r_f}{k_b r_f^2 + k_c}$ and $\beta = \dfrac{k_b k_c}{k_b r_f^2 + k_c}$

Table 5-4: Contribution from left finger to δg_b (rounded fingertip)

δg_x	$= -2\, k_a\, dx$
δg_y	$= 2(\alpha f - \beta)\, dy$
δg_z	$= \frac{1}{4}\left((\alpha f - \beta)w^2 + 2f(1 - \alpha r_f)w - 4f r_f\right) d\theta_z$

Table 5-5: Change in g_b due to motions dx, dy, and $d\theta z$ (rounded fingertips)

5.2.1 Discussion

The results in the x and y directions are identical to those for the point-contact example but the torque about the z axis has changed. As in the previous example, the expression for torque about the z axis simplifies for the limiting case in which k_c is large compared to k_b. The change in the torque about the z axis reduces to

$$\tfrac{1}{4}(-k_b w^2 + 2fw - 4f r_f)\, d\theta_z$$

In the above expression, if $r_f = \frac{w}{2}$ then the last two terms cancel each other out leaving only the restoring torque, $-\frac{1}{4} k_b w^2 \delta\theta_z$. In other words, the translation of the contact point due to rolling of the finger with respect to the object exactly cancels the effect of rotating the object. Thus for large radii of curvature, ($r_f \geq \frac{w}{2}$), the grasp is infinitesimally stable with respect to rotations *regardless* of the stiffness of the fingers.

5.3 Very Soft Fingers

For contacts with soft fingers a combined compliance matrix is established for the finger and fingertip as in Section 4.3. The combined compliance matrix is shown in Appendix C for a square fingertip. In the matrix, k_p is the elastic stiffness of the fingertip in compression. Since the shear modulus, G, of rubber-like materials is generally about one third the compression modulus, E, the shear stiffness can be written using equations (4.11) and (4.12) as $\frac{1}{3}k_p$. From equations (4.13)-(4.15), the bending and torsional stiffnesses are approximately $B\,k_p$ and $\frac{2}{3}B\,k_p$, where B is equal to one-twelfth the contact area.

The restoring force at the contact is $\delta g_{bp} = [Kbp]d_{bp}$. The restoring forces in joint coordinates are given by $\delta g_q = [Jfq]^t \delta g_{bp}$ and the corresponding motions in joint coordinates are given by $d_q = [Kq]^{-1}\delta d_q$. The motions are then expressed in fingertip coordinates as $d_{fp} = [Jfq]d_q$.

δg_x	$= -\dfrac{k_b k_p}{k_b + k_p}\, dx$
δg_y	$= \dfrac{2k_p k_b (k_c - f r_f)}{k_b k_p r_f^2 + k_c k_p + 3k_b k_c}\, dy$
δg_z	$= 0$
$\delta g_{\theta x}$	$= 0$
$\delta g_{\theta y}$	$= 0$
$\delta g_{\theta z}$	$= \dfrac{k_b k_p (f r_f - k_c) w^2 + 2fwk_p(k_b r_f^2 + k_c)}{2(k_b k_p r_f^2 + k_c k_p + 3k_b k_c)}\, d\theta z$

Table 5-6: Change in δg_b for small contact area (soft fingertips)

As in point contact and rolling contact, comparison between d_{bp} and d_{fp} determines the relative motion between the finger and the object, which appears in the differential jacobian $\Delta[Jf]^{-t}$.

The net change in g_{bp} is obtained by summing the restoring forces and the forces due to the change in geometry.

$$\delta g_{bp} = [Kbp]d_{bp} + \Delta[Jf]^{-t} g_f$$

5.3.1 Discussion

The general expression for Δg_b is lengthy, but it is simplified considerably for the limiting cases in which the contact area is very small, or very large. To further simplify the algebra in the following results, the finger joint stiffnesses in the a and b directions have been set equal so that $k_a = k_b$.

For a small contact area, $B \rightarrow 0$ and the bending and torsional stiffnesses become negligible in comparison

to the shear and compressive stiffnesses. For two fingers, the final results are given in Table 5-6. If it is further assumed that $k_p \gg k_b$, as is usually the case, it can be shown that the results for $\Delta \mathbf{g}_b$ become identical to those obtained in the point contact case.

For the case when the contact area is large, the bending and torsional stiffnesses become infinite. If it is again assumed that $k_p \gg k_b$, the problem reduces to that of a finger glued to the surface of the object and $\Delta \mathbf{g}_b$ is given in Table 5-7.

δg_x	$= -2k_b dx$
δg_y	$= -2k_b dy$
δg_z	$= 0$
$\delta g_{\theta x}$	$= 0$
$\delta g_{\theta y}$	$= 0$
$\delta g_{\theta z}$	$= -2(k_c + (\frac{w}{2} + r_f)^2 k_b) d\theta_z$

Table 5-7: Change in $\delta \mathbf{g}_b$ for large contact area (soft fingertips)

6. Summary

In Section 2 a procedure was listed for discovering the properties of a grip by moving the object slightly, observing the resulting finger motions and determining the changes in the forces on the object. The grip properties of stiffness, resistance to slipping and infinitesimal stability were introduced and it was shown that such properties could be used to compare grips. For specific tasks, one could then choose, for example, the grip that would be stiffest with respect to rotations or the grip that would resist the largest vertical force before slipping occurred.

Two-dimensional examples with point-contact fingers were used to demonstrate how the grip properties depended on finger stiffness, finger arrangement and gripping forces. In later sections a more complete three-dimensional analysis was developed. In the final example of Section 2, the instability of a coin held on-edge between two fingers was discussed, using the simplifying example of a rectangle held between two pointed fingers. When the rectangle was rotated slightly, the finger stiffnesses produced restoring forces that tended to stabilize the grip, but the differential change in geometry resulting from the rotation allowed the grasp forces to become unstable. The stability of the grip was a function of the finger stiffness, the length of the rectangle, and the magnitude of the initial grasping forces. Interestingly, the grip became less stable as the gripping forces were increased. Thus, while an increase in the gripping forces may make the fingers more resistant to slipping, it does not always make the grip more secure

The coin example also uncovered a limitation of the point-contact assumption used in previous analyses. With pointed fingers, a coin is *less* stable if held by fingers pressing against the two faces than if held on edge. For human fingers, this is obviously not the case. A more accurate model of the finger/object interaction (one that accounts for the deformation and rolling of the fingertips) explains why. Such a model is developed in Section 4. First, however, it is useful to establish a more general framework for determining the force/deflection relations of a grasp.

For three-dimensional problems it becomes convenient to use matrices to describe the grip. The matrix equations are developed in Sections 3.1, 3.3, and 3.4. When the procedure of Section 2 is applied to general, three-dimensional problems, the results depend on the number of degrees of freedom of the contact and the finger. For an arbitrary motion of the object, the finger motion can be classified as under determined, exactly determined or over determined. Different solutions are discussed for each case.

Section 4 took a closer look at the interactions between different kinds of fingertips and the object. The characteristics of pointed, curved, and soft fingers were compared. The different characteristics are reviewed below, and summarized in Table 6-1.

In Section 4.2, it was shown that the rolling of curved fingers causes the contact area to shift with respect to the object. This adds a new term to the differential change in the geometry of the grasp — one that may

Fingertips	Kinematic conditions	Friction conditions
(1) 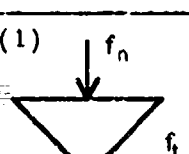 pointed	Point contact with friction. Translational motions and forces are transmitted, but rotations are not. Finger rotates about contact point which remains fixed on object. $\Delta[Jb]^t = [0]$ $\Delta[Jf]^{-t}$. rotation terms	Force tangent to object surface limited by Coulomb friction law $f_t \leq \mu f_n$
(2) 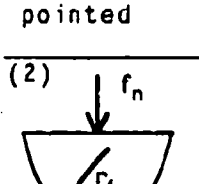 curved	Only translational forces and motions transmitted. Contact point moves as finger rolls. Approaches case (3) for $r_f \rightarrow \infty$ and case (1) for $r_f \rightarrow 0$ $\Delta[Jb]^t$: translation terms $\Delta[Jf]^{-t}$: translation & rotation terms	Force tangent to object surface limited by Coulomb friction law $f_t \leq \mu f_n$
(3) 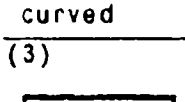 flat	Planar contact with friction. Translational and rotational forces and motions transmitted. No relative motion without slipping. $\Delta[Jb]^t = [0]$ $\Delta[Jf]^{-t} = [0]$	Distributed pressure and shear tractions allow transmission of forces and moments in plane of contact.
(4) 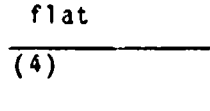 very soft	Add elastic fingertip compliance to finger compliance. Contact forces produce relative motion. Approaches case (1) for $A \rightarrow 0$ and case (3) for $A \rightarrow \infty$ $\Delta[Jb]^t = [0]$ $\Delta[Jf]^{-t}$: translation & rotation terms	Uniformly distributed pressure and shear tractions. High (adhesive) friction allows large forces and moments to be transmitted in plane of contact.
(5) 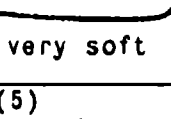 soft, curved	Elastic coupling + rolling motion. Combine cases (2) and (4). Approaches case (1) for $r_f \rightarrow 0$ and $A \rightarrow 0$ Approaches case (3) for $r_f \rightarrow \infty$ and $A \rightarrow \infty$ $\Delta[Jb]^t$: translation & rotation terms $\Delta[Jf]^{-t}$: translation & rotation terms	Non-uniform pressure distribution and shear tractions permit large forces and small moments to be transmitted in plane of contact.

Table 6-1: Summary of contact models derived in Section 4

help to stabilize it. As expected, when the radius of curvature of a curved finger becomes very small, the movement of the contact point becomes negligible and the contact behaves like a point-contact with friction. As the radius of curvature becomes very large, the finger approaches the limiting case of a flat-tipped finger having a planar contact with friction.

Fingers also deform, and a model was developed in Section 4.3 to investigate the importance of deformation. The model considers a very soft fingertip which conforms and possibly adheres to the object surface. The fingertip compliance is added to the finger joint compliance. As the area of contact becomes small, the fingertip becomes more compliant with respect to rotations than translations and approaches the

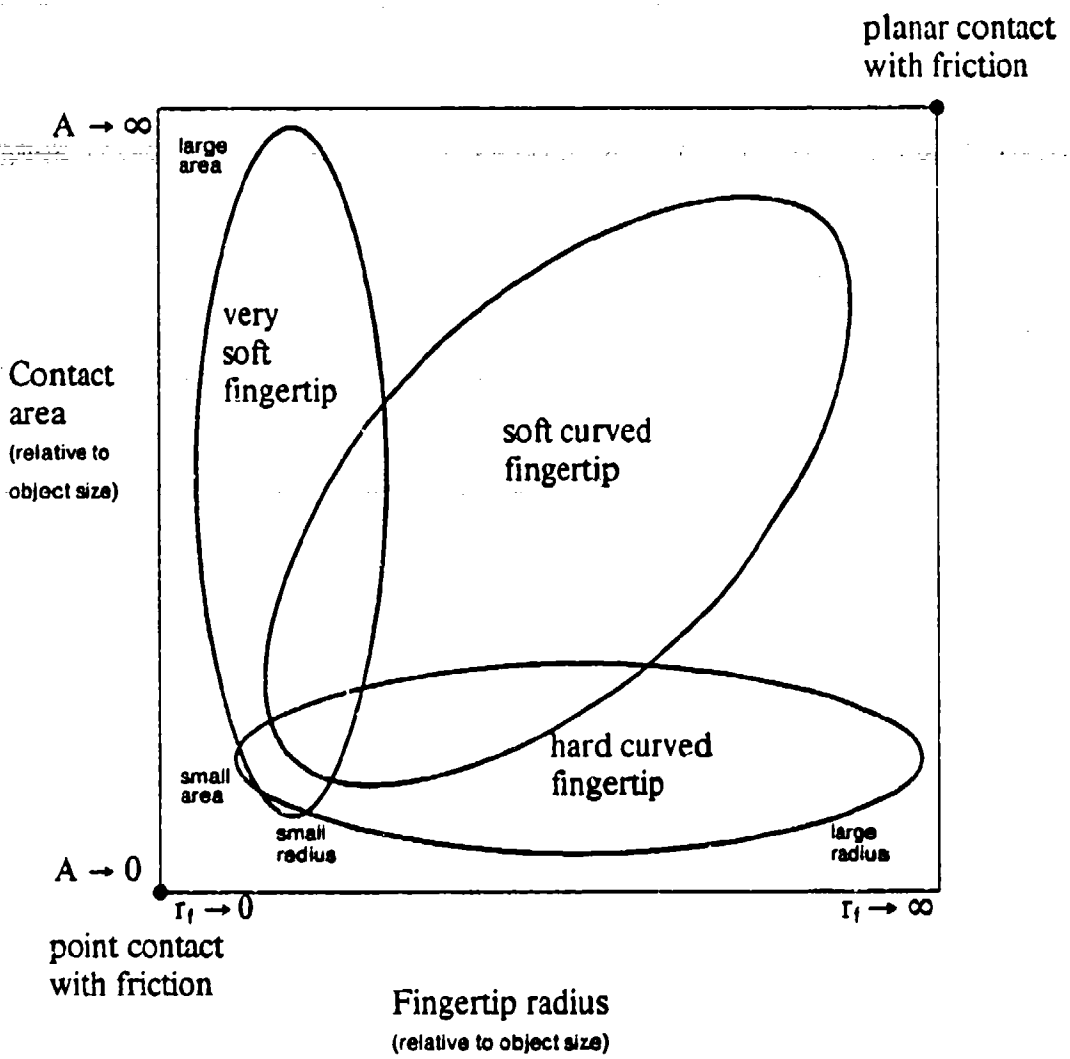

Figure 6-1: Relations between finger models

point-contact model. For large contact areas, the rotational compliance becomes much smaller than the translational compliance and the limiting case of a planar contact with friction is approached.

Fingertips such as those found on the human hand display both rolling and deformation. Section 4.4 addressed the properties of a soft, curved fingertip and found that they combined the attributes of the models in Sections 4.2 and 4.3. As the radius of curvature and the contact area became small, the fingertip could be approximated by a point-contact. For large radii of curvature and large contact areas, the fingertip approached the case of a planar contact with friction.

Figure 6-1 shows the regimes in which the different models developed in Section 4 apply, and indicates the limiting cases approached for very large or small radii of curvature and contact areas.

In Section 5, some simple examples were used to demonstrate the methods described in Sections 3.1-3.4

and to illustrate the differences between pointed, curved and soft fingers. When pointed fingertips were used, and only rotations of the object were considered, the problem reduced to the two-dimensional example given in Section 2. For curved fingertips, the stability of the grasp increased over the pointed-finger case due to rolling of the fingertips. If the fingertip radii were larger that one half the length of rectangle, the grip became stable with respect to rotational displacements no matter how small the finger stiffnesses were. The relationship between the fingertip radii and the length of the rectangle brings up an important point; the definitions of "large" or "small" radii of curvature and contact areas depend on the size of the object being handled. This is why the point-contact model is reasonable when we hold a basketball or a large box, but not a coin or a matchbox.

7. Applications to the Design and Control of Hands

The analysis presented in this paper has been part of an effort to describe the mechanical properties of a grip and to determine how they depend on finger shapes, contact conditions, finger stiffnesses and gripping forces. It has been shown that the predicted behavior depends strongly on the model used for the interaction between the fingertips and the object. In this section we consider how the results might be applied to the design and control of dextrous hands.

For controls purposes, the small-motion behavior of a grip amounts to a linearized description of the "plant," giving a relationship between displacements of the object and the resulting changes in force. The results show that point-contact finger models and stiffness-based control schemes are not always adequate. If only the stiffnesses of the fingers are considered, a displacement of the object always results in forces that tend to restore the object to its original position. However, a small change in the grip geometry may cause the grasping forces to produce something akin to positive feedback for displacements of the object. For stability, these must be canceled by increasing the grip stiffness in the corresponding directions.

The contribution of the geometric effect varies for pointed, round and soft fingers and its magnitude depends on the relative dimensions of the fingers and the object.

If a stiffness model as used in earlier analyses is not adequate, then what must be done to describe and control the grip? Unfortunately, a three-dimensional analysis of the grip becomes quite involved when finger rolling and deformation are considered. It seems unrealistic to expect a robot or gripper controller to perform a complete analysis in real-time.

Much of the complexity of the procedure results from its being a predictive or open-loop calculation in which only the motion of the object and the physical characteristics of the object and the fingers are assumed to be known. The forward force and displacement relations are relatively simple, but some complication arises in determining how displacements will be transmitted through the contact and how the finger will respond to them. Further difficulty arises in determining how finger stiffnesses, finger motions and grasp forces will interact to change the forces transmitted to the object. Much of the difficulty could be avoided if the *finger motions* and *contact forces* were available from another source. In practice, humans and animals use sensory information and experience to provide this kind of information.

When we manipulate objects with our fingers we do not use a kinematic analysis to predict how the forces at our fingertips will change in response to displacements of the object. Instead, we seem to acquire a database of general grip behavior and we use the sensors in our fingers and fingertips to modify our predictions while we work. A similar approach might also be used by a robot, provided the gripper had sufficient sensors to describe the behavior of the grasp. This prompts us to consider what kinds of sensors

would be useful. Based on the results of the analysis presented earlier, several types of sensory information are suggested:

- The measurement of normal and shear forces at the fingertips.
  If these can be measured, they do not have to be computed. The shear force can be compared with normal forces and, using information about the friction conditions, predictions can be made concerning how close each finger is to slipping.

- The location of the center of the contact area on the finger.
  Using this information, one can determine how the contact has moved since the last time step, and (by extrapolation), where it will be next. For curved fingers this allows one to track the movement of the contact with respect to the finger and to determine the degree of rolling motion. For fingers that do not roll, it shows that rate at which the finger is sliding against a surface.

- The size, uniformity and general shape of the pressure distribution of the contact area.
  The pressure distribution could be compared with typical profiles for point contacts, curved contacts and soft contacts and an estimate made of how closely the actual contact approaches each of these models.

- Sums and first moments of pressures and shear tractions.
  These allow the forces and moments transmitted through the contact to be determined.

To the above list of fingertip quantities would be added the joint angles and joint torques of the fingers, but already, the list is becoming unrealistic. Even if accurate sensors were available, computing first moments and matching pressure profiles might be just as time consuming as performing the analysis presented in this paper. Determining such quantities has much in common with feature extraction for grey-scale vision, which is notoriously slow unless performed on special-purpose hardware.

However, even if only the forces and an estimate of the contact size and location were available, the analysis could be simplified. Between these fingertip quantities and the finger joint angles, most of the information needed to describe the grip would be available through forward transformations. The finger joint torques are easily found from the fingertip forces and the fingertip motion is easily determined from the joint angles. An estimate of the contact size would indicate the degree of finger/object coupling and the contact location would allow the finger jacobians to be updated. A small number of fingertip sensors might be sufficient. Recent studies with human beings performing assembly-line tasks [22] suggest that a sparse array of sensory information (perhaps no more than eight points per fingertip) provides adequate information.

In Section 2 the possibility of discriminating between different grip geometries based on grip stiffness, stability and resistance to slipping was considered. The best grip would be the one that most closely matched the grip properties to the task requirements. Presumably the finger stiffnesses would be chosen near the middle of their achievable range. The next question is, once a suitable grip has been identified how should the finger stiffnesses (joint servo gains) and joint torques be adjusted? The problem is usually under determined if only the force on the object and its stiffness with respect to external loads are specified. Salisbury [2] specified additional internal forces and internal grip stiffnesses so that every finger joint torque and stiffness became determined. The internal grip forces and stiffnesses could be chosen to ensure that

fingers remained in contact with the object, to reduce the likelihood of crushing the object, or to reduce the danger of slipping.

As mentioned in Section 1, Orin and Oh [8] consider a similar problem in determining the most efficient distribution of joint forces for walking machines or multi-fingered grippers. The optimum force distribution is found subject to a number of constraints including linearized friction limitations. In grasping it is probably less important to minimize power consumption than it is in a walking machine. More important is the need to minimize gripping forces. This prevents objects from being damaged, avoids saturating the fingertip sensors and reduces the kind of instability demonstrated for the rectangle held between two fingers. Linear programming methods may be too slow for real-time control of joint torques, but could be useful for off-line estimation of grasp forces and stiffnesses. The fingertip models of Section 4 could be added to the kinematic description of the grasp.

In a current investigation, Kerr [23] has extended the kinematic analyses of Salisbury and has considered the optimum selection of internal grip forces. Like Orin and Oh [8], he suggests the use of "friction pyramids" to form a set of linear constraint equations for slipping at the fingertips.

Ideally, choosing and adjusting a grip is something that a robot should be able to do using a combination of computational methods (including those discussed above), sensory information and some "rules of thumb." The rules are difficult to define, but as we continue to explore the mechanics of gripping and to observe how humans and animals handle objects we can begin to make some suggestions such as:

- In general, grip as gently as possible without letting the object slip. A light grip helps to prevent damage to the object and the fingers, reduces the likelihood of instability, and keeps the sensors working near the lower end of their range (where they are often more sensitive).
- Try to match the stiffness of the grip to the requirements of the task. This will simplify the active control of the object.
- Spacing the fingers closer together results in a grip that is less stiff with respect to rotations.
- Point contacts are usually less stable than soft or rounded fingers.

Compared to the analysis and control of manipulator arms, the modeling and control of multi-fingered grippers are in an infant stage. Current efforts are directed not toward making them more precise and efficient but toward controlling them at all. Fortunately, it is unnecessary to develop a system that rivals the human hand. In fact, a gripper that could grasp and manipulate within its restricted environment as well as many animals do in theirs, would be extremely useful. The results of this and previous analyses suggest that for tasks involving small motions and solid objects, grips can be modeled and controlled. Experiments with grippers assembling parts, wielding tools and loading machines are now required to construct grasping rules, to determine what sensory information is most useful and to explore control strategies for manufacturing hands.

8. Acknowledgements

I am most grateful to my thesis advisor, Professor Paul Wright, for his assistance and constant encouragement in this project. Special thanks are also due to Professors Mark Nagurka and Matt Mason for their comments on the draft of this paper. The Phillip M. McKenna Foundation provided a fellowship that supported most of the work.

A. Matrix Identities

The finger positions and orientations may be expressed with 4x4 homogeneous transformation matrices, [T]:

$$[T] = \left[\begin{array}{c|c} A & r \\ \hline 0 & 1 \end{array}\right] = \left[\begin{array}{ccc|c} a_x & b_x & c_x & r_x \\ a_y & b_y & c_y & r_y \\ a_z & b_z & c_z & r_z \\ \hline 0 & 0 & 0 & 1 \end{array}\right]$$

[A] is a 3x3 orthonormal matrix of direction cosines, expressing the orientation of the finger (a,b,c) system of Figure 3-1 in terms of the global (x,y,z) system. r is a vector from the origin of the (x,y,z) system to the origin of the (a,b,c) system. If r_f is the vector in Figure 3-1 from f to fp in (a,b,c) coordinates then $[A]r_f$ gives the same vector in (x,y,z) coordinates. Consequently, the vector from o to fp in Figure 3-1 is $r = r_b - [A]\, r_f$.

The relationship between two six-element vectors ($d^t = [d_x,\ d_y,\ d_z,\ d_{\theta x},\ d_{\theta y},\ d_{\theta z}]$) of differential translations and rotations may be expressed as a 6x6 jacobian.

$$d_{bp} = [Jb]\, d_b$$

The jacobian is conveniently written in terms of 3x3 partitions:

$$\underset{(6x6)}{[Jb]} = \left[\begin{array}{c|c} A^t & A^t R^t \\ \hline 0 & A^t \end{array}\right] \quad \begin{matrix} \\ \\ (3x3) \quad (3x3) \end{matrix}$$

[A] is again a 3x3 matrix of direction cosines. In the above example, [A] expresses the orientation of the (l,m,n) coordinate system at bp in Figure 3-1 with respect to the (x,y,z) system. Since [A] is orthonormal it follows that $[A]^t = [A]^{-1}$.

[R] is an antisymmetric cross-product matrix formed from the elements of a vector r, such that if v is a three-component vector (for example, the three rotational components of d_b) then

$$[R]\ v = \begin{bmatrix} 0 & -r_z & r_y \\ r_z & 0 & -r_x \\ -r_y & r_x & 0 \end{bmatrix} \begin{bmatrix} v_x \\ v_y \\ v_z \end{bmatrix} = r \times v$$

Since is [R] is antisymmetric. $[R]^t = -[R]$ and $[R]^t v = v^t [R] = v \times r$.

Given the above identities for [R] and [A] the following relationships hold for [J]:

$$[Jb]^t = \left[\begin{array}{c|c} A & 0 \\ \hline RA & A \end{array}\right] \qquad [Jb]^{-1} = \left[\begin{array}{c|c} A & RA \\ \hline 0 & A \end{array}\right]$$

$$[Jb]^{-t} = \left[\begin{array}{c|c} A^t & 0 \\ \hline A^tR^t & A^t \end{array}\right]$$

A.1 Matrix Method for Under Determined Finger Motions

For the case in which the motion of the object does not completely determine the motion of the finger, the potential energy may be minimized subject to the *nc* constraint conditions in [P]. The constraint equations, C_i, are formed by multiplying one row of [P] by d_c. The *nf* auxiliary equations may then be written as [24]

$$\varphi_i = \frac{\partial P.E.}{\partial q_i} + \lambda_1 \frac{\partial C_1}{\partial q_i} + \lambda_2 \frac{\partial C_2}{\partial q_i} + \cdots + \lambda_{nc} \frac{\partial C_{nc}}{\partial q_i}$$

These are combined with the constraint equations to provide $nf + nc$ equations for $nf + nc$ unknowns. The equations may be conveniently expressed as,

$$\left[\begin{array}{c} d_q \\ \hline l \end{array}\right] = [L]^{-1} \left[\begin{array}{c} g_q \\ \hline d_c \end{array}\right]$$

where l is a column vector of the *nc* Lagrange multipliers and

$$[L] = \left[\begin{array}{c|c} Kq & P^t \\ \hline P & 0 \end{array}\right]$$

A.2 Differential Jacobians

In Section 3.1 the change in the jacobians, [J], as a result of small displacements of the object are considered. These terms, [ΔJ] and $[\Delta J]^t$, result from shifting of the contact area and rolling of the fingers. Products such as [ΔJ]·d contain very small terms and may be ignored, but products such as $[\Delta J]^t \cdot g$ may contain significant terms since the forces, g, may be large. As an example, if the contact area translates and rotates with respect to the object then change in the jacobian relating g_{bp} and g_b is

$$[\Delta Jb]^t = [Jb']^t - [Jb]^t$$

where $[Jb']^t$ is the jacobian relating to the new position and orientation of the contact area and $[Jb]^t$ is the original jacobian. By writing $[Jb']^t$ and $[Jb]^t$ in terms of partitions, $[\Delta Jb]^t$ is seen to be

$$\left[\begin{array}{c|c} \Delta A & 0 \\ \hline \Delta(RA) & \Delta A \end{array}\right]$$

where $\Delta(RA) = (RA)'-(RA) = [R][A] + [\Delta R][A] + [R][\Delta A] + [\Delta R][\Delta A] - [R][A]$. $[\Delta R][\Delta A]$ contains second order terms, and may be dropped so that $\Delta(RA) \approx [\Delta R][A] + [R][\Delta A]$.

$[\Delta R]$ and $[\Delta A]$ can be written in terms of differential translations and rotations, $(\delta r_x, \delta r_y, \delta r_z, \delta\theta_x, \delta\theta_y, \delta\theta_z)$.

$$[\Delta R] = [R'] - [R] = \begin{bmatrix} 0 & -\delta r_z & \delta r_y \\ \delta r_z & 0 & -\delta r_x \\ -\delta r_y & \delta r_x & 0 \end{bmatrix}$$

$$[\Delta A] = [A'] - [A] = \begin{bmatrix} 0 & -\delta\theta_z & \delta\theta_y \\ \delta\theta_z & 0 & -\delta\theta_x \\ -\delta\theta_y & \delta\theta_x & 0 \end{bmatrix}$$

$[\Delta A]$ and δr are also equivalent to the upper left 3x3 partition and right column respectively of the differential 4x4 homogeneous transform, $[\Delta]$, expressing a small translation and rotation of one coordinate system with respect to another [16].

B. Rolling Contact

$r'_{(s)} = r_{(s+\delta s)}$ and $u'_{(s)} = u_{(s+\delta s)}$ may be expanded in terms of $r_{(s)}$ as

$$r'_{(s)} = r_{(s)} + \delta s \frac{dr_b}{ds} + \frac{(\delta s)^2}{2!} \frac{d^2 r_b}{ds^2} + \cdots$$

$$u'_{(s)} = \frac{dr}{ds} + \delta s \frac{d^2 r}{ds^2} + \cdots$$

Then Δr becomes

$$\Delta r = \delta s \frac{dr}{ds} + \frac{(\delta s)^2}{2!} \frac{d^2 r}{ds^2} + \cdots = \delta s u + \frac{(\delta s)^2}{2!} \frac{du}{ds} + \cdots$$

Since the first derivatives of r_b and r_f are equal at the initial contact point, subtracting $\Delta r_b - \Delta r_f$ gives

$$\Delta r_b - \Delta r_f = \frac{(\delta s)^2}{2!} \left(\frac{d^2 r_b}{ds^2} - \frac{d^2 r_f}{ds^2} \right) + \cdots$$

or, $\Delta r_b - \Delta r_f \approx 1/2(\delta s)^2$ times the difference in curvature between $r_{b(s)}$ and $r_{f(s)}$.

The rotation of the contact point is given by the vector $(u_b \times u_b')$ and the rotation of the fingertip is given by $(u_f' \times u_b')$. Expanding u_f' and u_b' in terms of $r_{(s)}$ and discarding third and higher derivatives of r gives

$$u_b \times u_b' = u_b \times \left(u_b + \frac{du_b}{ds} \delta s \right) = (0) + \delta s \left(\frac{dr_b}{ds} \times \frac{d^2 r_b}{ds^2} \right)$$

and

$$u_f' \times u_b' = (u_f \times u_b) + \delta s \left(u_f \times \frac{du_b}{ds} \right) + \delta s \left(u_b \times \frac{du_f}{ds} \right) + (\delta s)^2 \left(\frac{d^2 r_f}{ds^2} \times \frac{d^2 r_b}{ds^2} \right)$$

$$= (0) + \delta s \left(\left(\frac{d^2 r_f}{ds^2} - \frac{d^2 r_b}{ds^2} \right) \times u \right) + (\delta s)^2 \left(\frac{d^2 r_f}{ds^2} \times \frac{d^2 r_b}{ds^2} \right)$$

where $u = u_b = u_f$ at the initial contact point.

For the case in which the object surface is flat and the fingertip is a segment of a circular arc, as in Figures 4-3 and 4-4, or 5-2 and 5-3, the rolling equations become

$$r_f = (r_c \sin\theta_f)\mathbf{i} + (r_c \cos\theta_f)\mathbf{j}, \quad r_b = (r_c \tan\theta_b)\mathbf{i} - r_c \mathbf{j}.$$

where θ_f is related to s as

$$\frac{d\theta_f}{ds} = 1/r_c$$

For $\theta_f = \theta_b = 0$ at the initial contact point, equations (4.5)-(4.7) become

$$\Delta r_b = (r_c \, \delta\theta_f)\, i + 0\, j$$

$$\Delta r_b - \Delta r_f = 0\, i + \frac{r_c (\delta\theta_f)^2}{2}\, j$$

$$u_b \times u_b' = 0$$

$$u_f' \times u_b' = \delta\theta_f$$

C. Details for examples in Section 5

$$[Jb] = \left[\begin{array}{ccc|ccc} 0 & 0 & 1 & 0 & \frac{w}{2} & 0 \\ 0 & 1 & 0 & 0 & 0 & \frac{w}{2} \\ -1 & 0 & 0 & 0 & 0 & 0 \\ \hline 0 & 0 & 0 & 0 & 0 & 1 \\ 0 & 0 & 0 & 0 & 1 & 0 \\ 0 & 0 & 0 & -1 & 0 & 0 \end{array}\right] \qquad [Jf] = \left[\begin{array}{ccc|ccc} 0 & 0 & 1 & 0 & r_f & 0 \\ 0 & 1 & 0 & 0 & 0 & r_f \\ -1 & 0 & 0 & 0 & 0 & 0 \\ \hline 0 & 0 & 0 & 0 & 0 & 1 \\ 0 & 0 & 0 & 0 & 1 & 0 \\ 0 & 0 & 0 & -1 & 0 & 0 \end{array}\right] \qquad [Jq] = \left[\begin{array}{ccc} 1 & 0 & 0 \\ 0 & 1 & 0 \\ 0 & 0 & 0 \\ \hline 0 & 0 & 0 \\ 0 & 0 & 0 \\ 0 & 0 & 1 \end{array}\right]$$

$$[Jfq] = \left[\begin{array}{ccc} 0 & 0 & 0 \\ \hline 0 & 1 & r_f \\ -1 & 0 & 0 \\ \hline 0 & 0 & 1 \\ 0 & 0 & 0 \\ 0 & 0 & 0 \end{array}\right][P] \qquad [M] = \left[\begin{array}{ccc|ccc} 1 & 0 & 0 & 0 & 0 & 0 \\ 0 & 1 & 0 & 0 & 0 & 0 \\ 0 & 0 & 1 & 0 & 0 & 0 \end{array}\right] \qquad [Kq] = \begin{bmatrix} k_a & 0 & 0 \\ 0 & k_b & 0 \\ 0 & 0 & k_c \end{bmatrix} \qquad [L] = \left[\begin{array}{ccc|cc} k_a & 0 & 0 & 0 & -1 \\ 0 & k_b & 0 & 1 & 0 \\ 0 & 0 & k_c & r_f & 0 \\ \hline 0 & 1 & r_f & 0 & 0 \\ -1 & 0 & 0 & 0 & 0 \end{array}\right]$$

$$[Cfp] = \left[\begin{array}{c|c|c|c|c} 0 & 0 & 0 & 0 & 0 \\ \hline 0 & \frac{k_b r_f^2 + k_c}{k_b k_c} & 0 & \frac{r_f}{k_c} & 0 \\ 0 & 0 & \frac{1}{k_a} & 0 & 0 \\ 0 & \frac{r_f}{k_c} & 0 & \frac{1}{k_c} & 0 \\ \hline 0 & 0 & 0 & 0 & 0 \\ 0 & 0 & 0 & 0 & 0 \end{array}\right] \qquad [Kfc] = \begin{bmatrix} k_b & 0 & -k_b r_f \\ 0 & k_a & 0 \\ -k_b r_f & 0 & k_b r_f^2 + k_c \end{bmatrix}$$

$$\begin{bmatrix} \frac{dq}{\lambda_1} \\ \lambda_2 \end{bmatrix} = [L]^{-1} \begin{bmatrix} \frac{gq}{dm} \\ dn \end{bmatrix}$$

Figure C-1: Matrices for Left Finger - pointed or rolling contact

$\Delta [Jf]^{-t}$ point contact

$$\left[\begin{array}{ccc|ccc} 0 & 0 & 0 & 0 & 0 & 0 \\ -\delta\theta & 0 & 0 & 0 & 0 & 0 \\ 0 & -\delta\theta & 0 & 0 & 0 & 0 \\ \hline 0 & 0 & 0 & 0 & 0 & 0 \\ 0 & 0 & 0 & -\delta\theta & 0 & 0 \\ 0 & 0 & -\delta\theta r_f & 0 & -\delta\theta & 0 \end{array}\right]$$

$\Delta [Jf]^{-t}$ rolling contact

$$\left[\begin{array}{ccc|ccc} 0 & 0 & 0 & 0 & 0 & 0 \\ -\delta\theta & 0 & 0 & 0 & 0 & 0 \\ 0 & -\delta\theta & 0 & 0 & 0 & 0 \\ \hline \delta\theta r_f & 0 & 0 & 0 & 0 & 0 \\ 0 & 0 & 0 & -\delta\theta & 0 & 0 \\ 0 & 0 & 0 & 0 & -\delta\theta & 0 \end{array}\right]$$

$\Delta [Jb]^{t}$ rolling contact

$$\left[\begin{array}{ccc|ccc} 0 & 0 & 0 & 0 & 0 & 0 \\ 0 & 0 & 0 & 0 & 0 & 0 \\ 0 & 0 & 0 & 0 & 0 & 0 \\ \hline \delta\theta r_f & 0 & 0 & 0 & 0 & 0 \\ 0 & 0 & 0 & 0 & 0 & 0 \\ 0 & 0 & \delta\theta r_f & 0 & 0 & 0 \end{array}\right]$$

	Object			Finger		
	d_b	d_{bp}	d_c	d_{fp}	d_f	d_q
1	dx	0	0	0	-dn	-dn
2	dy	dm	dm	dm	$\frac{\beta\ dm}{k_b}$	$\frac{\beta\ dm}{k_b}$
3	0	dn	dn	dn	0	
4	0	$d\theta_1$		αdm	0	
5	0	0		0	0	
6	$d\theta_z$	0		0	αdm	αdm

In the above,

$dn = -dx$

$dm = dy - \frac{w\ d\theta_z}{2}$

$d\theta_1 = d\theta_z$

$\delta\theta = d\theta_z - \alpha(dy - \frac{w\ d\theta_z}{2})$

$\beta = \frac{k_b k_c}{k_b r_f^2 + k_c}$

$\alpha = \frac{k_b r_f}{k_b r_f^2 + k_c}$

$d_{bp} = [Jb]\ d_b$

$d_c = [M]\ d_{bp}$

$d_{fp} = [Jf]\ d_f$

$d_f = [Jq]\ d_q$

Figure C-2: Matrices for left finger - pointed or rolling contact

Summary of matrix equations for left finger — point-contact example

1. $d_{bp} = [M][Jb]d_b$

2. $d_{fp} = [Jfq]d_q$

3.
$$\begin{bmatrix} d_q \\ \hline \lambda_1 \\ \lambda_2 \end{bmatrix} = [L]^{-1} \begin{bmatrix} g_q \\ \hline dm \\ dn \end{bmatrix}$$

4. $\delta g_q = [Kq]d_q$

5. $[Cfp] = [Jfq][Kq]^{-1}[Jfq]^t$

6. $[Cfc]$ = non-singular portion of $[Cfp]$

7. d_{fc} = subset of d_{fp} corresponding to $[Cfc]$

8. $\delta g_{fc} = [Cfp]^{-1}d_{fc}$

9. $\delta g_{fp} = \delta g_{fc} + \Delta[Jf]^{-t}g_f$

10. $\delta g_b = [Jb]^t[M]^t\delta g_{fp}$

$$[Cfp]$$

$$\begin{bmatrix} \frac{3}{k_p} & 0 & 0 & 0 & 0 & 0 \\ 0 & \frac{1}{\beta}+\frac{3}{k_p} & 0 & \frac{r_f}{k_c} & 0 & 0 \\ 0 & 0 & \frac{1}{k_b}+\frac{1}{k_p} & 0 & 0 & 0 \\ 0 & \frac{r_f}{k_c} & 0 & \frac{1}{Bk_p}+\frac{1}{k_c} & 0 & 0 \\ 0 & 0 & 0 & 0 & \frac{1}{Bk_p} & 0 \\ 0 & 0 & 0 & 0 & 0 & \frac{3}{2Bk_p} \end{bmatrix}$$

Combined compliance for finger and square fingertip
where $k_a = k_b$ in finger joint coordinates and

$$k_{comp} = k_p$$

$$k_{shear} = \frac{k_p}{3}$$

$$k_{bend} = Bk_p$$

$$k_{twist} = \frac{2k_p}{3}$$

$$B = \frac{Area}{12}$$

for the elastic fingertip.

Figure C-3: Compliance matrix for soft finger example

References

1. H. Asada, *Studies on Prehension and Handling by Robot Hands With Elastic Fingers*, PhD thesis, Kyoto University, April 1979.

2. J.K. Salisbury, *Kinematic and Force Analysis of Articulated Hands*, PhD thesis, Stanford University, July 1982.

3. T. Okada, "Computer Control of Multijointed Finger System for Precise Handling," *IEEE Transactions on Systems, Man and Cybernetics*, Vol. SMC-12, No. 3, May 1982, pp. 289-299.

4. T. Okada, " Object Handling System for Manual Industry," *IEEE Transactions on Systems, Man, and Cybernetics*, Vol. SMC-9, No. 2, February 1979, pp. 79-89.

5. J.K. Salisbury and J.J. Craig, "Articulated Hands: Force Control and Kinematic Issues," *Robotics Research*, Vol. 1, No. 1, 1982, pp. 4-17.

6. K. Salisbury, "Active Stiffness Control of a Manipulator in Cartesian Coordinates," *Proc. 19th IEEE Conference on Decision and Control*, Albuquerque, NM, December 1980, , pp. 87-97.

7. H. Hanafusa, K. Kobayashi and N. Terasaki, "Fine Control of the Object With Articulated Multi-Finger Robot Hands," *1983 International Conference on Advanced Robotics*, Tokyo, Japan, September 1983, , pp. 245-252.

8. D.E. Orin and S.Y. Oh, "Control of Force Distribution in Robotic Mechanisms Containing Closed Kinematic Chains," *Journal of Dynamic Systems, Measurement and Control (ASME)*, Vol. 102, June 1981, pp. 134-141.

9. M.T. Mason, *Manipulator Grasping and Pushing Operations*, PhD thesis, Massachusetts Institute of Technology, June 1982.

10. R. Malek, "The Grip and its Modalities," in *The Hand*, R. Tubiana, ed., W.B. Saunders Co., Philadelphia, PA, 1981, ch. 45.

11. T. Lozano-Perez, "Task Planning," in *Robot Motion Planning and Control*, M. Brady *et al*, ed., The MIT Press, Cambridge, MA, 1982, pp. 463-488, ch. 6.

12. T. Lozano-Perez, "Automatic Planning of Manipulator Transfer Movements," in *Robot Motion Planning and Control*, M. Brady *et al*, ed., The MIT Press, Cambridge, MA, 1982, pp. 489-526, ch. 6.

13. M. Mason, "Compliance and Force Control for Computer Controlled Manipulators," in *Robot Motion Planning and Control*, M. Brady *et al*, ed., The MIT Press, Cambridge, MA, 1982, pp. 373-404, ch. 5.

14. B.E. Shimano, *The Kinematic Design and Force Control of Computer Controlled Manipulators*, PhD thesis, Stanford University, March 1978.

15. N. Hogan and S.L. Cotter, "Cartesian Impedance Control of a Nonlinear Manipulator," *Robotics Research and Advanced Applications*, ASME Winter Annual Meeting, Phoenix, AZ, November 1982, , pp. 121-128.

16. R.P. Paul, *Robot Manipulators: Mathematics Programming and Control*, The MIT Press, Cambridge, MA, 1981.

17. S.H Crandall, N.C. Dahl and T.J. Lardner, *Theory of Elasticity*, McGraw-Hill, Inc., New York, 1972.

18. S.P. Timoshenko and J.N. Goodier, *Theory of Elasticity*, McGraw-Hill, Inc., New York, 1970.

19. J. Halling, *Principles of Tribology*, Macmillan Press, Ltd., London, 1975.

20. K.C. Ludema, "Friction of Rubber," in *Mechanics of Pneumatic Tires, NBS Monograph 122*, S.K. Clark, ed., U.S. Govt. Printing Office, Washington, D.C., 1971, pp. 41-54, ch. 1.2.

21. J.Y. Wong, *Theory of Ground Vehicles*, John Wiley and Sons, Inc., New York, 1978.

22. L.D. Harmon, "Robotic Taction for Industrial Assembly," *The International Journal of Robotics Research*, Vol. 3, No. 1, 1984, pp. 73-76.

23. J. Kerr, *Grasping*, PhD thesis, Stanford University, (to be submitted in 1984).

24. S.B. Hildebrand, *Advanced Calculus for Applications*, Prentice-Hall, Inc., Englewood Cliffs, N.J., 1976.